FUNCTIONAL NANOCOATINGS FABRICATED FROM AQUEOUS POLYMER COMPLEXES

A Dissertation

by

MERID MINASSE HAILE

Submitted to the Office of Graduate and Professional Studies of
Texas A&M University
in partial fulfillment of the requirements for the degree of

DOCTOR OF PHILOSOPHY

Chair of Committee,	Jaime Grunlan
Committee Members,	Mustafa Akbulut
	Zhengdong Cheng
	Abraham Clearfield
Head of Department,	Ibrahim Karaman

December 2016

Major Subject: Materials Science and Engineering

ABSTRACT

Layer-by-layer deposition has provided a framework in which coatings with a variety of functionality can be deposited from aqueous solutions in ambient conditions. Despite the many advantages of layer-by-layer assembly, the process requires many processing steps to deposit films of adequate thickness. The work in this dissertation focuses on using polyelectrolyte complex suspensions to deposit similar functional films more quickly and easily.

Impressive flame retardancy on cotton fabric was achieved by depositing polyethylenimine/poly(sodium phosphate) nanocoatings on cotton in a sol-gel process. By raising the pH of the suspension of the two oppositely-charged polyelectrolytes to 9.0, a stable complex was formed. After depositing these polymers onto cotton by wet-pickup, a simple treatment in acidic buffer yielded a durable, conformal film on the cotton fibers. The coating rendered the fabric self-extinguishing during vertical flame testing, as well as reduced the peak heat release rate by 88% during pyrolysis combustion flow calorimetry.

A polyelectrolyte complex coating consisting of poly(allyl amine) and poly(sodium phosphate) was deposited on polyester-cotton fabric. Not only did this nanocoating render the fabric self-extinguishing during vertical flame testing, with only 18 wt% coating, it outperformed a layer-by-layer assembled film of the same weight. This coating also showed impressive wash durability, maintaining flame retardancy after five home launderings and eight hours in boiling water.

A polyelectrolyte complex coacervate was rod coated onto PET to provide excellent oxygen barrier. After treating the coating in humidity and subsequent 150 °C thermal cross-linking, the film consisting of polyethylenimine and polyacrylic acid reduced the oxygen transmission of 127 µm PET by a factor of 120.

DEDICATION

I would like to dedicate this dissertation to my father, David Haile, for his constant support and encouragement throughout my graduate studies. I really needed someone that just always had my back these past few years and he was always there to lend a helping hand.

ACKNOWLEDGEMENTS

My greatest thanks goes to God, “merciful and gracious, slow to anger and abounding in steadfast love and faithfulness” (Psalm 86:15), even when I fall short of His design.

I would like to thank my committee chair, Professor Jaime Grunlan, for his guidance, and for providing a means of financial support throughout my graduate research. I would like to thank Dr. Mustafa Akbulut, Dr. Zhengdong Cheng, and Professor Abraham Clearfield, for serving on my committee, and for their helpful advice during my preliminary examination.

I would also like to thank all of the staff here at Texas A&M University, for their patience with me in trying to get my research done, particularly Dr. Wilson Serem and Yordanos Bisrat at the Materials Characterization Facility, Mitch Wittneben, Nicole Latham, Lindy Boss, Crystal Morris, Laura Rueda, Troy Mitchell and Jason Charanza in the Mechanical Engineering Department.

I am tremendously grateful to all of the members of the Polymer Nanocomposites Lab that I’ve had the pleasure to work with for their support and assistance, particularly Amanda Cain, David Hagen, Bart Stevens, Fangming Xiang, Ping Tzeng, Kevin Holder, Taylor Smith, Morgan Plummer, Tyler Guin, Dr. Chungyeon Cho, Dr. Marcus Leistner, Dr. Chaoqun Zhang, Dr. Chaowei Feng, Taylor Smith, Ryan Smith, Yixuan Song, Shuang Qin, Alyssa John, and Dr. Debrata Patra, for their guidance in helping me understand the science, being great coworkers, and for their friendship during the past three years. Thanks

also to the undergraduate assistants, who helped me produce much of the data presented in this dissertation: Sandra Fomete, Ilse Lopez, Owais Sarwar, Robert Henderson, Pablo Leon, and Luis Plata.

NOMENCLATURE

AFM	Atomic Force Microscopy
ASTM	American Society for Testing and Materials
LbL	Layer-by-Layer
MCC	Microcombustion Calorimetry
OTR	Oxygen Transmission Rate
PAA	Poly(acrylic acid)
PAAm	Poly(allyl amine)
PEC	Polyelectrolyte Complex
PECO	Polyester-cotton
PEI	Branched Polyethylenimine
PET	Poly(ethylene terephthalate)
PNC	Polymer Nanocomposites
PSP	Poly(sodium phosphate)
TGA	Thermogravimetric Analysis
UV-Vis	Ultraviolet-Visible Light Spectroscopy

TABLE OF CONTENTS

Page

LIST OF FIGURES

Page

LIST OF TABLES

Page

CHAPTER I

INTRODUCTION

1.1 Background

Layer-by-layer (LbL) assembly has attracted considerable attention as a highly versatile method to fabricate thin films on two-dimensional and three-dimensional substrates, as well as particles. The process typically builds films in ambient conditions using the electrostatic interactions between oppositely-charged polyelectrolytes.[1] The film is assembled using a "bottom-up" approach as each charged layer adsorbs onto a substrate as it is alternately immersed into aqueous polyelectrolyte solutions (or dispersions). These assemblies can be built from polymers,[2] nanoparticles,[3-6] or biomolecules[7-10] to deposit thin films without altering the desired properties of the bulk material.[2] This technique is attractive for its ambient processing from aqueous solutions, providing a low-cost and environmentally friendly alternative to other coating processes, such as chemical vapor deposition and solution casting. LbL assembly has been used to apply multilayered films with desirable properties such as drug release,[2,9,11-13] chemical sensing,[9,14-16] antimicrobial,[17-21] flame retardancy[22,23] and oxygen barrier.[24-31]

Over the past ten years fabrics made of synthetic fibers, such as polyester, have emerged as the largest component of the textile industry and continue to increase in demand.[32] Polyester-cotton (PECO) blends are used to combine comfort and breathability (of cotton) with strength and durability (of polyester).[33] The high flammability of these textiles, however, pose a significant danger. More than 4300 serious

burn injuries associated with clothing occur annually in the United States.[34] The hazard associated with PECO-based apparel is further worsened by polyester's tendency to melt, clinging to the wearer's body and causing severe burning.[35] Reducing fabric flammability is a challenge due to the combination of melting polyester and non-melting cotton fibers that tend to produce a scaffolding effect, resulting in greater flammability than that of the individual components.[35] Approaches developed to reduce PECO flammability include the use of organohalogen additives and flame retardant (FR) back-coatings.[36-39] Using additives at the fiber spinning stage often result in weaker fibers as well as difficulties in spinning.[40,41] Furthermore, halogen-based additives have been linked to biological persistence and toxicity.[42,43] Although halogen-containing flame retardants have been effective in reducing fire-related deaths and property damage, concerns over their potential threat to the environment and human health have prompted efforts in finding safer alternatives.[44-48] LbL assembly has proven to be an effective method to impart non-halogenated FR coatings on polyurethane foam,[31,44,49-58] as well as other flammable materials such as cotton,[59-69] nylon,[21,70,71] and polyester fabric.[59,65,72]

Thin films for gas barrier are highly desirable for applications such as protection of flexible electronics, pressurized systems, and food packaging.[73,74] Multilayered films, fabricated using LbL deposition have shown extraordinarily low oxygen transmission and are of high interest due to their robustness, tailorability and ease of fabrication.[27] Despite all the benefits and impressive properties of these multilayered nanocoatings, the long deposition times and high number of processing steps are an impediment to industrial viability. This dissertation presents an exciting framework in which polyelectrolyte

complexes of oppositely charged polyions can be deposited as functional thin films with properties competitive to LbL-deposited thin films. In most cases, only three or four processing steps are needed to achieve good flame retardant or gas barrier behavior.

1.2 Outline of Dissertation

Chapter II provides an overview of the layer-by-layer process and efforts toward reducing the number of processing steps and speeding up deposition time. The gas barrier and flame retardant applications are highlighted and polyelectrolyte complexation is introduced as an alternative to LbL deposition.

Chapter III investigates the deposition of polyelectrolyte complexes onto cotton fabric for flame retardancy. The pH-dependent stability of these complexes in water and the pH-dependent solidification of the complex onto cotton fibers is investigated. Composition of the films as well as their effective flame retardancy are assessed.

Chapter IV expands the investigation of flame retardant polyelectrolyte complexes by comparing the poly(allyl amine) and poly(sodium phosphate) system directly with a layer-by-layer deposited coating. These coatings are compared with regard to composition and overall flame retardancy and the wash durability of the polyelectrolyte coating is presented.

Chapter V explores the use of polyelectrolyte complexes as gas barrier thin films. A coacervate suspension of tailored viscosity is prepared with polyethylenimine and polyacrylic acid which are kept stabilized by high sodium chloride concentration. The suspension was rod-coated onto a substrate and treated with citric acid to generate an effective oxygen barrier thin film on PET. This study demonstrates a rapid, scalable

process for depositing similar gas barrier layer-by-layer films in line with current continuous coating technology.

Chapter VI presents conclusions and proposes topics for future research. This dissertation provides several examples where polyelectrolyte complexes can be deposited to achieve functional thin films.

CHAPTER II

LITERATURE REVIEW

2.1 Functional Layer-by-Layer Coatings

Layer-by-layer assembly was first described in 1966 when Iler fabricated films using alternating immersions into suspensions of positively and negatively-charged colloidal particles.[75] The film thickness grew in proportion to the number of layers deposited and the resulting coating could not be rinsed off with water. The exploration of this technology was revived more recently, after Decher and coworkers assembled negatively and positively-charged polymers from water.[76] They demonstrated that discrete thicknesses of films could be targeted by varying the number of positive-negative dip cycles used, each cycle of which is referred to as a bilayer (BL). LbL has since been used to deposit films using clay particles,[6,28-31,49,77,78] metal oxides,[79] biomolecules,[8,9,12,80] dendrimers,[81,82] quantum dots,[83] and carbonaceous materials.[25,84-86] Various films have been assembled by layer-by-layer and have demonstrated a variety of properties including optical,[83,87,88] biomedical,[11,89] and electrical.[6,84,90,91] This deposition process has attracted significant attention for its use of ambient processing, water-based suspensions and ease of tunability. A key advantage also lies in the versatility LbL assembly provides, as it can be applied to a variety of surfaces, including substrates with both 2-D and 3-D structures.

In most studies, LbL systems rely on electrostatic self-assembly. Negative moieties of the polyanion bind to the positive moieties of the polycation through

coulombic attraction. After every deposition layer, charge reversal occurs at the film surface that allows for another oppositely-charged layer to be deposited.[92] Strong polyelectrolytes maintain their degree of ionization but the charge density of weak polyelectrolytes is greatly dependent on solution pH, as their functional groups can be in the basic or acidic form. In addition to pH, LbL assembly can be affected by ionic strength,[92,93] polyelectrolyte concentration,[94] temperature,[95] and deposition time.[96,97] Although, electrostatic forces are the prevailing interaction, LbL assembly has been facilitated by other intermolecular forces such as hydrogen-bonding,[98] charge-transfer,[99] biological,[100,101] and covalent bonding.[102]

Most LbL systems reported in literature rely on immersive deposition in solutions or suspensions of charged polyelectrolytes, as shown in Figure 2.1a.[1] The substrate is submerged in an aqueous solution from anywhere between one second to several minutes. Often there is a rinsing step in between depositions to remove excess material, is sometimes followed by a drying step. Other studies have explored alternate deposition methods to improve film properties and make this multilayer process more industrially viable. Spray-assisted LbL assembly, where films are assembled by the deposition of aerosolized suspensions, has proven to be faster than similar dip processing, and aligns well with current industrial processes.[2,72,103-106] Rubner and coworkers demonstrated both dipping and spraying could assemble highly reflective Bragg stack films, but the time required to deposit one bilayer using spraying was 90 s, while it was 36 min for dipping assembly.[107] A gas barrier film assembled by dipping LbL assembly was improved by

Xiang and coworkers by adapting the process to spray-coating, achieving a barrier film of sufficient thickness with fewer bilayers.[108]

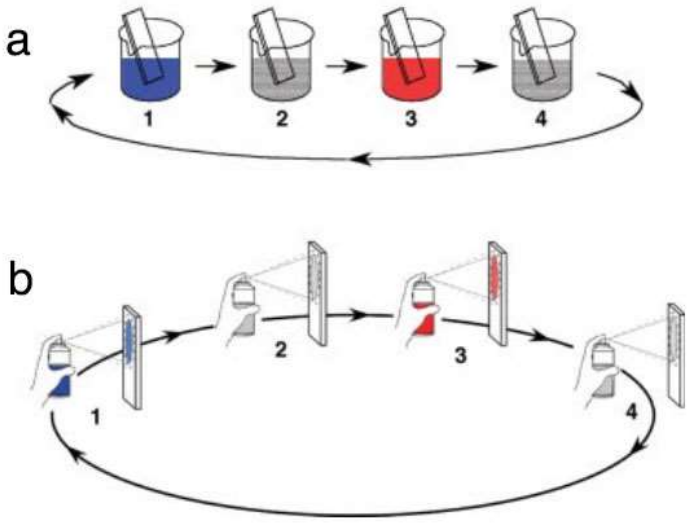

Figure 2.1. Schematic of the LbL deposition process using the (a) dipping and (b) spraying methods.[1] A substrate is treated with a positively charged polyelectrolyte solution (1), rinsed (2) then treated with a negatively charged solution (3). The substrate is finally rinsed (4) and the process is repeated until the desired number of bilayers are deposited.[1] Reprinted with permission from Decher, G.; Schlenoff, J. B. *Multilayer Thin Films: Sequential Assembly of Nanocomposite Materials*; 2nd ed.; Wiley-VCH: Weinheim, Germany **2012.**

Spin-assisted layer-by-layer, or spin assembly, rapidly spins a substrate during fluid deposition. Spin assembly is much faster than immersive techniques, reducing the time of each layer deposition (including drying and rinsing steps) to 30 seconds or less. This technique also produces more homogeneous films by exploiting centrifugal, air shear, and viscous forces to remove weakly adsorbed material and dry the film.[106] The multilayers are substantially more organized, producing more stratified layers than

immersive processes. This has been especially useful in producing optical films with transparency and homogeneous color.[109,110] Unlike immersive and spray processes, spin assembly is not a continuous process, limiting its industrial viability.

Process improvements to layer-by-layer assembly has reduced the processing time considerably. By the addition of salt or buffer, layers have been deposited with greater thickness.[111,112] Altering the immersion time can also achieve thicker coatings with fewer bilayers.[97] Despite these improvements, multilayer deposition fundamentally requires a high number of processing steps relative to established coating processes, which presents a major challenge to commercial viability.

2.1.1 Flame Retardant Nanocoatings on Fabric

In the United States, more than 4300 serious burn injuries associated with clothing occur annually.[34] While cellulosic materials such as cotton remain the most prevalent material in clothing, only a minority of it is rendered flame retardant. Cotton-synthetic blends have emerged as the greatest component of the textile industry and continue to increase in demand.[32] One such blend, polyester-cotton (PECO) is desirable as it combines comfort and breathability (of cotton) with strength and durability (of polyester).[33] The hazard associated with clothing containing synthetic fibers is worsened as the fibers tend to melt, clinging to the wearer's body and cause severe burning.[35] Reducing the flammability of these fiber blends is a challenge due to the combination of melting synthetic and non-melting cotton fibers that tend to produce a scaffolding effect, resulting in greater flammability than that of the individual components.[35]

Approaches developed to reduce synthetic fiber flammability include the use of organohalogen additives and flame retardant (FR) back-coatings.[36-39] Using additives at the fiber spinning stage often result in weaker fibers as well as difficulties in spinning, and cannot be used for non-melting natural fibers such as ramie and cotton.[40,41] Furthermore, halogen additives have been linked to biological persistence and toxicity.[42,43] These concerns have prompted the development of non-halogenated coatings for cotton and cotton-blends. Phosphorus in particular has been proven to be a very effective FR agent for cellulose-based fabrics. Phosphorus compounds are used in the more commercially prevalent flame retardant coatings for cotton: Proban CC and Pyrovatex CP. These flame retardants use the synergy of nitrogen and phosphorus to produce a highly efficient char-forming effect on cotton when subjected to flame. Organophosphorus compounds degrade to form phosphoric acid during burning, which phosphorylates the C(6) and C(4) hydroxyl moieties of the glucose monomers of cellulose, as shown in Figure 2.2.[38,113,114] This prevents the pyrolysis of the fabric to levoglucosan that fuels flame spread. Instead, the cellulose can undergo alternative degradation pathways and allow for its dehydration and cross-linking to form aliphatic char. This char helps to protect underlying material from the heat of the flame as well as locks in flammable volatiles from the fire.[38,115]

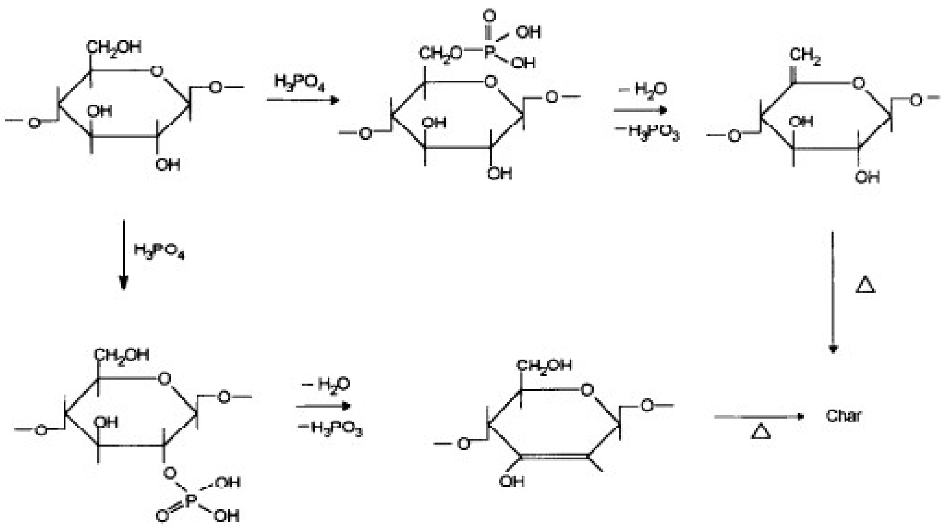

Figure 2.2. Degradation of cellulose catalyzed by phosphoric acid.[114] Reprinted with permission from Kandola, B. K.; Horrocks, A. R. Complex char formation in flame-retarded fibre-intumescent combinations: Thermal analytical studies. *Polym. Degrad. Stab.* **1996**, *54*, 289.

Although providing highly effective protection of cotton and ramie, Proban CC requires complex processing in an ammonia chamber and Pyrovatex CP produces harmful formaldehyde as a byproduct. LbL assembly in aqueous suspensions may provide an environmentally benign alternative in which flame retardant coatings can be applied to fabric. The first demonstration of flame retardant multilayer nanocoatings on fabric made use of polyethylenimine and clay to promote the charring of cotton fabric.[116] Since then, a variety of phosphorus-based layer-by-layer approaches have been used on textiles. Li and co-workers deposited poly(sodium phosphate) with poly(allylamine) to produce a film on cotton fabric that extinguished fire during vertical flame testing (VFT).[117] A film composed of renewable polyelectrolytes, phytic acid and chitosan, extinguished flame on cotton during VFT as well as reduced the total heat release of the fabric by 76% during

microcombustion calorimetry.[64] These two coating systems were elegant flame retardant treatments for cellulosic textiles, and most subsequent studies involving phosphorus coatings have been quite similar, often showing no further improvement in flame retardancy. A recent review by Malucelli lists off dozens of studies whose only novelty is the simple replacement of the polycation or polyanion.[118] Although there is a considerable amount of effort focused on reducing the number of processing steps for these FR recipes,[72,103,111,119] assembling coatings one layer at a time remains a considerable hurdle toward commercialization.

2.1.2 Gas Barrier of Layer-by-Layer Thin Films

Polymers are a common material for food packaging due to their low-cost, flexibility, and thermal and chemical stability.[120] Their impermeability to oxygen and water increases the shelf-life and freshness of their contents. This impermeability is also highly desirable for polymers used for pressurized system and flexible electronics. The moisture and oxygen transmission rate requirements for these applications are shown in Figure 2.3.[121] The most prevalent high barrier for food packaging is metallized plastic, prepared by physical vapor deposition, a highly scalable roll-to-roll process that has been widely used since the 1970's.[122] Metal deposition is done in high vacuum as a metal target is heated to vaporize. As the vaporized metal atoms assemble on the substrate, a gas-impermeable film is formed. Although this technology is mature, it is non-recyclable, non-microwavable and opaque. Thin oxide films provide gas barrier, while being microwavable and often transparent, but they have a tendency to crack when flexed and require high vacuum processing.[123]

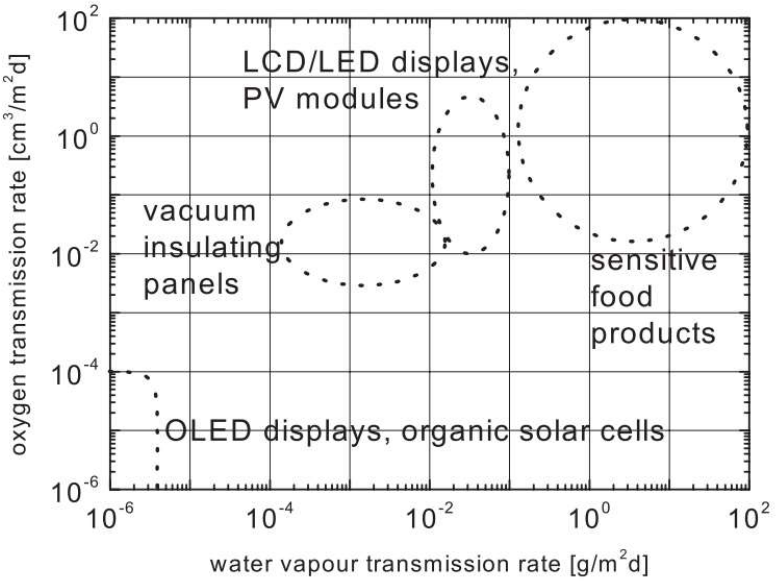

Figure 2.3. Barrier requirements for different technologies.[121] Reprinted with permission from Charton, C.; Schiller, N.; Fahland, M.; Holländer, A.; Wedel, A.; Noller, K., Development of high barrier films on flexible polymer substrates. *Thin Solid Films* **2006**, *502*, 99.

The first LbL film for oxygen barrier was fabricated by Kotov and coworkers in 1998, when 50 bilayers of polydiallyldimethylammonium chloride (PDDA) and montmorillonite clay (MMT) were deposited on PET. The oxygen transmission rate was reduced from 80 to 10 $cm^3/(m^2 \cdot day \cdot atm)$. Grunlan and colleagues later fabricated similar LbL films consisting of polycations and MMT on PET with orders of magnitude improvement in oxygen barrier.[78,94,124-127] In one study, a polyethylene (PEI)/MMT film of only 20 bilayers reduced the oxygen transmission rate of PET to 0.078 $cm^3/(m^2 \cdot day \cdot atm)$.[94] By precisely tuning the spacing between clay layers, Grunlan et al. reduced the oxygen transmission rate of PET to a level undetectable by commercial testing equipment (< 0.005 $cm^3/(m^2 \cdot day \cdot atm)$).[78] Polymer-clay coatings constructed by LbL

assembly have especially high clay-loading (>50 wt%) but maintain fairly good transparency due to their highly aligned "nanobrick wall" structure. The barrier of these coatings rely on oxygen molecules taking a "tortuous path" around the impermeable clay platelets as they move through the barrier coating. The tortuous path model was first described by Nielsen in 1967, modelling a gas molecule as diffusing through a polymer matrix perpendicular to the normal direction of the film, passing through areas between impermeable particles, shown schematically in Figure 2.4.[128]

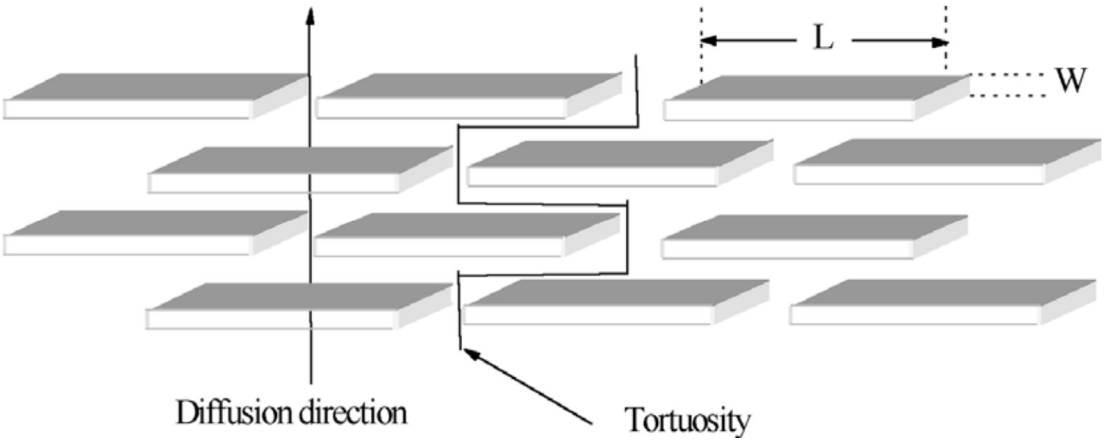

Figure 2.4. Schematic of the Nielsen model of gas diffusion through a nanocomposite.[128] Reprinted with permission from Nielsen, L. E., Models for the permeability of filled polymer systems. *J. Macromol. Sci. A* **1967**, *1*, 929.

All-polymer LbL films have also demonstrated excellent gas barrier. Yang and cowokers prepared a film consisting of PEI and polyacrylic acid (PAA) that reduced the oxygen transmission rate of PET to < 0.005 $cm^3/(m^2 \cdot day \cdot atm)$ with only 8 bilayers.[24] These films also have excellent H_2/CO_2 selectivity (190:1) and reasonable flux, making them an excellent option for gas separation.[129] Due to the strong electrostatic interactions

of the polyelectrolytes, the free volume of polyelectrolyte multilayers tend to be lower than that of typical polymers, giving them very low gas permeability. The relationship between permeability and free volume can be described by Equation 2.1:

$$P = A \exp\left(-\frac{B}{f}\right) \qquad (2.1)$$

where A and B are constants depending on the permeant molecule and f is the fractional free volume described by the fraction of the polymer matrix unoccupied by polymer chains.

2.2 Polyelectrolyte Complexes

Polyanions and polycations can associate in water to form polyelectrolyte complexes (PECs) that provide an alternative to LbL assembly in fabricating functional thin films.[130] Just like the interactions governing LbL assembly, PECs arise from the Columbic attraction of oppositely-charged polymer chains and is driven by a positive change in entropy. As the polyions associate, small counterions (associated with polymers) are liberated into solution, as shown in Figure 2.5.[131] PEC formation is typically endothermic, as the polymers must undergo conformational changes to associate with each other, resulting in steric energy contributions not present in their association of small counterions. PECs can also be formed from the association of polyelectrolytes with charged particles, such as colloidal silica.

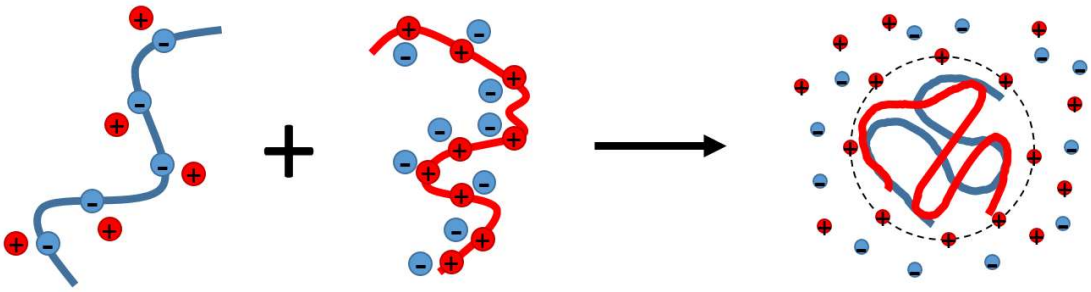

Figure 2.5. A polycation and polyanion associate to form a polyelectrolyte complex.

The stability of a polyelectrolyte complex in water arises from its structure. Water-soluble PECs are often formed when oppositely charged polyions are weakly associated. Loosely-associated polyelectrolytes sometimes form less stable morphologies and become complex coacervates.[132,133] The solution mixture phase-separates into polymer-rich and polymer-poor phases. This coacervate is often transient, as the polymer rich phase collapses over time to exclude solvent and becomes a single aggregate.[132] Colloidal stable PECs are formed when aggregation of strongly associated polyelectrolytes halts at a colloidal level (radii of 10-100 nm), and usually occur in fairly dilute solutions.[134] An electrical charge on the particles prevents further aggregation due to electrostatic repulsion. Flocculation occurs when strongly associated polyelectrolytes form larger networks, resulting in macroscopic sedimentation.[131,133,135-137]

The stability of PECs in solution is very relevant to their application as flocculants. The speed of flocculation, as well as particle cohesion and size, is important in paper-making.[132,137-139] Polyelectrolytes can also be used in wastewater treatment in order to remove unwanted suspended particles.[137] These complexes have also proven to be effective in membrane applications (pervaporation and nanofiltration).[140-142] In this case,

PECs are designed to be highly hydrophilic, but at the same time insoluble in the medium they come in contact with. Controlling the characteristics of PECs is of great interest to researchers in the field of drug delivery. PECs can solubilize and protect drugs from hostile environments as well as respond to environmental stimuli.[143-148] When the complex undergoes a change in ionic strength and pH, the structure to selectively release its contents.[148,149]

The controlled self-assembly of polyelectrolyte complexes is a valuable scientific and engineering topic. These complexes are built in aqueous and ambient conditions and can be applied to a range of applications. PECs are insoluble in organic solvents, have no glass transitions, and have tunable surface charge.[141] Many of the inter-polymer interactions that take place in PECs are similar to those in polyelectrolyte multilayers.[150] PECs can be used in the fabrication of thin polymer films using far fewer processing steps than LbL assembly by controlling the interaction of the oppositely charged components.

2.2.1 Controlling Polyelectrolyte Complex Formation

Solution conditions such as pH, ionic strength, and composition greatly affect the complexation behavior of PECs. Intrinsic properties of the polyelectrolytes, such as molecular weight and degree of substitution, can also provide a handle for controlling polymer interactions. One way to alter PEC structure and stability is by changing the ratio of the two component polyelectrolytes. Many PEC experiments consist of the titration of a solution of a polyion with an oppositely charged polyelectrolyte and observing the characteristics of the resulting complexes.[131] Typically, complexes become larger and less stable as the polyelectrolytes reach a 1:1 monomer stoichiometry. This relationship

between colloidal stability and mixing ratio is observed in numerous studies.[132-134,136] As the overall electrical charge of the complexes decrease, there is less electrostatic repulsion between them and aggregation, followed by flocculation, occurs. Aggregation is prevented by an excess binding of the major component. Dautzenberg and coworkers studied this effect as shown in Figure 2.6.[136] In suspensions of various ionic strength, the radius of gyration (R_g) as well as the molecular weight (M_w) of PECs increases dramatically as the molar ratio of cationic polydiallyldimethylammonium chloride (PDDA) and anionic sodium poly(styrene sulfonate) [PSS] approaches 1.0.

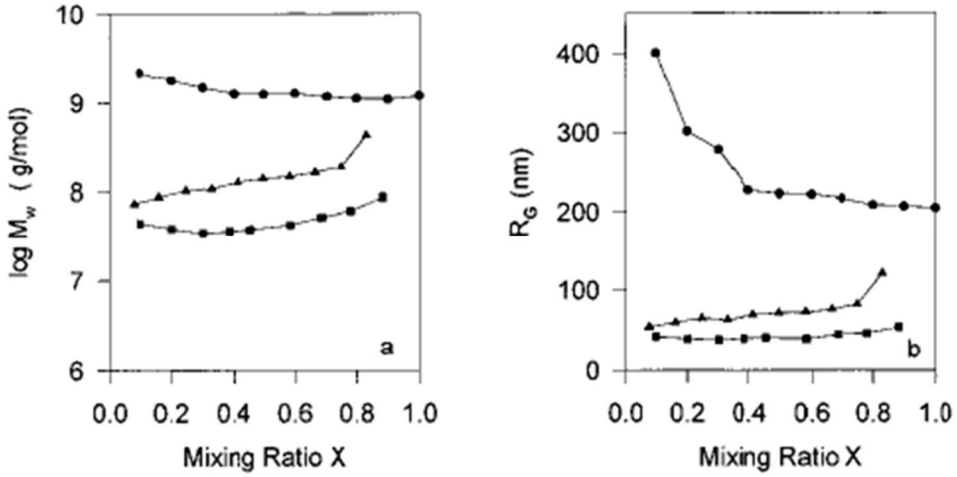

Figure 2.6. Particle mass (M_w) and size (R_g) of PSS/PDDA complexes as a function of molar ratio at varying ionic strengths: pure water (circles), I = 1 x 10^{-2} M (squares), I = 1 x 10^{-1} M (triangles).[136] Reprinted with permission from Dautzenberg, H., Polyelectrolyte complex formation in highly aggregating systems. 1. effect of salt: Polyelectrolyte complex formation in the presence of NaCl. *Macromolecules* **1997,** *9297*, 7810.

Ionic strength has a large influence on the formation and stability of polyelectrolyte complexes and is often the chief variable in studies. The addition of salt to a PEC-

containing solution often causes aggregation until coacervation and flocculation occurs.[151] When the concentration of salt is much higher, PECs can be stabilized again.[133] Figure 7 illustrates this behavior by measuring the concentration of polycationic poly(*N*-ethyl-4-vinylpyridinium) bromide (QPVP) in solution as a function of sodium chloride concentration as the polycation complexes with poly(methyl acrylate) [PMA].[152] In region I, the QPVP/PMA complex is solubilized in aqueous solution. As the concentration of salt and ionic strength increases in region II, the polyelectrolytes aggregate and phase separation is observed. The author claims this transition is reversible, but it is difficult to understand how ascertaining this would be possible. Increasing ionic strength is simple with the addition of salt, but the study does not present a procedure to decrease solution ionic strength, while also maintaining polyelectrolyte concentration. The aggregation likely occurs due to the salt ions screening the charged sphere of the complexes, reducing the Coloumbic PEC-PEC repulsion. The complexes coalesce and precipitate as larger particles.[131]

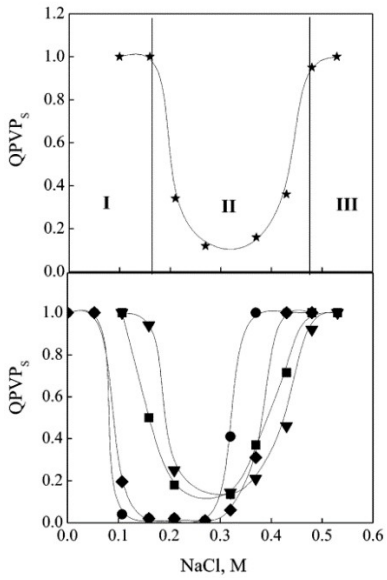

Figure 2.7. Fraction of QPVP and QPVPS, remaining in supernatants of QPVP/PMAA mixtures for PMAA with different molecular weights [350K (top panel); 7K (circles), 25K (rhombuses), 72K (squares), and 150K (triangles) (bottom panel)] as a function of salt concentration.[152] Reprinted with permission from Izumrudov, V.; Kharlampieva, E.; Sukhishvili, S. A., Salt-Induced multilayer growth: correlation with phase separation in solution. *Macromolecules* **2004**, *37*, 8400.

At higher ionic strength (region III in Figure 2.7), the polyelectrolytes are solubilized. Sukhisvili et al. observed the polyelectrolytes being completely soluble in solution, however, another study shows coacervation as an intermediate step to a stable solution.[133,150,153] Wang et al. observed PEC undergoing a transition from solid aggregates to complex coacervates all the way to dissociated polyelectrolytes.[133] This return to solubility is due to the screening individual polymer chain charges by high salt concentration.[131,133,152]

The charge density of associating polyelectrolytes often influences structure and stability of the resulting PECs. Dautzenberg et al. investigated how polycations of varying charge affect the formation of PECs when paired with PSS.[154] The results were

interesting, as PDDA-acetamide copolymers of greater charge density formed PECs of greater colloidal stability in pure water. The addition of salt affected PECs containing highly charged polycations much less than it did for PECs containing lightly-charged polycations. When 0.05 M sodium chloride was added, PECs containing lightly-charged polycations were consumed and the polyelectrolytes dissociated. This is due to the high mismatch in charges between the polyion pairs, making the highly charged PECs sensitive to changes in ionic strength.

Vanerek et al. investigated the PECs formed by cationic-functionalized polyacrylamide (cPAM) of various degrees of quaternary substitution.[132] The experiment showed that the charge density of the polycation had no observable effect on the relative proportion of PECs forming complex coacervates versus stable colloidal particles. Non-ionic PAM was unable to form a coacervate complex with sulfonated kraft lignin, which suggests electrostatic attraction is necessary for the formation of PECs. The charge density of the polycationic cPAM had a substantial influence on the stoichiometry of the PECs formed. Unsurprisingly, a higher charge density on cPAM results in a higher sulfonate kraft lignin composition in the insoluble PECs. The degree of ionization's effect on PEC stability seems to be an issue of debate. Vanerek's study suggests that it has no effect on PEC stability,[132] in contrast to Dautzenberg's study.[154] It is likely that degree of ionization does affect the colloidal stability of PECs. Vanerek's study did not evaluate whether this non-effect persists in varying ionic strengths (like Dautzenberg did). The Vanerek study also uses sulfonate kraft lignin which are large molecules, but are not strictly polymers.

Changing the pH of the polyelectrolyte solutions greatly affects the degree of ionization of weak polyelectrolytes. This parameter is more manageable than changing the intrinsic character of the polyelectrolyte being used. Cundall et al. showed the stoichiometry of polyions could be altered with changes in solution pH.[151] The polycation/polyanion stoichiometric ratio could be increased by higher pH corresponding to a deionization of a cationic polybase or ionization of a polyacid. Changes in pH can also influence the zeta potential of PEC particles, as shown in Figure 2.8. In this study, low pH allows the chitosan to be highly charged, forming positively-charged PECs with pectin. As the pH approaches 6, this net charge is lowered and the particles cannot maintain mutual electrostatic repulsion and flocculation occurs. At much higher pH, pectin is highly charged and chitosan is almost entirely neutral. The authors speculate the zeta potentials ≥ pH 8 may be from unassociated pectin rather than PECs.[155]

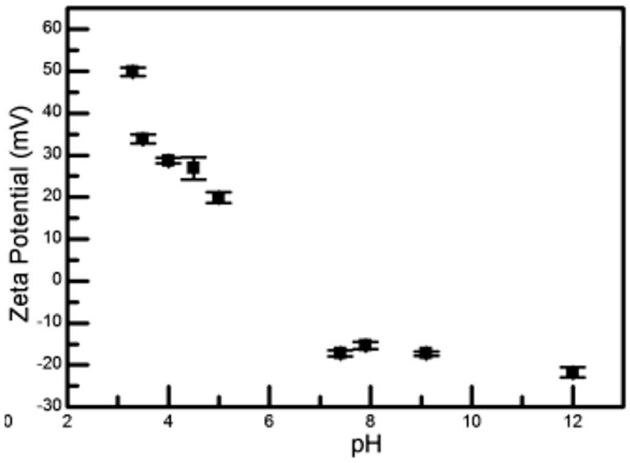

Figure 2.8. Zeta potential of PECs of chitosan/pectin as a function of solution pH.[155] Reprinted with permission from Birch, N. P.; Schiffman, J. D., Characterization of self-assembled polyelectrolyte complex nanoparticles formed from chitosan and pectin. *Langmuir* **2014**, *30*, 3441.

The influence of pH on PEC size plays an important role in responsive drug delivery systems.[156-158] PECs for oral delivery must be robust and maintain structure in a wide range of pH, as well as maintain stability in the human body until it reaches the site of interest. Lin et al. demonstrated the utility of pH-dependent swelling of PEC gel microspheres composed of chitosan, dextran sulfate and sodium tripolyphosphate (all biologically-compatible ingredients).[157] These complexes were used to encapsulate ibuprofen. The rate of ibruprofen release was greatly affected by solution pH. Using UV spectrophotometry, the researchers determined that the release rate increases with higher pH in the range pH 1.4 to 9. Most importantly, the drug release is very slow at pH 1.4, an acidity corresponding to the acidity of the stomach, and much faster at more neutral pH 6.8, corresponding to the acidity of the small intestine (where the drug could be absorbed). Adjusting for the relative time durations when the drug would likely reside in the organs, only 7% of ibuprofen is released after 3 hours in simulated gastric fluid and 94% of the ibuprofen is released after 6 hours in simulated intestinal fluid. The pH-responsive release was due to the ability of the PECs to swell in size at higher pH as the degree of ionization of the contained chitosan is reduced.

The formation of PECs can also be influenced by switching the order of addition of the polycations and polyanion. Dautzenberg measured PECs of greater density when PDDA was added to PSS rather than the other way around (a difference of 0.2 g/mL at any given mixing ratio).[136] Particle size and stoichiometry of PECs can also be altered by the order of addition.[155,159] Ball et al. investigated the change in zeta potential of PECs over time after mixing, as shown in Figure 2.9.[135] The zeta potential of PEC particles

change after a long polycation (poly(allylamine hydrochloride) [PAH]) and anionic oligomer (poly(sodium phosphate) [PSP]) are mixed. The particles are positively charged when the solutions are initially mixed. As time goes on, the charges neutralize, approaching a slightly negative zeta potential. When the starting solution is PSP, the particles grow faster and neutralize from a more negative zeta potential. The particles approach equilibrium from a more positive zeta potential when the starting solution is PAH.

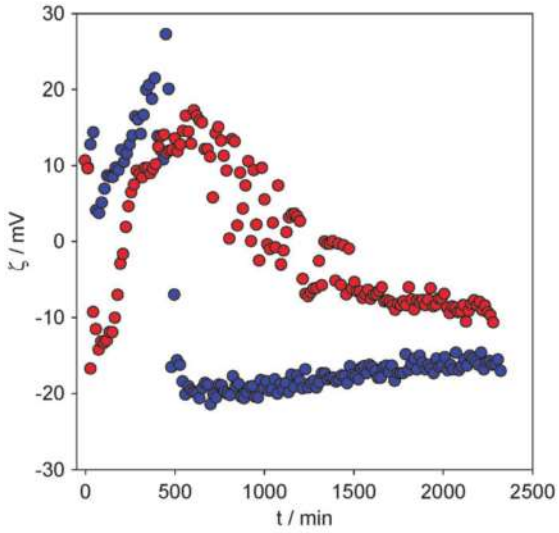

Figure 2.9. Zeta potential of PAH-PSP complexes when solution of PAH is added to a solution of PSP (blue) or when PSP is added to PAH (red).[135] Reprinted with permission from Cini, N.; Tulun, T.; Blanck, C.; Toniazzo, V.; Ruch, D.; Decher, G.; Ball, V., Slow complexation dynamics between linear short polyphosphates and polyallylamines: analogies with "layer-by-layer" deposits. *PCCP* **2012**, *14*, 3048.

Most polyelectrolyte complex mixtures are created by titrating one polyion with the other. This likely causes localized high concentration of the titrant polyelectrolyte, even while stirring or using some other means of agitation. This could affect the

complexation of the polyelectrolytes and vary complexation from the first addition drop to the last. It could also be a major contributor to the high polydispersity of PECs as measured by static light scattering.[136] One study uses jet mixing to make a fast homogenous mixture and control PEC size.[160] Future studies could incorporate jet mixing to observe if any differences occur and assess the benefits of applying this technology to paper-making.

2.2.2 Polyelectrolyte Complexes as Solid Materials

Whereas LbL assembly requires a number of processing steps to fabricate films of thickness greater than 1 μm, polyelectrolyte complexes provide a simple avenue for incorporating similar polymer interactions into materials with macroscopic dimensions. Ionic strength is a key component of PEC processing, as high salt concentration is used to suspend and plasticize the material and low salt concentration water is used to solidify and compact it. Schlenoff and coworkers termed the salt-dependent mechanical properties of PECs as "saloplasticity" and exploited it to successfully extrude PDDA/PSS complexes as fibers, tapes and rods.[161,162] PAH/PAA complexes were compacted into rods using ultracentrifugation as well. By varying the sodium chloride doping of the PECs, they could target specific moduli and microstructure.[163]

PEC nanocomposites have also become possible. By incorporating iron oxide nanoparticles in one such PEC, Schlenoff and coworkers afforded an extruded nanocomposite that could be heated remotely by radio frequency.[164] The use of PECs allows for a sol-gel process that can be processed at low temperatures and ambient conditions, removing the possibility of damaging the contained nanoparticles. Dispersing

nanoparticles in PECs has also been used for gas barrier. Gao and coworkers dispersed graphene oxide in carboxymethyl cellulose (CMCNa) and PDDA complexes. Complexes were prepared by simple sedimentation, then dispersion, followed by solution casting as shown in Figure 2.10.[165] 1.5 wt% of graphene oxide reduced the gas permeability of these composites by as much as 4 orders of magnitude.

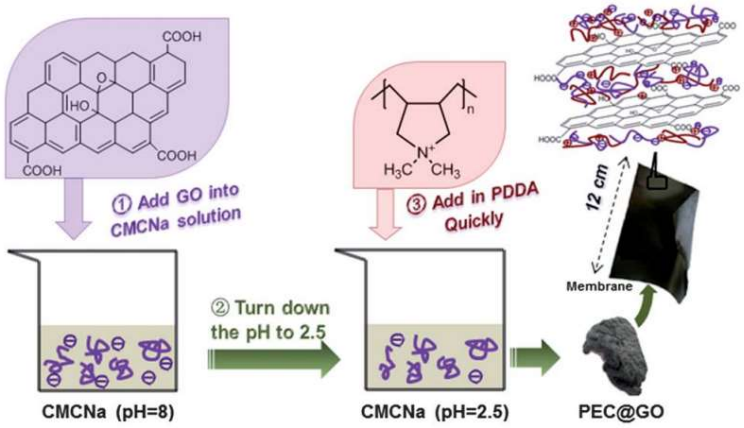

Figure 2.10. Schematic preparation of graphene oxide-loaded PEC membranes.[165] Reprinted with permission from Zhao, Q.; An, Q.-F.; Liu, T.; Chen, J.-T.; Chen, F.; Lee, K.-R.; Gao, C.-J., Bio-inspired polyelectrolyte complex/graphene oxide nanocomposite membranes with enhanced tensile strength and ultra-low gas permeability. *Polym. Chem.* **2013**, *4*, 4298.

In the interest of reducing processing time and steps, attention has been focused on preparing thin films from PECs that are similar to existing coatings prepared by LbL assembly. The ease of preparing PEC films may be more amenable to industry. Ball and colleagues prepared thin polyelectrolyte films from the simple sedimentation of PECs.[166] PECs prepared from weak polyelectrolytes were able to coalesce in a uniform film, but those from strong polyelectrolytes formed an inconsistent snow-flake structure. Although this process requires very few processing steps, it requires time to allow the complex to

flocculate from suspension and film thickness is difficult to control. In a similar process, Cain and coworkers used the sedimentation of polyethylenimine and poly(sodium phosphate) to coat cotton fibers with a flame retardant thin film.[167] The weight gain coating could be controlled by the time in which the slow flocculation is allowed to occur. Using this process, films prepared on cotton could self-extinguish during vertical flame testing. Schlenoff and coworkers prepared PDDA/PSS films from the spin-coating of polyelectrolyte complex coacervates.[168] By affecting the concentration of potassium bromide in the coacervate, they controlled the viscosity of the suspension suitable for spin-coating. The coating was then solidified by dipping in water to remove the plasticizing salt to afford a transparent free-standing PDDA/PSS film. These 15 μm thick films would have required hundreds of bilayers to achieve using layer-by-layer deposition.

The following chapters demonstrate PEC systems capable of flame retarding various fabrics and imparting high gas barrier to PET substrates. It is believed that properly engineered PEC-based coatings can provide and industrially viable alternative to LbL assembly with little sacrifice in properties.

CHAPTER III

WATER-SOLUBLE POLYELECTROLYTE COMPLEXES THAT EXTINGUISH FIRE ON COTTON FABRIC WHEN DEPOSITED AS PH-CURED NANOCOATING*

3.1 Introduction

The layer-by-layer (LbL) process requires multiple cycles of immersion to deposit enough coating to achieve appreciable flame suppression. Deposition of oppositely-charged polyelectrolytes from a single solution provides an opportunity to achieve effective flame retardant (FR) behavior in a single coating step. It is well-known that oppositely-charged polyelectrolytes can associate to form polyelectrolyte complexes (PECs) in solution.[150] Complex solubility is largely dependent on concentration, ionic strength, and in the case of weak polyelectrolytes, solution pH.[169] Thin films have recently been deposited from sedimentation of PECs.[166] More recently, the flocculation of poly(sodium phosphate) with polyethyleneimine was used to deposit this flame retardant combination onto cotton fabric.[167] The time in which the cotton was submerged in the phase-separating suspension dictated the amount of FR material deposited on the fabric. Unfortunately, this unstable PEC suspension could only be used once and for a limited amount of time after preparation.

*Reprinted with permission from Haile, M.; Fincher, C.; Fomete, S.; Grunlan, J. C. Water-soluble polyelectrolyte complexes that extinguish fire on cotton fabric when deposited as pH-cured nanocoating. *Polym. Degrad. Stab.* **2015**, 60-64. Copyright 2015 Elsevier.

In this chapter, a stable polyelectrolyte complex suspension is reported that is capable of imparting flame retardant behavior to cotton fabric in a single deposition step (now known as a stable OnePot coating system). A stable water-soluble PEC (WPEC) suspension can be made using weak polyelectrolytes, which allows for multiple uses of the suspension over time and a prolonged shelf life, in contrast to the established sedimentation processes.[166,167] Using the pH-dependent stability of polyelectrolyte complexation, the deposited polyelectrolytes are rendered insoluble after the initial coating. Soaking cotton fabric for 30 s in OnePot solution yields a coating that is 23 wt%, reduces cotton heat release by 88% and self-extinguishes during vertical flame testing. This OnePot nanocoating system is an effective treatment that imparts flame resistance to fabric quickly and easily.

3.2 Experimental

3.2.1 Materials

Bleached, desized cotton print cloth with an approximate weight of 100 g m^{-2} (3 oz yd^{-2}) was purchased from Testfabrics, Inc (West Pittston, PA). Poly(phosphate sodium salt) [PSP] (crystalline, +200 mesh, 96%) and branched polyethylenimine (molecular weight, Mw ~ 25,000 g mol^{-1}) [PEI], purchased from Sigma-Aldrich (Milwaukee, WI), were used as received. The number average molecular weight of PSP was determined to be 3450 g mol^{-1} by end group titration done according to a literature procedure.[170] Citric acid monohydrate and sodium citrate dihydrate were purchased from Macron Fine Chemicals (Center Valley, PA) and were used to make buffer solutions. 1 M NaOH (made from sodium hydroxide pellets, anhydrous; reagent grade, ≥ 98%) and 5 M HCl (made

from hydrochloric acid; ACS reagent, 37%), purchased from Sigma-Aldrich, were used to adjust the pH of the deposition and treatment solutions. All individual solutions were prepared with 18.2 MΩ·cm deionized water.

3.2.2 Preparation and Deposition of Stable OnePot Solution

Previous work with a PEI/PSP OnePot solution was done at pH 7,[167] where the degree of cationic charge of PEI was substantial enough to cause strong electrostatic interactions with negatively charged PSP. The result was agglomeration driven by entropy, as sodium counterions and solvating water molecules were excluded from the complexes.[171] Further investigation of the PEI/PSP system showed that polyelectrolytes are stable together at pH ≥ 9. The solution pH is considerably higher than the polymer's pKa of 8.25, the amine groups of PEI are largely unprotonated and the polyelectrolyte has low positive charge.[172] This situation causes the electrostatic interaction between PEI and the polyphosphate to weaken, allowing stable WPECs to form. In order to achieve high weight gain with a single dip, this OnePot solution contained high concentrations of the oppositely charged polyelectrolytes. An equal weight of 10% PEI solution (adjusted to pH 9) was poured into a 20% PSP solution to produce a transparent homogenous 5% PEI/10% PSP solution (i.e., the stable OnePot solution). To minimize base-catalyzed hydrolysis of the PSP, acid was added to lower the solution pH to 9. The suspension was completely transparent and homogeneous at this pH. The average particle size was measured to be 22 nm after 1 h and 23 nm after 48 h, suggesting this was a stable suspension. Cotton was dipped in the OnePot solution for 30 s immediately after preparation. Fabrics were then squeezed and hung to dry in a 70℃ oven for 1 h prior to treatment and testing. Buffer

solutions at pH 2, 3, 4, 5, and 6 were prepared using 50 mM citric acid/sodium citrate. NaCl was added to each buffer solution to achieve an ionic strength of 300 mM. Coated fabric was treated by soaking in 1 L of the appropriate buffer solution for 5 min, then rinsed vigorously in deionized water to remove citrate and excess polymer. The fabric was then dried at 70 °C for 2 h prior to testing.

3.2.3 Non-Thermal Characterization

Coated and uncoated cotton substrates were mounted on aluminum stubs and sputter coated with 4 nm of platinum/palladium (Pt/Pd) alloy in preparation for imaging performed with a field-emission scanning electron microscope (FESEM, Model JSM-7500F, JEOL; Tokyo, Japan). XPS measurements were conducted using a PHI Quantera XPS, using a focused monochromatic Al Kα X-ray (1486.7 eV) source (using 50W, 15kV and a 200μm diameter). The vacuum pressure during analysis was 5×10^{-8} torr. XPS survey scan spectra in the 0-1100 eV binding energy range were recorded in 0.5eV steps, with a pass energy of 140.0 eV. The pKa of PEI was determined to be 8.25 using potentiometric titration, with 0.05 M NaOH standard. pH was measured with a IntelliCAL pH electrode (Hach, Loveland,CO). Average particle size of water soluble polyelectrolyte complexes was determined by analysis of a diluted OnePot solution using a Brookhaven ZetaPALS instrument (Brookhaven Instruments Corp., Holtsville, NY).

3.2.4 Thermal Stability and Flammability of Fabric

Thermal stability of uncoated and OnePot coated cotton fabric (approximately 30 mg) was evaluated in triplicate using a Q-50 thermogravimetric analyzer (TA Instruments,

New Castle, DE), under a controlled heating ramp of 20℃ min^{-1}, from ambient temperature up to 600℃, with a sample purge flow of 60 mL s^{-1} air and a balance purge flow of 40 mL s^{-1} nitrogen. Fabric samples were cut into 3 x 12 in. strips that were vertically hung in a metal clamp within a model VC-2 vertical flame cabinet (Govmark, Farmingdale, NY). Samples were exposed to the flame from a Bunsen burner for 12 sec to measure time after-flame and after-glow times, in accordance with ASTM D6413-08. All fabric was run in triplicate for microscale combustion calorimetry at a 1℃ sec^{-1} heating rate, from 150-550℃, using method A of ASTM D7309 (pyrolysis under nitrogen) at the University of Dayton Research Institute (Dayton, OH).

3.3 Results and Discussion

The PEI/PSP coating was deposited by dipping cotton in the OnePot solution for 30 s, resulting in an average weight gain of 23%. Cotton coated with this procedure, with no further treatment or rinsing, will be designated as “untreated coating” throughout the rest of the text. It was initially believed that the polyelectrolyte was adsorbed purely through wet-pickup. In this case, the composition of the coating on the fabric would be identical to the composition of the OnePot solution, but XPS revealed that the atomic composition in the coating was different from that in solution. This disparity can be explained conceptually as water-soluble polyelectrolyte complex particles adsorbing onto the cotton fiber from the stable solution, similar to what is observed in LbL deposition.[1,173] The WPECs consist of weakly associated polyphosphate and PEI, with small counterions such as sodium excluded. As the phosphorus-containing complexes actively adsorb onto cotton through electrostatic and hydrogen bonding, sodium cations

(as well as non-associated polyelectrolytes) are present in the coating due to being dissolved in the water left on the fabric after squeezing. This results in the high P/Na ratio observed by XPS, summarized in Table 3.1. The low P/N ratio is likely due to the cotton surface having stronger association with free PEI chains, rather than PSP, or it could be reflective of the stoichiometric ratio of the polyelectrolytes contained in the WPEC particles.

Table 3.1. Atomic composition of OnePot solution and coated fabric.

	Solution	**Coated Fabric**
Atomic ratio P/Na	1	3.13
Atomic ratio P/N	0.84	0.38

As expected, most of the coating was removed when the cotton fabric was rinsed and dried. The weight gain after rinsing fell from 23 to 6.3%. The same weak intermolecular forces that allowed for the complexes to remain stable in water were also present in the coating on fabric, allowing the polyelectrolytes to be redispersed in water. Realizing that these polyelectrolytes sediment at lower pH, the coated fabric was treated in citric acid/sodium citrate buffer at varying pH in an effort to "cure" the coating (to resist damage during rinsing). Coated fabric was treated by dipping in buffer solutions with pH values from 2 to 6. As the pH of the buffer treatment was lowered, more coating weight remained on the treated cotton after rinsing. Similar to what was observed in solution, the PEI/PSP PEC-based coating is insoluble in water under pH 9. Below this pH, the degree of protonation of the PEI chains is sufficiently high to electrostatically bind with PSP and

the negatively-charged cotton surface, generating an insoluble gel. The resulting coating is resistant to vigorous rinsing and reaches weight gains similar to those that would be reached only with many dipping cycles (> 20) using LbL assembly. All coating and treatment processes maintained the whiteness and hand of the uncoated cotton. A schematic of the coating procedure is shown in Figure 3.1.

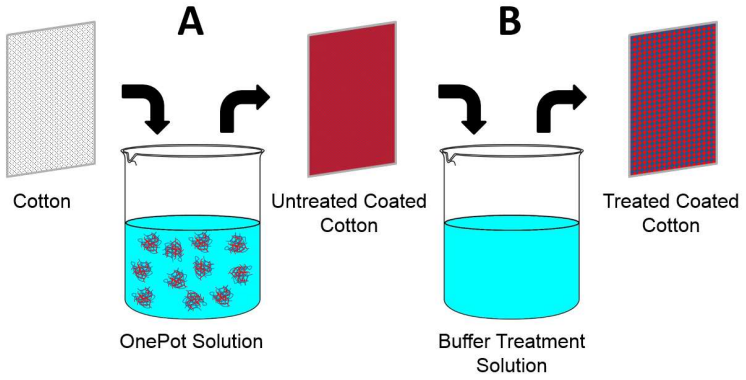

Figure 3.1. General procedure for the OnePot flame retardant coating of cotton fabric. The untreated cotton is first dipped in the OnePot solution to produce the untreated coated fabric (A), which is subsequently submerged in the appropriate pH buffer treatment solution for 5 min, (followed by rinsing and drying) to make the treated coated fabric (B).

Studies have reported that the composition of LbL films can be modified by changing the pH of the polyelectrolyte solutions.[64,174] Altering the pH allows for control over the degree of ionization of weak polyelectrolytes. It was hypothesized that similar changes in composition could be tailored by exposing the OnePot coating to changes in pH. Compositional analysis with XPS indicated that phosphorus content in the deposited films increases when the coated fabric is treated with decreasing buffer solution pH, as shown in Figure 3.2. As observed in multilayer films, weak polycations such as PEI

approach a maximum degree of ionization when dissolved in a solution pH much lower than their isoelectric point.[92,174] When a lower pH treatment solution is used, a larger portion of the phosphates on PSP are protonated and the negative charge is reduced. The highly charged PEI in the film is then at a greater stoichiometric excess due to this diminished charge it needs to balance. This excess PEI is removed in the rinsing step, which results in a higher P/N ratio in the coating with decreasing pH buffer treatment. Treatment and subsequent rinsing appears to remove sodium and chlorine, as their signals are no longer present in XPS measurements.

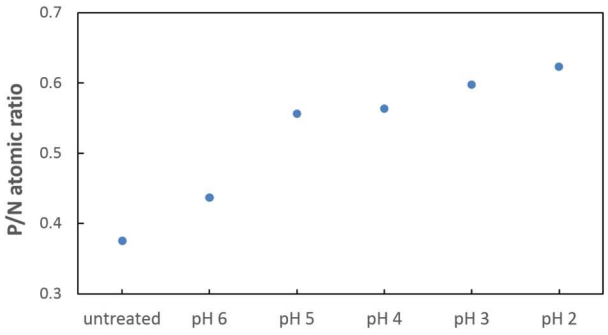

Figure 3.2. Phosphorus/nitrogen ratios of PEI/PSP OnePot coatings on cotton fabric, treated with varying buffer solution pH.

Uncoated fabric, along with untreated and treated PEI/PSP coated cotton, was heated from ambient temperature up to 600℃ in oxidizing conditions using a thermogravimetric analyzer (TGA) at a heating rate of 20℃ min^{-1}, as shown in Figure 3.3a. All coated fabric exhibited earlier onset degradation temperatures compared to the uncoated cotton (321 °C), indicative of a thermally-triggered mechanism interrupting the combustion cycle of cellulose. The formation of a swollen insulating layer retards flame

when it occurs earlier than the onset of cellulose degradation. At 600℃, the uncoated fabric is completely consumed, but all coated samples retain residue of greater weight than the coating. These results suggest that the coating converted a portion of the cellulose into a less combustible material through an intumescent mechanism.[67,175]

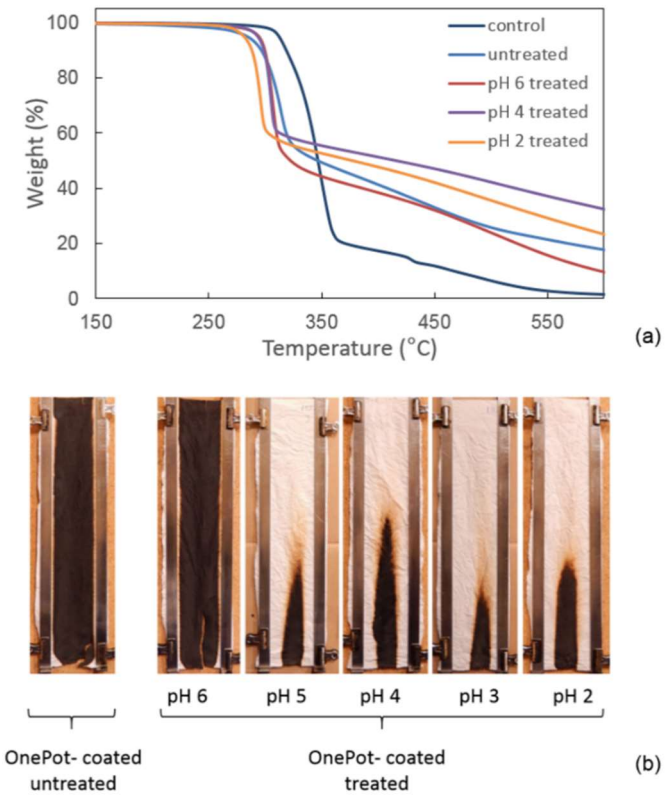

Figure 3.3. (a) Representative weight loss as a function of temperature for uncoated (control) fabric, and OnePot coated cotton fabric measured in an oxidizing atmosphere. (b) Images of treated and untreated fabric after vertical flame testing.

During vertical flame testing (VFT), uncoated cotton was ignited and engulfed in flame for an average of 19 s, at which point it was completely consumed. Ashes along the metal holder edges radiated with afterglow for an average of 20 s. No coated fabric

exhibited afterglow when the flame was removed. Untreated coated fabric had the highest weight gain (23%) without further rinsing, but the flame front travelled up the length of the fabric, leaving a residue of 39.5 ± 0.3 wt%. Buffer treatment of the coating improved performance, despite considerably decreasing the coating weight gain. Treatment with pH 6 buffer yielded the lowest weight gain and showed a moderate increase in char residue (44.1 ± 1.8 wt%). Coatings treated with ≤ pH 5 buffer completely stopped flame propagation, showing remarkable self-extinguishing behavior (most of the cotton was untouched). The residues of the coated fabric following VFT are shown in Figure 3.3b.

Figure 3.4 shows SEM micrographs of the coated fabric that reveal a radial polyelectrolyte coating around individual fibers. Additionally, micrographs of afterburn residues show that the structure and shape of the coated fibers were remarkably well-preserved. The bubbles observed in afterburn images of pH 2 and 4 treated coatings are evidence of an intumescent FR mechanism. The charred nanocoatings of the treated fabric have varying levels of bubbling, with pH 2 treated char containing the greatest amount. This intumescent response is the source of the self-extinguishing behavior found with these coated and buffer-treated samples. This mechanism is not visibly present in the char of the untreated coated fabric, underscoring the reason for its poor VFT performance.

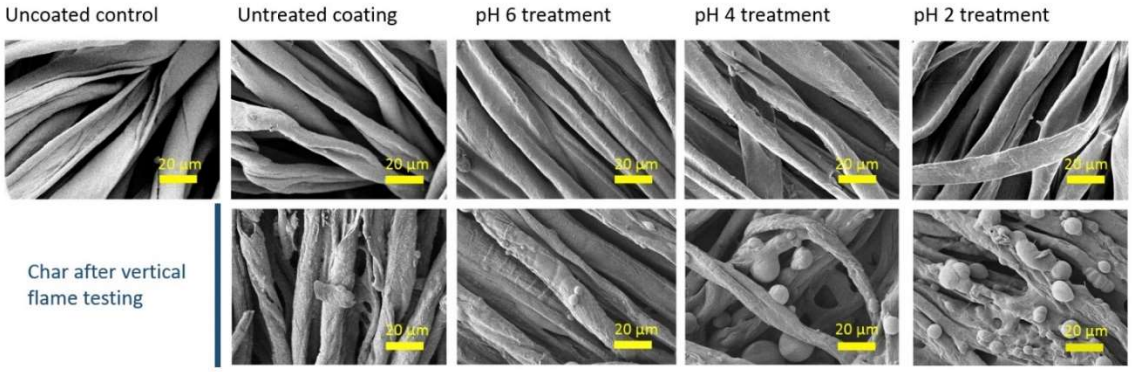

Figure 3.4. SEM images of uncoated cotton fabric and fabric coated with the PEI/PSP OnePot solution, untreated and treated in varying pH buffers. Uncoated cotton was completely consumed in fire testing, so there was no residue to be imaged.

Uncoated, treated and untreated OnePot FR fabrics were assessed for heat release rate (HRR) using microscale combustion calorimetry (MCC). The peak HRR is a quantitative measurement of the rate at which the fabric releases heat during a fire, which propagates the combustion cycle. This is why fire spreads very quickly over cotton clothing, reducing the time in which the wearer can remove the fabric before injury.[176] Coating the fabric with the PEI/PSP complex solution reduces total heat release (THR) and peak HRR significantly. These results also indicate the buffer treatment improves the flame retardancy of the coating, increasing char yield and reducing peak HRR and THR with a lower weight coating (pH 2 treated coating reduces the THR of cotton by 88% with only 16.5 wt% coating).

3.4 Conclusions

Cotton fabric was rendered flame retardant with a stable solution of water-soluble polyelectrolyte complexes to form a rinse-resistant flame retardant coating. Fabric soaked

in this aqueous PEI/PSP mixture had an average weight gain of 23%, but the coating largely eroded when rinsed in water. Treating the fabric with an acidic buffer "cured" the coating to resist rinsing. Coatings treated in acidic buffer at pH 6, 5, 4, 3, and 2 had weight gains of 11.5%, 11.6%, 15.4%, 14.6%, and 16.5%, respectively. SEM micrographs of the coatings show a conformal coating that uniformly covers individual cotton fibers. Flame retardant behavior of this OnePot coating was evaluated by TGA, VFT, and MCC. Buffer treatment of coated fabric greatly improved the flame retardant behavior of the coating. The best OnePot deposition on cotton, treated with pH 2 buffer, achieved an 81% reduction in peak HRR and 88% reduction in total heat release in comparison to uncoated cotton fabric. This two-step, water-based process produces flame retardant fabric more quickly, using less coating weight than most commercial treatments.

CHAPTER IV

WASH-DURABLE POLYELECTROLYTE COMPLEX THAT EXTINGUISHES FLAME ON POLYESTER-COTTON FABRIC*

4.1 Introduction

Many of the challenges associated with flame retardant approaches for fabric have been recently overcome by applying conformal coatings using layer-by-layer (LbL) assembly.[23,60,175,177] This technology has been shown to render polyester,[4,178] ramie,[179] and cotton[64,67,177,178,180,181] fabric flame retardant using environmentally-benign aqueous solutions applied under ambient conditions. LbL assembly involves the deposition of thin films by alternate layering of oppositely charged polyelectrolytes that impart the desired functionality onto a substrate.[1,100,182] Although these treatments are effective, the LbL process involves multiple cycles of immersion to deposit enough flame retardant to achieve appreciable flame suppression. In an effort to apply FR coatings of similar chemistry onto fabric with very few processing steps, a method involving water-soluble polyelectrolytes complexes (PEC) from a single solution was recently developed.[66,183] Two different fabric types were rendered self-extinguishing by applying a nanocoating in just two or three steps using the pH-dependent solubility of PECs. Complex solubility is largely dependent on concentration, ionic strength, and in the case of weak

* Reprinted with permission from Haile, M.; Leistner, M..; Sarwar, O.; Henderson, R.; Grunlan, J. C. A wash-durable polyelectrolyte complex that extinguishes flames on polyester–cotton fabric. *RSC Adv.* **2016**, 33998-34004. Copyright 2016 Royal Society of Chemistry.

polyelectrolytes, solution pH.[150,169,170] The flame retardant PECs were kept stable at high pH and deposited onto fabric. After drying, the PEC was rendered water-insoluble by exposure to an acidic buffer solution. Figure 4.1 compares the LbL and PEC deposition processes.

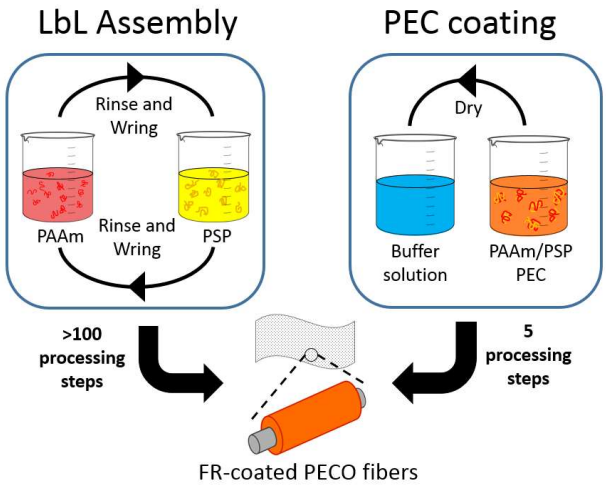

Figure 4.1. Schematic of the LbL assembly and PEC coating procedures for applying poly(allylamine) and poly(sodium phosphate) onto polyester-cotton blend fabric.

To better demonstrate the effectiveness of the PEC-deposition technique, this study set out to directly compare flame retardant PEC and LbL coatings prepared with the same polyelectrolytes. Coatings deposited layer-by-layer with poly(allylamine) and poly(sodium phosphate) were previously shown to promote char formation on cotton fabric.[67] This multilayered nanocoating is compared to a polyelectrolyte complex coating presented in this work in terms of flame retardancy, weight gain, and composition. A greater reduction in peak heat release rate has been achieved using the PEC coating (78%

reduction for cotton, 31% for polyester) relative to the LbL deposited coating (45% for cotton, 19% for polyester). PAAm/polyphosphate complex coatings self-extinguish PECO fabric with less added weight (17.9%) than those assembled layer-by-layer (22.2%). Investigation into the possible cause for this improved FR effect revealed a significant difference in composition between coatings produced with these two techniques. The PEC coating also proved to be durable to washing, maintaining flame retardancy after five home launderings and 8 h in boiling water. PEC coatings provide a powerful opportunity to reduce the flammability of blended fabrics, using water-based ingredients and very few processing steps.

4.2 Experimental

4.2.1 Materials

Polyester-cotton fabric with a weight of 4.5 oz yd^{-2} (65% polyester) and 1993 AATCC standard detergent were purchased from Testfabrics, Inc (West Pittston, PA). Sodium hexametaphosphate (crystalline, +200 mesh, 96%) [PSP] was purchased from Sigma-Aldrich (Milwaukee, WI). Poly(allylamine hydrochloride) (Mw ~ 15,000 g mol^{-1}) [PAAm hydrochloride] was purchased from Beckmann-Kenko (Bassum, Germany) and used as received. Citric acid monohydrate and sodium citrate dihydrate were purchased from Sigma-Aldrich and used to make buffer solutions. 1 M NaOH made from pellets (anhydrous; reagent grade, ≥ 98%), and 5 M HCl, made from concentrated acid (ACS reagent, 37%), both purchased from Sigma-Aldrich, were used to adjust the pH of the deposition and treatment solutions. All individual solutions were prepared with 18.2 MΩ cm deionized water.

4.2.2 Preparation and Deposition of PEC Coating

PAAm and PSP were found to be stable in the same suspension at pH ≥ 12. Below this pH, the polyelectrolytes associate and flocculate from the suspension. The pKa of PAAm is 8.7, so its amine groups are largely unprotonated and the polyelectrolyte has very little positive charge and pH 12.[184] Under these conditions there are only weak interactions between PAAm and polyphosphate, allowing for a stable polyelectrolyte suspension to form. In order to achieve high weight gain with a single dip, the PEC solution contained high polymer concentrations. PEC coating solutions were prepared using a 7:12 ratio of PAAm hydrochloride to PSP (near equimolar proportion of the two polymers by monomer units). The PEC suspension was prepared with 9.2 wt% PAAm hydrochloride and 15.8 wt% PSP (25 wt% solids in water). PAAm hydrochloride was dissolved in water, while an equimolar amount of NaOH was added to neutralize the hydrochloride. PSP was dissolved in a separate solution. The two solutions were added together and stirred vigorously to generate a pearlescent suspension. The pH of the stable suspension was ~12. Medium and low concentration PEC suspensions were prepared according to the same procedure using lower polyelectrolyte concentrations. Medium concentration consisted of 7.4 wt% PAAm hydrochloride and 12.6 wt% PSP (20 wt% solids), while low concentration consisted of 5.5 wt% PAAm hydrochloride and 9.5 wt% PSP (15 wt% solids).

PECO fabric was dipped in a PEC solution for 30 s immediately after preparation. Fabric was then squeezed and hung to dry in a 70℃ oven for 1 h prior to buffer treatment. A pH 4 buffer solution was prepared using 100 mM citric acid/sodium citrate. Coated

PECO was treated by soaking in 300 mL of the buffer solution for 5 min. The acidic environment of the buffer treatment protonated the PAAm contained in the coating. The positively-charged PAAm then strongly complexed with the anionic polyphosphate, forming an insoluble complex. The fabric was then rinsed vigorously in water to remove citrate and free polymer, then dried at 70 °C for 2 h prior to testing.

4.2.3 Layer-by-Layer Assembly

The LbL assembly of PAAm/PSP films was modified from an earlier literature procedure.[67] 2 wt% PSP and 1 wt% PAAm hydrochloride solutions, both at pH 4, were prepared with deionized water (18.2 MΩ·cm) as separate deposition solutions. Multilayer nanocoatings were deposited on PECO fabric by dipping into the polyelectrolyte solution, alternating between cationic PAAm and anionic PSP, with each cycle corresponding to one bilayer (BL). The first dip into each mixture was for 5 min, beginning with cationic poly(allylamine). Subsequent dips were for 1 min each. Between dips, the fabric was wrung and rinsed in deionized water to remove excess polymer. After the desired number of bilayers were reached, the fabric was hung to dry for 2h at 70 ˚C prior to testing.

4.2.4 Characterization

The X-ray photoelectron spectroscopy and scanning electron microscopy methodology used in this study was described in Chapter 3 (Section 3.2). Elemental analyses were performed by Midwest Microlab LLC (Indianapolis, IN).

Thermal stability of uncoated and PEC-coated cotton fabric (approximately 30 mg) was evaluated in triplicate using a Q-50 thermogravimetric analyzer (TGA; TA

Instruments, New Castle, DE), under a controlled heating ramp of 20℃ min^{-1}, from ambient temperature up to 600℃, with a sample purge flow of 60 mL s^{-1} air and a balance purge flow of 40 mL s^{-1} nitrogen. Fabric samples were cut into 3 x 12 in. strips that were vertically hung in a metal clamp within a model VC-2 vertical flame cabinet (Govmark, Farmingdale, NY) and vertical flame testing was performed according to ASTM D6413-08. All fabric was run in triplicate for microscale combustion calorimetry at a 1℃ sec^{-1} heating rate, from 150-550℃, using method A of ASTM D7309 (pyrolysis under nitrogen) at the University of Dayton Research Institute (Dayton, OH). Home laundering was performed according to AATCC 135, however the water temperature was 30 ˚C using a Samsung 4 cubic foot top-load washer (purchased at Home Depot, College Station, TX). Coating durability was also tested by refluxing 5 g (9 x 4 in.) of fabric in 400 mL of water for 8 h.

4.3 Results and Discussion

4.3.1 Flame Retardant Behavior

Polyester-cotton blended fabric was coated with poly(allylamine)-polyphosphate complexes of varying concentration in water. Similar to earlier reports of flame retardant complex coatings,[66,183] sufficient weight gain on fabric was achieved with very few processing steps. High concentration polyelectrolyte complexes (HPEC) achieved the highest average coating weight gain of 17.9 wt%. Low and medium concentration complexes (LPEC and MPEC) achieved weight gain of 8.7% and 13.7%, respectively. These coatings maintained the whiteness of the fabric, although there was some increase in fabric stiffness. For direct comparison to multilayer coatings, PAAm/PSP multilayers

were applied to PECO fabric using LbL assembly adapted from the procedure reported by Li et al.[67] Fabric was alternately dipped into cationic PAAm and PSP solutions until the desired number of bilayers were deposited. 20, 25, and 30 BL achieved coatings of weight gain 12.3, 17.2, and 22.2%, respectively. Weight gain and vertical flame test results for all PECO samples are summarized in Table 4.1.

Table 4.1. Vertical flame test results of coated and uncoated PECO fabric.

Coating system	Sample	Wt gain (%)	Afterflame (s)	Char length (in.)	Residue (wt%)
Control	-	-	14 ± 2	consumed	45 ± 2
LbL	20 BL	12.3 ± 0.6	10 ± 4	entire sample	75 ± 4
	25 BL	17.2 ± 1.1	10 ± 3	entire sample	73 ± 5
	30 BL	22.2 ± 0.8	<1	6.3 ± 0.2	95 ± 3
PEC	LPEC	8.7 ± 0.2	20 ± 3	entire sample	61 ± 4
	MPEC	13.7 ± 0.3	inconsistent	inconsistent	inconsistent
	HPEC	17.9 ± 0.6	<1	6.3 ± 0.8	94 ± 2

The flame retardancy of LbL and PEC coatings was evaluated with vertical flame testing (VFT). Uncoated control fabric ignited and was almost completely consumed in an average of 14 s, leaving 45% residue from melted remains at the sides, with no visible charring. Both polyelectrolyte coating systems showed improved VFT performance by an evident charring mechanism. 20 and 25 BL PAAm/PSP coatings were able to produce significant char residue. 30 BL achieved sufficient weight gain (22.2%) to cause PECO to self-extinguish during burn testing, yielding a 6.3 inch char length. PEC coatings on PECO performed significantly better than the LbL coatings, with lower coating weight needed to impart self-extinguishing behavior. MPEC was able to inconsistently self-extinguish with

only 13.7% coating weight, suggesting this was a borderline weight for effective flame retardancy. HPEC and 25 BL LbL coatings had the same weight gain (17%), but polyelectrolyte complex (deposited in just two steps) consistently self-extinguished, while the 25 BL fabric burned over the entire sample.

To further investigate the flame retardancy of the coatings, pyrolysis-combustion flow calorimetry (PCFC) was used to obtain the heat release rate (HRR) of uncoated, PEC and LbL FR fabrics. HPEC and 25 BL coatings result in similar weight on PECO and both reduce the total heat release (THR) of the fabric by 30%, as shown in Figure 4.2. This is due to the coatings' ability to promote the formation of char, reducing the amount of flammable material available for pyrolysis and heat release. Although both systems have the same reduction in THR, HPEC shows a greater reduction in peak HRR. The peak heat release rate is a measure of the maximum rate at which fabric releases heat during a fire. This released heat continues the combustion cycle, propagating fire (i.e., greater peak HRR correlates to greater material flammability). In addition to reducing the peak HRR, both coating systems decrease the temperature at which these peaks occur.

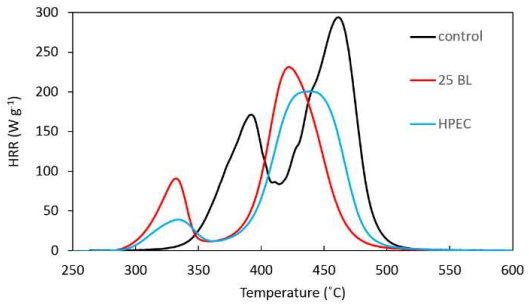

Figure 4.2. Heat release rate as a function of temperature for uncoated fabric and PECO coated with 25 PAAm/PSP bilayers or high concentration polyelectrolyte complex, as measured by pyrolysis-flow combustion calorimetry.

This earlier decomposition temperature is actually desirable, because it changes the decomposition pathway of the fabric. The first peak for uncoated PECO (Figure 4.2) corresponds to cotton decomposition at 392˚C, while the larger second peak is from polyester (at 461˚C). The HPEC coating reduces the peak HRR of cotton by 78% and the peak HRR of polyester by 31%, both of which are greater reductions than those achieved by the 25 BL coating at 45% and 19%, respectively.

Table 4.2. Pyrolysis-combustion flow calorimetry results for uncoated and coated PECO fabric.

Coating System	Wt gain (%)	PCFC		VFT (Table 1)
		pHRR (W g^{-1})	THR (kJ g^{-1})	
Control	-	170 at 392˚C 294 at 461˚C	15.6 ± 0.1	burned
25 BL	17.2 ± 1.1	93 at 322˚C 237 at 423˚C	11.0 ± 0.1	burned
HPEC	17.9 ± 0.6	38 at 334˚C 203 at 438˚C	10.9 ± 0.2	self-extinguishing

Scanning electron microscopy was used to visualize the PAAm/PSP coatings on the polyester-cotton fabric, as shown in Figure 4.3. The micrographs of both systems (HPEC and 25 BL) look very similar owing to their similar weight. Layer-by-layer deposition produces a conformal coating on the polyester-cotton fibers, maintaining the overall weave structure. Low solution concentration (≤ 2 wt% polyelectrolyte), and rinsing between layers, minimizes polyelectrolyte aggregation and fiber bridging with the LbL process. This process affords higher-quality nanocoatings, but requires a large number of processing steps (over 100 for 25 BL). The HPEC-coated fabric has a few more aggregated particles (Figure 4.3), but appears nearly as good as the LbL-coated fabric and requires only two processing steps. SEM micrographs of the char after VFT testing (bottom images in Figure 4.3) show that both FR coating systems preserve the weave of the fabric. Evidence of a bubbled intumescent charring mechanism can be observed in the char residues. Polyester can be observed as melted residue surrounding the fibers.

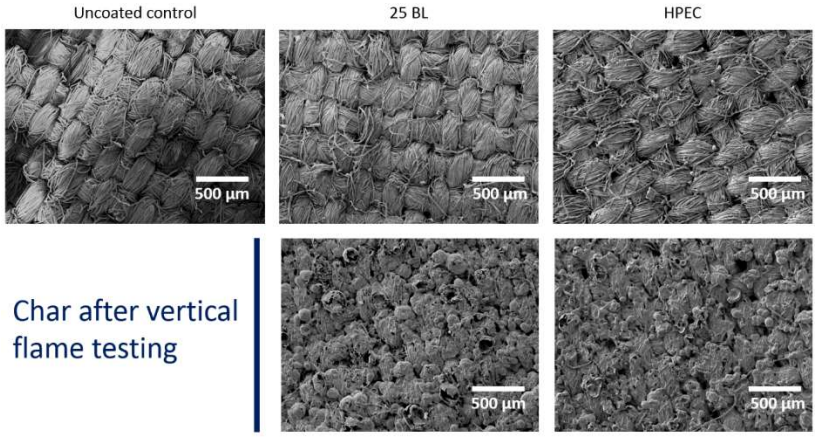

Figure 4.3. SEM micrographs of coated and uncoated PECO fabric.

Durability of the polyelectrolyte complex coating was demonstrated by laundering with detergent. No appreciable weight loss was observed for HPEC-coated PECO after five home-laundering cycles with ionic detergent. Additionally, much of the original softness and flexibility of the fabric was restored. After five home launderings, the samples were still able to self-extinguish during VFT, with a char length of 6.2 ± 0.6 in. and 90% residue. HPEC-coated PECO also maintained its flame retardant behavior after 8 h in boiling water. Although not fully understood, HPEC-coated fabrics lost on average 1.6 ± 0.1 wt% after boiling, but VFT performance improved, resulting in an average char length of 5.0 ± 0.8 in. Figure 4.4 shows HPEC coated fabric after vertical flame testing and washing. This is the first FR polyelectrolyte coating to show such impressive wash-durability on fabric, likely due to the insolubility of the polyelectrolyte complex, even at high solution pH.[61]

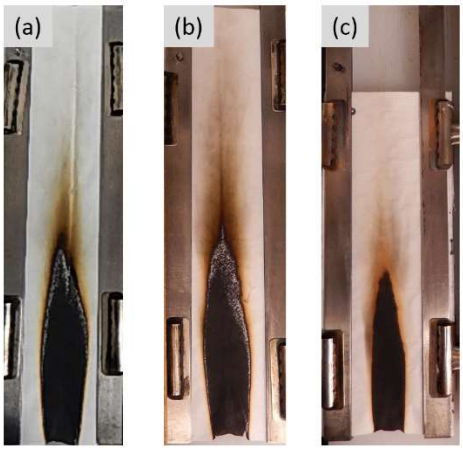

Figure 4.4. Representative VFT results of HPEC coated PECO fabric: (a) unwashed, (b) after five home launderings, and (c) after 8 h in boiling water.

4.3.2 Coating Composition

Although both 25 BL and HPEC coatings have the same weight, the difference in FR performance is likely due to differences in composition. Phosphorus and nitrogen concentration are indicative of the amount of polyphosphate and PAAm in the coating, respectively. These concentrations were determined by elemental analysis and revealed differences between the two coating systems. A polyelectrolyte complex obtained from the simple mixing of dilute PSP and PAAm solutions (both at pH 4), had a molar phosphorus-nitrogen ratio (P/N) of 0.93, close to what would be expected for charge-neutral stoichiometric complexation (P/N = 1). HPEC-coated fabric had a P/N ratio of 0.74, which is a stoichiometric excess of PAAm units and in agreement with a prior study of complexes containing polyethylenimine and polyphosphate.[183] This suggests the protonation of PAAm in the HPEC coating during buffer treatment was incomplete. In contrast, the P/N ratio of the LbL film was 1.26, indicative of a stoichiometric excess of polyphosphate, likely due to from incomplete charge neutralization during polymer adsorption.[132] Table 4.3 summarizes elemental analysis of these systems.

Table 4.3. Elemental analysis of flame retardant coatings.

	Phosphorus (wt%)	Nitrogen (wt%)	P/N (mol/mol)	Na/C
25 BL	3.11 ± 0.08	1.11 ± 0.04	1.26 ± 0.01	8.87×10^{-3}
HPEC	2.85 ± 0.08	1.74 ± 0.12	0.74 ± 0.03	4.90×10^{-3}
From solution	17.38 ± 0.04	8.45 ± 0.01	0.93 ± 0.00	-

Polyphosphate in the films phosphorylate the C(6) unit of the glucose monomer, preventing cellulose pyrolysis and promoting char formation. As the active flame retardant ingredient, it is often proposed that higher phosphorus content leads to a greater FR effect.[64,67,183] This makes the poorer flame retardant performance of the 25 BL system unexpected, given its greater phosphorus content relative to the self-extinguishing HPEC-coated PECO. While polyphosphate may function as an acid source for char formation during burning, it may function most efficiently when its surrounding environment contains protons. The availability of protons allows the polyphosphate to decompose into phosphoric acid, the charring catalyst in a fire. The FR performance of two polyphosphates with different counterions, ammonium (APP) and sodium (PSP), provides a useful demonstration of this concept. The protons available from the ammonium counterion allow APP to decompose at 150 ˚C, while aprotic PSP is stable all the way up to 500 ˚C..

When these polyphosphates were adsorbed on PECO fabric by wet pickup, similar weight gains were obtained (17%), but APP outperformed PSP as a flame retardant during VFT. PECO fabric coated with APP was able to self-extinguish, while PECO coated with PSP only left 33% char residue. Polyphosphate on the PSP-coated PECO has no available protons during burning. In contrast, the APP readily decomposes through the deprotonation of ammonium. In the case of the LbL and PEC films, the protonated amines of PAAm are an effective source of these protons for polyphosphate decomposition. The excess of PAAm in the HPEC coating means there are enough available protons to decompose polyphosphate completely, leading to more efficient char formation. The 25 BL films have a P/N ratio of 1.26, so there is only enough PAAm available in the film to

protonate (at maximum) 79% of the polyphosphate units. The negative charge of the excess polyphosphate is neutralized by sodium ions, as suggested by the atomic composition determined by X-ray photoelectron spectroscopy (XPS). The sodium-carbon atomic ratio (Na/C) is much higher for 25 BL (8.87×10^{-3}) than it is for PAAm/polyphosphate HPEC (4.90×10^{-3}). The excess positive charge expected for the HPEC film may be neutralized by the negative surface charge of the cotton or residual citrate. No chloride was detected by elemental analysis in any of the films.

4.4 Conclusions

Polyester-cotton fabric was rendered flame retardant with a stable polyelectrolyte complex of poly(allylamine) and polyphosphate, which formed a wash durable coating. In addition to having far fewer processing steps than a multilayer coating using the same polymers, the PEC exhibited improved flame retardancy when adjusted for weight gain, owing to its higher nitrogen content contributing to the strong charring of the system. The high concentration complex was able to successfully maintain the whiteness and microscopic weave of the fabric, while also maintaining the hand after washing. With only 17.9% weight gain, HPEC-coated PECO was able to self-extinguish in VFT and reduce the peak HRR by 78% and 31% for the cotton and polyester, respectively. After five home launderings with detergent, this coated fabric maintained its flame retardant behavior, which is the first time wash resistance has been demonstrated for these polyelectrolyte complex coatings. This water-based process provides a powerful framework to apply durable films to textiles of high commercial interest.

CHAPTER V

POLYELECTROLYTE COACERVATES DEPOSITED AS HIGH GAS BARRIER THIN FILMS

5.1 Introduction

Optically transparent, flexible thin films that provide high oxygen barrier are highly desirable for applications such as pressurized systems, food packaging and protection of flexible electronics.[73,185] Prevailing technologies, such as SiO_x and Al_xO_y thin films, provide a relatively impermeable layer to oxygen, but tend to have poor adhesion, flexibility and require costly vacuum-based processing.[186,187] Multilayer films deposited from water using layer-by-layer (LbL) assembly have shown extraordinarily low oxygen permeability and are of high interest due to their robustness, tailorability and ease of fabrication.[24,27,29,30,188] Despite all of the advantages associated with LbL assembly, the large number of processing steps remains a considerable challenge for commercial use.[1,189] In order to apply films composed of oppositely-charged polyelectrolytes to substrates using just one or two deposition steps, solutions containing polyelectrolyte complexes (PECs) can be employed.[66,141,166,183] PECs are formed by the entropy-driven association of oppositely charged polyelectrolytes in water and can exist as stable colloids, flocculants, or metastable coacervates.[133,150,169,171] Governed by conditions such as pH and ionic strength, PEC coacervation is marked by a liquid-liquid phase separation, where a polymer rich coacervate phase is in equilibrium with a polymer poor solution phase. PEC coacervates are composed of weakly bound polyelectrolytes,

and have viscous liquid-like behavior that can be exploited to quickly apply them as thin films.[133,168,190-192]

This chapter describes polyelectrolyte coacervates applied to substrates using Meyer rod coating (a common type of blade coating),[193] in an effort to quickly fabricate thin oxygen barrier films in a single step. The Meyer rod is drawn across a substrate, doctoring off coating fluid, using formed or wired grooves to deposit a specific wet film thickness. The coating fluid used for this process must have sufficient viscosity to resist dewetting and contain enough polymer to deposit a uniform layer. A polyelectrolyte complex coacervate suitable for the Meyer rod process was formulated by controlling the ionic strength of aqueous solutions containing two oppositely charged weak polyelectrolytes, cationic polyethylenimine (PEI) and anionic polyacrylic acid (PAA). These two polymers had been previously reported to exhibit high oxygen barrier when assembled layer-by-layer,[24] and were successfully adapted to the present PEC coating process as shown in Figure 5.1. After coating using a Meyer rod, the electrostatic interaction of the polyelectrolytes was increased by exposure to acidic buffer that produces an insoluble thin film. The oxygen permeability of the film was further improved by exposure to high humidity and thermal crosslinking. This simple and powerful technique adapted a highly effective multilayer coating to a process that is much more amenable to conventional coating techniques.

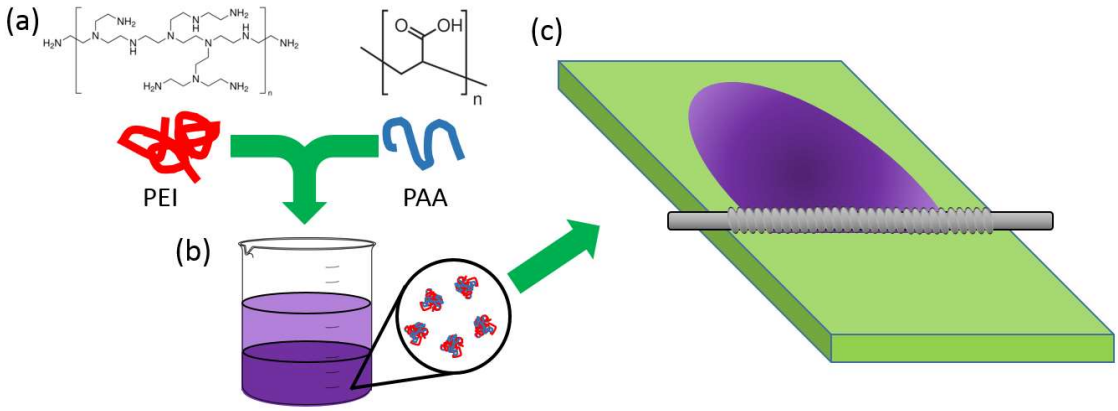

Figure 5.1. Schematic of the coacervate coating process. In the first step, (a) both polyelectrolytes are mixed together in a single suspension to form (b) dilute and coacervate phases. The coacervate phase is decanted and used for the (c) rod coating process to form the wet PEC film.

5.2 Experimental

5.2.1 Materials

Branched polyethylenimine (M_w = 25,000 g/mol, ρ=1.10 g/cm^3) was purchased from Sigma-Aldrich (St. Louis, MO) and used as a 0.1 wt% DI water solution. Natural sodium montmorillonite clay (trade name Cloisite NA+), provided by Southern Clay Products, Inc. (Gonzales, TX), was dispersed as a 1 wt% suspension in deionized (DI) water by rolling in bottles overnight. MMT platelets have a reported density of 2.86 g/cm^3, diameter ranging from 10-1000 nm, and thickness of 1 nm.[194] Zeta potential of MMT suspensions was measured with a Zeta Phase Angle Light Scattering (ZETA PALS) instrument (Brookhaven Instruments Corporation, Holtsville, NY).

5.2.2 Preparation of Polyelectrolyte Suspensions

All aqueous solutions were prepared with 18.2 MΩ·cm deionized water. The pH of individual 20 wt% solutions of PEI and PAA were adjusted to 8.0 using 5 M HCl and NaOH, respectively. After achieving pH 8.0, the solutions were diluted to 10 wt% polymer and the pH was adjusted to 8.0 again. The PEC suspensions were prepared by taking equal volumes of the two solutions and adding sodium chloride to achieve the desired concentration NaCl. PEI was added dropwise to the PAA while stirring vigorously. A solution pH of 8 was used because it reduced localized flocculation during mixing relative to lower pH processing. The suspensions were stirred for 10 min and then allowed to sit for 1 h. Coacervates and solutions were "annealed" in an oven for 2 h at 70 °C prior to characterization.

5.2.3 Fabrication of Coacervate Coatings

PEI/PAA coacervate prepared using 1.0 M NaCl was separated from the dilute phase by pipet. PET substrates were corona treated immediately before coating. Silicon and PET substrates were mounted on glass and coacervate fluid was deposited using a #2 Meyer rod from R.D. Specialites (Webster, NY). The rod was 0.5 in. in diameter, 16 in. long and had an "equivalent wire diameter" of 0.05 mm. The substrate was then dipped in 100 mM citric acid/citrate buffer for 1 min, followed by spraying with water to rinse and drying with a stream of filtered air. Humidity post-treatment involved placing the film in a chamber with humidity varying from 93 -97% for 12 h. Thermal crosslinking was done by placing films in an oven at 150 °C for 2 h. All films were stored in a drybox for 24 h or more prior to characterization.

5.2.4 Characterization

Film thickness was measured as a function of bilayers deposited with a P6 profilometer (KLA-Tencor, Milpitas, CA). Film thickness was measured on silicon wafers with a P-6 profilometer (KLA-Tencor, Milpitas, CA). Surface morphology was imaged using a JSM-7500F FESEM (JEOL, Tokyo, Japan). Prior to imaging, each film was sputter coated with 5 nm of platinum/palladium to reduce surface charging. Atomic force microscopy was done using a Bruker Dimension Icon AFM. All mapping measurements were conducted under ambient conditions (24 °C, 45% RH) using tapping mode. Oxygen transmission rate measurements were performed by MOCON (Minneapolis, MN) using an Oxtran 2/21 ML oxygen permeability instrument (in accordance with ASTM Standard D-3985) at 23 °C and at 50% RH. Viscosity (η) was measured using an AR G2 Rheometer (TA Instruments, New Castle, DE) using a 40 mm, 2° steel cone. Shear-stress experiments were performed at 25 °C over frequency range 1-100 Hz. Transmittance of PEC films was measured using a USB2000 UV-Vis spectrometer (Ocean Optics, Dunedin, FL).

5.3 Results and Discussion

The When polyelectrolyte complexes are formed, there is a large entropic driving force as small bound counterions are excluded and released into solution (Figure 5.2a). The addition of salt to the solution inhibits this counterion release, and also increases the ionic strength of the suspension, softening the electrostatic interactions of the polymers.[192] The effect of salt concentration on the complexation of the polyelectrolytes was studied by varying the concentration of sodium chloride in PEI and PAA solutions before mixing them together. In a range of 0 to 0.25 M NaCl, PEI and PAA strongly

associate into larger networks and form a macroscopic precipitate that is unsuitable for the rod coating process. At concentrations of 1.50 M and above, the ionic strength is high enough for PEI and PAA to be dissolved as individual chains, creating a true solution of polyelectrolytes. Coacervation is achieved at intermediate NaCl concentrations (0.50 – 1.00 M), where phase separation of the polymer-rich coacervate layer and a polymer-poor dilute layer is observed. Samples of varying salt concentration 1 h after mixing are shown in Figure 5.2b. To further coalesce microphase droplets and better identify which suspensions phase separate, both the solutions and coacervates were "annealed" for 2 h at 70 °C, resulting in optically transparent phases. All coacervate phases were decanted for further characterization.

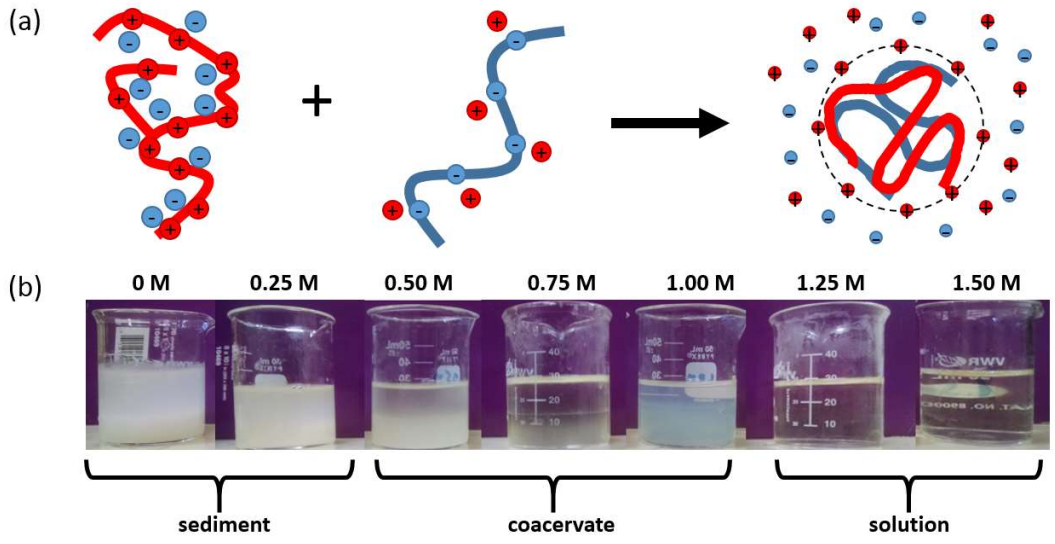

Figure 5.2. Schematic of (a) polycation and polyanion associating to form a polyelectrolyte complex as small counterions are driven into solution. (b) Photograph of polyethylenimine and polyacrylic acid suspensions one hour after mixing at various concentrations of sodium chloride. All solutions were pH 8.0 and contained 10 wt% polymer with a 1:1 weight ratio of PEI to PAA.

Rheology was performed on the PEI/PAA solutions as well as the lower salt concentration coacervate phases to determine which PEC sample was suitable as the coating fluid for Meyer bar coating. Figure 5.3 shows the viscosity of coacervate phases at varying NaCl concentration. The free chain polyelectrolyte solutions (1.25 – 1.50 M NaCl) have viscosities much lower than those of the coacervates (0.50 M- 1.0 M NaCl), where there is stronger interaction between polymer chains. The viscosities of the free chain polyelectrolyte solutions were considerably higher than water, indicating critical overlap concentration was achieved.[195] To achieve a Meyer rod coating with minimal defects, the viscosity of the fluid should be high enough to resist secondary flows induced by dewetting and surface tension.[193,196] The coacervate suspensions are suitable candidates for these coatings as they remain within the range of viscosity suitable for the Meyer rod technique (300 – 800 mPa·s).[197] The complex coacervate with 1.0 M NaCl was used for the gas barrier film because its viscosity remains suitable over a wide range of shear rates (0.2 – 100.0 s^{-1}).

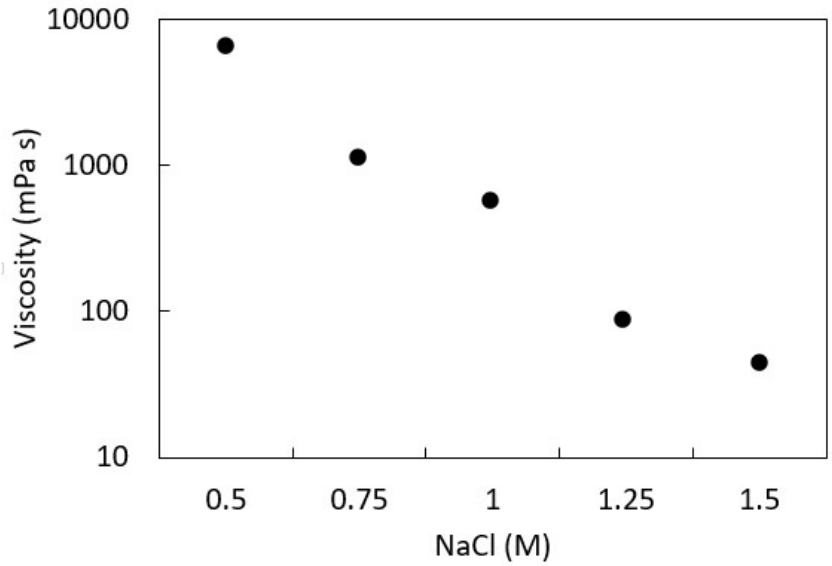

Figure 5.3. Viscosity of PEC suspensions as a function of sodium chloride concentration, measured at a shear rate of 1 s^{-1}. Viscosity measurements of 0.50 - 1.00 M NaCl suspensions were determined from the lower coacervate phase.

After separating from the top dilute phase of the polyelectrolyte complex, the coacervate prepared with 1.0 M NaCl was applied to substrates using a hand drawn rod (Figure 1c). The PEC film was then dipped in water to extract sodium chloride, allowing the polyelectrolyte chains to more strongly associate and solidify the complex. Because the polyelectrolyte coacervate is above critical overlap concentration, the complex solidifies into a coherent film rather than individual colloidal particles.[168] Subsequent spray rinsing appeared to erode the film and there was noticeable undesirable stickiness, likely due to the incomplete ionization of PEI at pH 8 in the film. When PEI is not completely protonated, there are less ammonium groups to ionically bond with the carboxylate ions of PAA.

After rod coating, the films were immersed into citric acid/citrate buffer solutions at pH 6, 4, and 2 to fully protonate PEI, which improved its association with PAA. In addition to improving the film's durability to rinsing, acid buffer treatment produces higher cohesive energy density,[198] which prevents gas molecules from moving aside polymer chains.[199] Spray rinsing removed buffer, persistent salt and excess polymer and the films were finally dried by a stream of air. PEC films on silicon, treated by pH 6 buffer, were depleted in some areas and coatings treated at pH 2 could not remain adhered after spray rinsing. Using pH 4 buffer proved to be the most effective treatment and produced highly conformal films, with average thickness of 1.63 ± 0.09 μm.

Scanning electron micrographs of pH 4 treated PEC films reveal a considerable amount of porosity (Figure 5.4a). Furthermore, atomic force microscopy (AFM) reveal pores spanning the thickness of the film, inhibiting the film's ability to reduce gas permeability. These pores likely arise from the fast evaporation of water from the film during air drying and are not present in films assembled layer-by-layer. Pores are eliminated by a 12 h exposure to 95% humidity. Water acts as a plasticizer, allowing polymer to fill the coating's pores. Both SEM and AFM of humidity-treated films reveal very smooth coatings (Figure 5.4d-f). Roughness of treated films was reduced two orders of magnitude (from 395 nm to 2.60 nm) and thickness increased to 1.91 ± 0.08 μm.

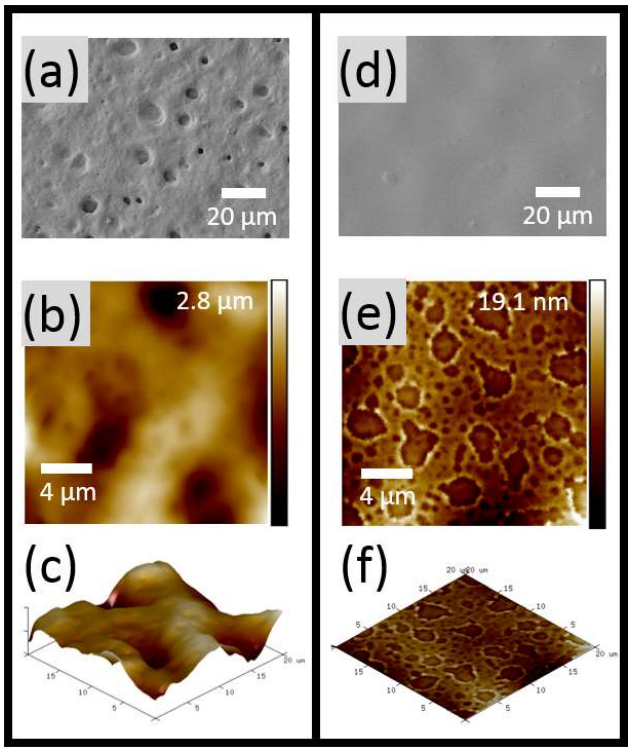

Figure 5.4. Scanning electron micrographs (top), atomic force micrographs (middle), and 3-dimensional topography maps for pH 4 treated polyethylenimine/polyacrylic acid coacervate deposited films (bottom) before (left) and after (after) humidity post-treatment. Film thickness was 1.63 ± 0.09 µm before post-treatment and 1.91 ± 0.08 µm after humidity exposure.

Although unsuccessful on silicon, PEC films treated by pH 2 and 6 buffer were successfully deposited on poly(ethylene terephthalate) [PET], along with pH 4 treated films. pH 4 and 6 treatments resulted in hazy films, with visible light transmittance of 14 and 11%, respectively. Films treated with pH 2 buffer were completely opaque (3% visible light transmittance). Figure 5.5 shows that pH 4 treatment results in the best oxygen barrier on PET, reducing the oxygen transmission rate (OTR) of 0.127 mm thick PET from 9.51 to 1.46 $cm^3/(m^2 \cdot day \cdot atm)$. Humidity treatment of the PEC coating reduced the porosity of the film, marked by the elimination of coating haziness (98% transparent), resulting in

further reduction of OTR to 0.384 $cm^3/(m^2 \cdot day \cdot atm)$. An even further reduction in OTR resulted with thermal crosslinking of the humidified film, achieving an OTR of 0.08 $cm^3/(m^2 \cdot day \cdot atm)$. Thermal crosslinking bonds the PEI to PAA, creating amide bonds. Unlike an earlier study incorporating thermal crosslinking,[200] no contraction was observed here, with the film maintaining a thickness of 1.99 ± 0.06 μm. It is likely that crosslinking reduces swelling during OTR testing, resulting in lower free volume and permeability. Oxygen barrier testing was done at 50% relative humidity and 23 °C according to typical indoor conditions.[201]

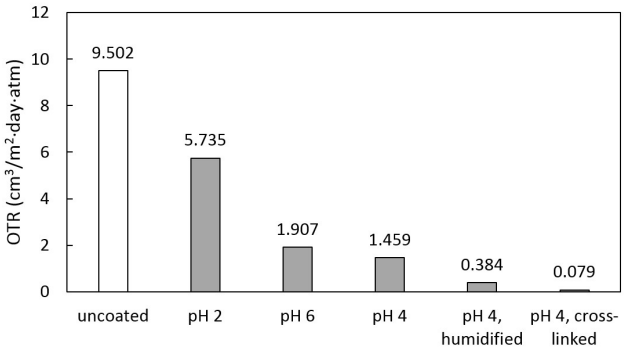

Figure 5.5. Oxygen transmission rate (measured at 50% relative humidity) of 0.127 mm PET without a coating and coated with a PEI/PAA coacervate treated with varying pH buffer and post-treatments.

The rod coating of polyelectrolyte coacervate suspensions provides a framework in which multi-polyelectrolyte films can be deposited in a single step. With this technique, it is likely that many of the multilayer gas barrier coatings reported in the literature can be more quickly and simply deposited. By altering salt concentration, coacervates of sufficient viscosity can be formed to resist fluid flow and the film can be cured by using

an appropriate pH buffer. Post-treatments of the film improved the oxygen barrier enormously by combining humidity and crosslinking treatments, these PEC-based films provided PET with a two order of magnitude reduction in oxygen transmission rate, while also achieving optical transparency. Although unable to match the super barrier of layer-by-layer deposition of PEI and PAA,[24] the significant reduction in processing steps afforded by coacervate coating should make this a useful industrial opportunity for a variety of packaging applications. This environmentally benign process offers the opportunity for scalable, low cost barrier films.

CHAPTER VI

CONCLUSIONS AND FUTURE WORK[*†]

6.1 Improvements on Gas Barrier Thin Films

This dissertation described several novel coating methods to deposit functional thin coatings from single-suspension stable polyelectrolyte complexes. Immersion deposition was successfully employed to deposit flame retardant nanocoatings onto cotton and polyester-cotton and rod-coating was used to successfully deposit a highly effective oxygen barrier on PET. All coatings were sol-gel processes that used the solution-dependent phase behavior of PECs to effectively stabilize them as well as solidify them post-deposition. Existing functional coatings assembled layer-by-layer can be adapted to the PEC-coating process described in this dissertation. Using this technique, flame retardant and high gas barrier films that are more easily processed and commercially viable can be achieved.

[*]Reprinted with permission from Haile, M.; Fincher, C.; Fomete, S.; Grunlan, J. C. Water-soluble polyelectrolyte complexes that extinguish fire on cotton fabric when deposited as pH-cured nanocoating. *Polym. Degrad. Stab.* **2015**, 60-64. Copyright 2015 Elsevier.

[†]Haile, M.; Leistner, M..; Sarwar, O.; Henderson, R.; Grunlan, J. C. A wash-durable polyelectrolyte complex that extinguishes flames on polyester–cotton fabric. *RSC Adv.* **2016**, 33998-34004. Copyright 2016 Royal Society of Chemistry.

6.1.1 Water-soluble Polyelectrolyte Complexes that Extinguish Fire on Cotton Fabric when Deposited as pH-Cured Nanocoating

It was shown in Chapter III that a OnePot mixture consisting of polyethylenimine and poly(sodium phosphate) imparts self-extinguishing behavior to cotton in a single step. This nanocoating maintains the fabric's weave structure by conformally coating individual fibers. Appreciable weight gain (23%) is achieved with just a single 30 s immersion in the WPEC suspension. Treatment of this coating with acidic buffer further renders it insoluble in water and durable to rinsing. Uncoated cotton is readily consumed during vertical flame tests, while OnePot-coated fabric, followed by buffer treatment of pH 5 or lower (16.5% weight gain or less), self-extinguishes through an intumescent mechanism. Microscale combustion calorimetry reveals a total heat release reduction of 88% and peak heat release rate reduction of 81%. This work demonstrates the ability of a WPEC nanocoating to prevent ignition of cotton fabric with few processing steps and relatively low weight gain.

6.1.2 Wash-Durable Polyelectrolyte Complex that Extinguishes Flame on Polyester-Cotton Fabric

To demonstrate the versatility of fire suppressing PEC coatings, Chapter IV describes application to polyester-cotton fabric, a commercially prevalent, but highly flammable textile. Treatment of this one-step coating with an acidic buffer (technically a second step) yields a nanocoating capable of extinguishing flames on PECO during vertical flame testing, outperforming a similar multilayer coating assembled layer-by-layer. Pyrolysis-combustion flow calorimetry revealed a total heat release reduction of 30% for PECO coated with 18 wt% PEC. The coated fabric also exhibited a 78% and 31%

reduction in peak heat release for cotton and polyester, respectively. In addition to stopping fire, this coating is durable to five home laundering cycles and eight hours in boiling water without losing any flame retardant activity. Although microscopy revealed identical structures in LbL and PEC coatings, elemental analysis revealed a difference in composition. The PEC coating showed greater flame retardancy than layer-by-layer assembled coatings using the same ingredients, while also greatly reducing the number of processing steps, making this a promising treatment for commercial fabric protection.

6.1.3 Polyelectrolyte Coacervate Gas Barrier

A rapid method of depositing oxygen barrier PEC coatings, consisting of polyethylenimine and polyacrylic acid, was explored in Chapter V. Coacervate suspensions of the two polymers were prepared using sodium chloride to alter stability and suspension viscosity. Coatings were successfully rod-coated onto PET and solidified using a combination of low pH and ionic strength. One such coating, treated with humidity and thermal cross-linking, successfully reduced the oxygen transmission rate of PET by a factor of 120. PEC-coatings providing high gas barrier suggests this technique can generate films with other desirable properties.

6.2 Future Research Direction

6.2.1 Single Suspension Clay Deposition

Previous studies have suggested that the multi-step depositions of LbL assembly is necessary for the proper alignment of clay.[29,30,78,94,202] This alignment allows for a more tortuous path, reducing the permeability of gas molecules. Breu and coworkers reported

the deposition of a clay-polyurethane film using doctor-blading of an organically-functionalized montmorillonite suspension.[201] These clay platelets were highly aligned due to the high shear applied by blade coating. Simple dyring of graphene oxide in a polyelectrolyte complex showed that the platelets in the film were highly aligned after drying.[165] These results suggest that alignment of impermeable platelets in a film may be possible without layer-by-layer deposition. Aligned coatings may be attained by suspensions of anionic clay and polycations cast onto a substrate and then complexed using low pH or low ionic strength solution. These films can provide high impermeability to gas using far fewer processing steps than existing multilayer clay-polymer thin films.

6.2.2 Stretchable Gas Barrier Interpolymer Complexes

The PEI/PAA films presented in Chapter V provide excellent gas barrier, but crack under strain, making them unsuitable to reduce the gas barrier of elastomeric substrates. Grunlan and coworkers have shown good stretchability while maintaining reasonable oxygen barrier with films assembled by hydrogen bonding interactions.[203,204] Using the pH-controlled interpolymer complexation of hydrogen-bonding polymers, it might be possible to deposit similar films in a few steps without the need for LbL assembly. Initial experiments yielded poor films, likely due to the low solubility of H-bond accepting poly(ethylene oxide), preventing the achievement of critical overlap concentration. Shifting from rod coating to spray coating may yield better quality films.

6.2.3 Conductive PEC films

Many reported LbL films incorporate conductive carbonaceous materials. Films incorporating carbon nanotubes have been fabricated, with very low resistance and small thickness.[84,205-207] Many of these LbL films require many layer to attain appreciable thickness, which involves a latge number of processing steps. Some graphene oxide free-standing films have been prepared by vacuum filtration,[208] but it would be desirable to develop a continuous scalable process to deposit conductive polymer-nanoparticle films from water. Multiwalled carbon nanotubes were dispersed in a PDDA/PSS coacervate by sonication and were successfully deposited onto PET. Although these films showed heating in microwave field, no appreciable electrical conductivity was observed by four-point probe testing. The coacervate suspension has very high polymer concentration (> 10 wt%) while likely only achieving less than 0.1 wt% suspended nanotubes. By lowering the polymer concentration to less than 1 wt% and using a true solution instead of coacervate suspension, higher carbon nanotube loading can be attained and high conductive may be achieved. The viscosity of such a suspension will be too low for drawdown technique so spray-coating can be used.

REFERENCES

[1] Decher, G.; Schlenoff, J. B. *Multilayer Thin Films: Sequential Assembly of Nanocomposite Materials*; 2nd ed.; Wiley-VCH: Weinheim, Germany **2012**.

[2] Ariga, K.; Hill, J. P.; Ji, Q., Layer-by-layer assembly as a versatile bottom-up nanofabrication technique for exploratory research and realistic application. *PCCP.* **2007**, *9*, 2319.

[3] Hao, W.; Pan, F.; Wang, T., Photocatalytic activity TiO_2 granular films prepared by layer-by-layer self-assembly method. *J. Mater. Sci.* **2005**, *40*, 1251.

[4] Carosio, F.; Laufer, G.; Alongi, J.; Camino, G.; Grunlan, J. C., Layer-by-layer assembly of silica-based flame retardant thin film on PET fabric. *Polym. Degrad. Stab.* **2011**, *96*, 745.

[5] Chapel, J. P.; Berret, J. F., Versatile electrostatic assembly of nanoparticles and polyelectrolytes: Coating, clustering and layer-by-layer processes. *Curr. Opin. Colloid Interface Sci.* **2012**, *17*, 97.

[6] Srivastava, S.; Kotov, N. A., Composite layer-by-layer (LbL) assembly with inorganic nanoparticles and nanowires. *Acc. Chem. Res.* **2008**, *41*, 1831.

[7] Xu, X. H.; Ren, G. L.; Cheng, J.; Liu, Q.; Li, D. G.; Chen, Q., Layer by layer self-assembly immobilization of glucose oxidase onto chitosan-graft-polyaniline polymers. *J. Mater. Sci.* **2006**, *41*, 3147.

[8] Lvov, Y.; Ariga, K.; Ichinose, I.; Kunitake, T., Molecular film assembly via layer-by-layer adsorption of oppositely charged macromolecules (linear polymer, protein and clay) and concanavalin A and glycogen. *Thin Solid Films* **1996**, *284*, 797.

[9] Hammond, P. T., Building biomedical materials layer-by-layer. *Mater. Today* **2012**, *15*, 196.

[10] Lutkenhaus, J. L.; Hammond, P. T., Electrochemically enabled polyelectrolyte multilayer devices: from fuel cells to sensors. *Soft Matter* **2007**, *3*, 804.

[11] Costa, R. R.; Mano, J. F., Polyelectrolyte multilayered assemblies in biomedical technologies. *Chem. Soc. Rev.* **2014**, *43*, 3453.

[12] Saurer, E. M.; Flessner, R. M.; Sullivan, S. P.; Prausnitz, M. R.; Lynn, D. M., Layer-by-layer assembly of DNA- and protein-containing films on microneedles for drug delivery to the skin. *Biomacromolecules* **2010**, *11*, 3136.

[13] Such, G. K.; Johnston, A. P. R.; Caruso, F., Engineered hydrogen-bonded polymer multilayers: from assembly to biomedical applications. *Chem. Soc. Rev.* **2011**, *40*, 19.

[14] Nohria, R.; Khillan, R. K.; Su, Y.; Dikshit, R.; Lvov, Y.; Varahramyan, K., Humidity sensor based on ultrathin polyaniline film deposited using layer-by-layer nano-assembly. *Sens. Actuator B-Chem.* **2006**, *114*, 218.

[15] Kim, B.-S.; Park, S. W.; Hammond, P. T., Hydrogen-bonding layer-by-layer assembled biodegradable polymeric micelles as drug delivery vehicles from surfaces. *ACS Nano* **2008**, *2*, 386.

[16] Boudou, T.; Crouzier, T.; Nicolas, C.; Ren, K.; Picart, C., Polyelectrolyte multilayer nanofilms used as thin materials for cell mechano-sensitivity studies. *Macromol. Biosci.* **2011**, *11*, 77.

[17] Richert, L.; Lavalle, P.; Payan, E.; Shu, X. Z.; Prestwich, G. D.; Stoltz, J. F.; Schaaf, P.; Voegel, J. C.; Picart, C., Layer by layer buildup of polysaccharide films: Physical chemistry and cellular adhesion aspects. *Langmuir* **2004**, *20*, 448.

[18] Nepal, D.; Balasubramanian, S.; Simonian, A. L.; Davis, V. A., Strong antimicrobial coatings: Single-walled carbon nanotubes armored with biopolymers. *Nano Lett.* **2008**, *8*, 1896.

[19] Lichter, J. A.; Van Vliet, K. J.; Rubner, M. F., Design of antibacterial surfaces and interfaces: Polyelectrolyte multilayers as a multifunctional platform. *Macromolecules* **2009**, *42*, 8573.

[20] Dvoracek, C. M.; Sukhonosova, G.; Benedik, M. J.; Grunlan, J. C., Antimicrobial behavior of polyelectrolyte-surfactant thin film assemblies. *Langmuir* **2009**, *25*, 10322.

[21] Dubas, S. T.; Kumlangdudsana, P.; Potiyaraj, P., Layer-by-layer deposition of antimicrobial silver nanoparticles on textile fibers. *Colloids Surf., A* **2006**, *289*, 105.

[22] Weil, E. D., Fire-protective and flame-retardant coatings - a state-of-the-art review. *J. Fire Sci.* **2011**, *29*, 259.

[23] Morgan, A. B.; Gilman, J. W., An overview of flame retardancy of polymeric materials: application, technology, and future directions. *Fire Mater.* **2013**, *37*, 259.

[24] Yang, Y.-H.; Haile, M.; Park, Y. T.; Malek, F. A.; Grunlan, J. C., Super gas barrier of all-polymer multilayer thin films. *Macromolecules* **2011**, *44*, 1450.

[25] Yang, Y.-H.; Bolling, L.; Priolo, M. A.; Grunlan, J. C., Super gas barrier and selectivity of graphene oxide-polymer multilayer thin films. *Adv. Mater.* **2013**, *25*, 503.

[26] Svagan, A. J.; Akesson, A.; Cardenas, M.; Bulut, S.; Knudsen, J. C.; Risbo, J.; Plackett, D., Transparent films based on PLA and montmorillonite with tunable oxygen barrier properties. *Biomacromolecules* **2012**, *13*, 397.

[27] Priolo, M. A.; Holder, K. M.; Guin, T.; Grunlan, J. C., Recent advances in gas barrier thin films via layer-by-layer assembly of polymers and platelets. *Macromol. Rapid Commun.* **2015**, *36*, 866.

[28] Priolo, M. A.; Holder, K. M.; Gamboa, D.; Grunlan, J. C., Influence of clay concentration on the gas barrier of clay-polymer nanobrick wall thin film assemblies. *Langmuir* **2011**, *27*, 12106.

[29] Priolo, M. A.; Gamboa, D.; Holder, K. M.; Grunlan, J. C., Super gas barrier of transparent polymer-clay multilayer ultrathin films. *Nano Lett.* **2010**, *10*, 4970.

[30] Priolo, M. A.; Gamboa, D.; Grunlan, J. C., Transparent clay-polymer nano brick wall assemblies with tailorable oxygen barrier. *ACS Appl. Mater. Interfaces* **2010**, *2*, 312.

[31] Laufer, G.; Kirkland, C.; Cain, A. A.; Grunlan, J. C., Clay-chitosan nanobrick walls: completely renewable gas barrier and flame-retardant nanocoatings. *ACS Appl. Mater. Interfaces* **2012**, *4*, 1643.

[32] Shui, S.; Plastina, A. *World Apparel Fiber Consumption Survey*, International Cotton Advisory Committee, **2013**.

[33] Day, M.; Suprunchuk, T.; Wiles, M., Combustibility study of gaseous pyrolysates produced by polyester/cotton blends. In *Fire Safety Science: Proceedings of the First International Symposium*; Grant, P. J. P. C. E., Ed.; Hemisphere Publishing: New York, NY, **1986,** 401.

[34] Hoebel, J.; Damant, G.; Spivak, S.; Berlin, G., Clothing-related burn casualties: an overlooked problem *Fire Technol.* **2010**, *46*, 765.

[35] Jarvis, C.; Barker, R., Flammability of cotton-polyester blend fabrics. In *Flame Retardant Polymeric Materials*; Lewin, M., Atlas, S. M., Pearce, E. M.; Springer: New York City, NY **1978,** p 133.

[36] Horrocks, A. R.; Wang, M. Y.; Hall, M. E.; Sunmonu, F.; Pearson, J. S., Flame retardant textile back-coatings. Part 2. Effectiveness of phosphorus-containing flame retardants in textile back-coating formulations. *Polym. Int.* **2000**, *49*, 1079.

[37] Weil, E. D.; Levchik, S. V., Flame retardants in commercial use or development for textiles. *J. Fire Sci.* **2008**, *26*, 243.

[38] Horrocks, A. R.; Kandola, B. K., Flame retardant textiles. In *Plastics Flammability Handbook: Principles, Regulations, Testing, and Approval*; 3rd ed.; Troitzsch, J., Ed.; Hanser Gardener: Cincinnati, OH **2004**, p 182.

[39] Drevelle, C.; Lefebvre, J.; Duquesne, S.; Le Bras, M.; Poutch, F.; Vouters, M.; Magniez, C., Thermal and fire behaviour of ammonium polyphosphate/acrylic coated cotton/PESFR fabric. *Polym. Degrad. Stab.* **2005**, *88*, 130.

[40] Lewin, M.; Sello, S. B. *Handbook of Fiber Science and Technology: Functional Finishes. Chemical Processing of Fibers and Fabrics*; Taylor & Francis: London, United Kingdom **1984.**

[41] Yang, H.; Yang, C. Q., Durable flame retardant finishing of the nylon/cotton blend fabric using a hydroxyl-functional organophosphorus oligomer. *Polym. Degrad. Stab.* **2005**, *88*, 363.

[42] de Wit, C. A., An overview of brominated flame retardants in the environment. *Chemosphere* **2002**, *46*, 583.

[43] Kim, Y. R.; Harden, F. A.; Toms, L.-M. L.; Norman, R. E., Health consequences of exposure to brominated flame retardants: A systematic review. *Chemosphere* **2014**, *106*, 1.

[44] Babrauskas, V.; Blum, A.; Daley, R.; Birnbaum, L., Flame retardants in furniture foam: benefits and risks. *Fire Safety Sci.* **2011**, *10*, 265.

[45] Watanabe, I.; Sakai, S.-i., Environmental release and behavior of brominated flame retardants. *Environ. Inter.* **2003**, *29*, 665.

[46] Renner, R., Watch: EPA won't regulate dioxin in sewage sludge. *Environ. Sci. Technol.* **2004**, *38*, 14.

[47] Wolska, A.; Goździkiewicz, M.; Ryszkowska, J., Thermal and mechanical behaviour of flexible polyurethane foams modified with graphite and phosphorous fillers. *J. Mater. Sci.* **2012**, *47*, 5627.

[48] Gavgani, J.; Adelnia, H.; Gudarzi, M., Intumescent flame retardant polyurethane/reduced graphene oxide composites with improved mechanical, thermal, and barrier properties. *J. Mater. Sci.* **2014**, *49*, 243.

[49] Cain, A. A.; Nolen, C. R.; Li, Y.-C.; Davis, R.; Grunlan, J. C., Phosphorous-filled nanobrick wall multilayer thin film eliminates polyurethane melt dripping and reduces heat release associated with fire. *Polym. Degrad. Stab.* **2013**, *98*, 2645.

[50] Cain, A. A.; Plummer, M. G. B.; Murray, S. E.; Bolling, L.; Regev, O.; Grunlan, J. C., Iron-containing, high aspect ratio clay as nanoarmor that imparts substantial thermal/flame protection to polyurethane with a single electrostatically-deposited bilayer. *J. Mater. Chem. A* **2014**, *2*, 17609.

[51] Carosio, F.; Di Blasio, A.; Cuttica, F.; Alongi, J.; Malucelli, G., Self-assembled hybrid nanoarchitectures deposited on poly(urethane) foams capable of chemically adapting to extreme heat. *RSC Adv.* **2014**, *4*, 16674.

[52] Chen, M.-J.; Shao, Z.-B.; Wang, X.-L.; Chen, L.; Wang, Y.-Z., Halogen-free flame-retardant flexible polyurethane foam with a novel nitrogen-phosphorus flame retardant. *Ind. Eng. Chem. Res.* **2012**, *51*, 9769.

[53] Haile, M.; Fomete, S.; Lopez, I.; Grunlan, J., Aluminum hydroxide multilayer assembly capable of extinguishing flame on polyurethane foam. *J. Mater. Sci.* **2016**, *51*, 375.

[54] Holder, K. M.; Huff, M. E.; Cosio, M. N.; Grunlan, J. C., Intumescing multilayer thin film deposited on clay-based nanobrick wall to produce self-extinguishing flame retardant polyurethane. *J. Mater. Sci.* **2015**, *50*, 2451.

[55] Kim, Y. S.; Li, Y.-C.; Pitts, W. M.; Werrel, M.; Davis, R. D., Rapid growing clay coatings to reduce the fire threat of furniture. *ACS Appl. Mater. Interfaces* **2014**, *6*, 2146.

[56] Laufer, G.; Kirkland, C.; Morgan, A. B.; Grunlan, J. C., Exceptionally flame retardant sulfur-based multilayer nanocoating for polyurethane prepared from aqueous polyelectrolyte solutions. *ACS Macro Lett.* **2013**, *2*, 361.

[57] Li, Y.-C.; Kim, Y. S.; Shields, J.; Davis, R., Controlling polyurethane foam flammability and mechanical behaviour by tailoring the composition of clay-based multilayer nanocoatings. *J. Mater. Chem. A* **2013**, *1*, 12987.

[58] Wang, J. Q.; Chow, W. K., A brief review on fire retardants for polymeric foams. *J. Appl. Polym. Sci.* **2005**, *97*, 366.

[59] Alongi, J.; Carosio, F.; Malucelli, G., Layer by layer complex architectures based on ammonium polyphosphate, chitosan and silica on polyester-cotton blends: flammability and combustion behaviour. *Cellulose* **2012**, *19*, 1041.

[60] Alongi, J.; Malucelli, G., Cotton flame retardancy: State of the art and future perspectives. *RSC Adv.* **2015**, *5*, 24239.

[61] Carosio, F.; Alongi, J., Few durable layers suppress cotton combustion due to the joint combination of layer by layer assembly and UV-curing. *RSC Adv.* **2015**, *5*, 71482.

[62] Carosio, F.; Di Blasio, A.; Alongi, J.; Malucelli, G., Green DNA-based flame retardant coatings assembled through layer by layer. *Polymer* **2013**, *54*, 5148.

[63] Guin, T.; Krecker, M.; Milhorn, A.; Grunlan, J. C., Maintaining hand and improving fire resistance of cotton fabric through ultrasonication rinsing of multilayer nanocoating. *Cellulose* **2014**, *21*, 3023.

[64] Laufer, G.; Kirkland, C.; Morgan, A. B.; Grunlan, J. C., Intumescent multilayer nanocoating, made with renewable polyelectrolytes, for flame-retardant cotton. *Biomacromolecules* **2012**, *13*, 2843.

[65] Leistner, M.; Abu-Odeh, A. A.; Rohmer, S. C.; Grunlan, J. C., Water-based chitosan/melamine polyphosphate multilayer nanocoating that extinguishes fire on polyester-cotton fabric. *Carbohydr. Polym.* **2015**, *130*, 227.

[66] Leistner, M.; Haile, M.; Rohmer, S.; Abu-Odeh, A.; Grunlan, J. C., Water-soluble polyelectrolyte complex nanocoating for flame retardant nylon-cotton fabric. *Polym. Degrad. Stab.* **2015**, *122*, 1.

[67] Li, Y.-C.; Mannen, S.; Morgan, A. B.; Chang, S.; Yang, Y.-H.; Condon, B.; Grunlan, J. C., Intumescent all-polymer multilayer nanocoating capable of extinguishing flame on fabric. *Adv. Mater.* **2011**, *23*, 3926.

[68] Pan, H.; Song, L.; Ma, L.; Pan, Y.; Liew, K.; Hu, Y., Layer-by-layer assembled thin films based on fully biobased polysaccharides: chitosan and phosphorylated cellulose for flame-retardant cotton fabric. *Cellulose* **2014**, *21*, 2995.

[69] Pan, H.; Wang, W.; Pan, Y.; Zeng, W.; Zhan, J.; Song, L.; Hu, Y.; Liew, K., Construction of layer-by-layer assembled chitosan/titanate nanotubes based nanocoating on cotton fabrics: flame retardant performance and combustion behavior. *Cellulose* **2015**, *22*, 911.

[70] Apaydin, K.; Laachachi, A.; Ball, V.; Jimenez, M.; Bourbigot, S.; Toniazzo, V.; Ruch, D., Polyallylamine-montmorillonite as super flame retardant coating assemblies by layer-by layer deposition on polyamide. *Polym. Degrad. Stab.* **2013**, *98*, 627.

[71] Apaydin, K.; Laachachi, A.; Ball, V.; Jimenez, M.; Bourbigot, S.; Toniazzo, V.; Ruch, D., Intumescent coating of (polyallylamine-polyphosphates) deposited on polyamide fabrics via layer-by-layer technique. *Polym. Degrad. Stab.* **2014**, *106*, 158.

[72] Carosio, F.; Di Blasio, A.; Cuttica, F.; Alongi, J.; Frache, A.; Malucelli, G., Flame retardancy of polyester fabrics treated by spray-assisted layer-by-layer silica architectures. *Ind. Eng. Chem. Res.* **2013**, *52*, 9544.

[73] Graff, G. L.; Burrows, P. E.; Williford, R. E.; Praino, R. F., Barrier layer technology for flexible displays. In *Flexible Flat Panel Displays*; John Wiley & Sons: Weinheim, Germany **2005**, p 57.

[74] Yam, K. L.; Lee, D. S., Emerging food packaging technologies. In *Emerging Food Packaging Technologies: Principles and Practice*; Woodhead: Cambridge, United Kingdom **2012**, p 1.

[75] Iler, R., Multilayers of colloidal particles. *J. Colloid Interface Sci.* **1966**, *21*, 569.

[76] Decher, G.; Hong, J. D.; Schmitt, J., Buildup of ultrathin multilayer films by a self-assembly process: III. Consecutively alternating adsorption of anionic and cationic polyelectrolytes on charged surfaces. *Thin Solid Films* **1992**, *210*, 831.

[77] Yang, Y.-H.; Malek, F. A.; Grunlan, J. C., Influence of deposition time on layer-by-layer growth of clay-based thin films. *Ind. Eng. Chem. Res.* **2010**, *49*, 8501.

[78] Priolo, M. A.; Holder, K. M.; Greenlee, S. M.; Stevens, B. E.; Grunlan, J. C., Precisely tuning the clay spacing in nanobrick wall gas barrier thin films. *Chem. Mater.* **2013**, *25*, 1649.

[79] Ratanatawanate, C.; Perez, M.; Gnade, B. E.; Balkus, K. J., Jr., Layer-by-layer assembly of titanate nanosheets/poly-(ethylenimine) on PEN films. *Mater. Lett.* **2012**, *66*, 242.

[80] Alongi, J.; Carletto, R. A.; Di Blasio, A.; Cuttica, F.; Carosio, F.; Bosco, F.; Malucelli, G., Intrinsic intumescent-like flame retardant properties of DNA-treated cotton fabrics. *Carbohydr. Polym.* **2013**, *96*, 296.

[81] Crespo-Biel, O.; Dordi, B.; Reinhoudt, D. N.; Huskens, J., Supramolecular layer-by-layer assembly: Alternating adsorptions of guest- and host-functionalized molecules and particles using multivalent supramolecular interactions. *J. Am. Chem. Soc.* **2005**, *127*, 7594.

[82] Zacharia, N. S.; Modestino, M.; Hammond, P. T., Factors influencing the interdiffusion of weak polycations in multilayers. *Macromolecules* **2007**, *40*, 9523.

[83] Kharlampieva, E.; Kozlovskaya, V.; Zavgorodnya, O.; Lilly, G. D.; Kotov, N. A.; Tsukruk, V. V., pH-responsive photoluminescent LbL hydrogels with confined quantum dots. *Soft Matter* **2010**, *6*, 800.

[84] Park, H. J.; Oh, K. A.; Park, M.; Lee, H., Electrical properties and conductivity mapping of thin multilayered films containing different types of carbon nanotubes. *J. Phys. Chem. C* **2009**, *113*, 13070.

[85] Park, Y. T.; Ham, A. Y.; Grunlan, J. C., High electrical conductivity and transparency in deoxycholate-stabilized carbon nanotube thin films. *J. Phys. Chem. C* **2010**, *114*, 6325.

[86] Sarker, A. K.; Hong, J.-D., Electrochemical reduction of ultrathin graphene oxide/polyaniline films for supercapacitor electrodes with a high specific capacitance. *Colloids Surf., A* **2013**, *436*, 967.

[87] Altman, M.; Shukla, A. D.; Zubkov, T.; Evmenenko, G.; Dutta, P.; Boom, M. E. v. d., Controlling structure from the bottom-up: structural and optical properties of layer-by-layer assembled palladium coordination-based multilayers. *J. Am. Chem. Soc.* **2006**, *128*, 7374.

[88] Fernandez, R.; Ocando, C.; Fernandes, S. C. M.; Eceiza, A.; Tercjak, A., Optically active multilayer films based on chitosan and an azopolymer. *Biomacromolecules* **2014**, *15*, 1399.

[89] Boudou, T.; Crouzier, T.; Ren, K.; Blin, G.; Picart, C., Multiple functionalities of polyelectrolyte multilayer films: new biomedical applications. *Adv. Mater.* **2010**, *22*, 441.

[90] Alemu, D.; Wei, H.-Y.; Ho, K.-C.; Chu, C.-W., Highly conductive PEDOT:PSS electrode by simple film treatment with methanol for ITO-free polymer solar cells. *Energ. Environ. Sci.* **2012**, *5*, 9662.

[91] Yu, B.; Liu, X. M.; Cong, H. L.; Wang, Z. H.; Tang, J. G., Fabrication of stable ultrathin transparent conductive graphene micropatterns using layer by layer self-assembly. *Sci. Adv. Mater.* **2013**, *5*, 1533.

[92] Dubas, S. T.; Schlenoff, J. B., Factors controlling the growth of polyelectrolyte multilayers. *Macromolecules* **1999**, *32*, 8153.

[93] Patel, P. A.; Dobrynin, A. V.; Mather, P. T., Combined effect of spin speed and ionic strength on polyelectrolyte spin assembly. *Langmuir* **2007**, *23*, 12589.

[94] Priolo, M. A.; Holder, K. M.; Gamboa, D.; Grunlan, J. C., Influence of clay concentration on the gas barrier of clay–polymer nanobrick wall thin film assemblies. *Langmuir* **2011**, *27*, 12106.

[95] Tan, H. L.; McMurdo, M. J.; Pan, G.; Van Patten, P. G., Temperature dependence of polyelectrolyte multilayer assembly. *Langmuir* **2003**, *19*, 9311.

[96] Xiang, F.; Tzeng, P.; Sawyer, J. S.; Regev, O.; Grunlan, J. C., Improving the gas barrier property of clay–polymer multilayer thin films using shorter deposition times. *ACS Appl. Mater. Interfaces* **2014**, *6*, 6040.

[97] Hagen, D. A.; Foster, B.; Stevens, B.; Grunlan, J. C., Shift-time polyelectrolyte multilayer assembly: fast film growth and high gas barrier with fewer layers by adjusting deposition time. *ACS Macro Lett.* **2014**, *3*, 663.

[98] Zhang, H.; Wang, D.; Wang, Z.; Zhang, X., Hydrogen bonded layer-by-layer assembly of poly(2-vinylpyridine) and poly(acrylic acid): Influence of molecular weight on the formation of microporous film by post-base treatment. *Eur. Polym. J.* **2007**, *43*, 2784.

[99] Shimazaki, Y.; Mitsuishi, M.; Ito, S.; Yamamoto, M., Preparation and characterization of the layer-by-layer deposited ultrathin film based on the charge-transfer interaction in organic solvents. *Langmuir* **1998**, *14*, 2768.

[100] Borges, J.; Mano, J. F., Molecular interactions driving the layer-by-layer assembly of multilayers. *Chem. Rev.* **2014**, *114*, 8883.

[101] Hodak, J.; Etchenique, R.; Calvo, E. J.; Singhal, K.; Bartlett, P. N., Layer-by-layer self-assembly of glucose oxidase with a poly(allylamine)ferrocene redox mediator. *Langmuir* **1997**, *13*, 2708.

[102] Liang, Z.; Dzienis, K. L.; Xu, J.; Wang, Q., Covalent layer-by-layer assembly of conjugated polymers and CdSe nanoparticles: multilayer structure and photovoltaic properties. *Adv. Funct. Mater.* **2006**, *16*, 542.

[103] Izquierdo, A.; Ono, S. S.; Voegel, J. C.; Schaaf, P.; Decher, G., Dipping versus spraying: Exploring the deposition conditions for speeding up layer-by-layer assembly. *Langmuir* **2005**, *21*, 7558.

[104] Krogman, K. C.; Lowery, J. L.; Zacharia, N. S.; Rutledge, G. C.; Hammond, P. T., Spraying asymmetry into functional membranes layer-by-layer. *Nat. Mater.* **2009**, *8*, 512.

[105] Saetia, K.; Schnorr, J. M.; Mannarino, M. M.; Kim, S. Y.; Rutledge, G. C.; Swager, T. M.; Hammond, P. T., Spray-layer-by-layer carbon nanotube/electrospun fiber electrodes for flexible chemiresistive sensor applications. *Adv. Funct. Mater.* **2014**, *24*, 492.

[106] Richardson, J. J.; Björnmalm, M.; Caruso, F., Technology-driven layer-by-layer assembly of nanofilms. *Science* **2015**, *348*, 411.

[107] Nogueira, G. M.; Banerjee, D.; Cohen, R. E.; Rubner, M. F., Spray-layer-by-layer assembly can more rapidly produce optical-quality multistack heterostructures. *Langmuir* **2011**, *27*, 7860.

[108] Xiang, F.; Givens, T. M.; Grunlan, J. C., Fast spray deposition of super gas barrier polyelectrolyte multilayer thin films. *Ind. Eng. Chem. Res.* **2015**, *54*, 5254.

[109] Thomas, I. M., Single-layer TiO_2 and multilayer TiO_2–SiO_2 optical coatings prepared from colloidal suspensions. *Appl. Opt.* **1987**, *26*, 4688.

[110] Seo, J.; Lutkenhaus, J. L.; Kim, J.; Hammond, P. T.; Char, K., Effect of the layer-by-layer (LbL) deposition method on the surface morphology and wetting behavior of hydrophobically modified PEO and PAA LbL films. *Langmuir* **2008**, *24*, 7995.

[111] Guin, T.; Krecker, M.; Milhorn, A.; Hagen, D. A.; Stevens, B.; Grunlan, J. C., Exceptional flame resistance and gas barrier with thick multilayer nanobrick wall thin films. *Adv. Mater. Interfaces* **2015**, *2*.

[112] Guin, T.; Krecker, M.; Hagen, D. A.; Grunlan, J. C., Thick growing multilayer nanobrick wall thin films: super gas barrier with very few layers. *Langmuir* **2014**, *30*, 7057.

[113] Hull, T. R.; Kandola, B. K. *Fire Retardancy of Polymers: New Strategies and Mechanisms*; Royal Society of Chemistry: London, United Kingdom **2009**.

[114] Kandola, B. K.; Horrocks, A. R. Complex char formation in flame-retarded fibre-intumescent combinations: Thermal analytical studies. *Polym. Degrad. Stab.* **1996**, *54*, 289.

[115] Hull, T. R.; Stec, A. A., Polymers and fire. In *Fire Retardancy of Polymers: New Strategies and Mechanisms,* Royal Society of Chemistry: London, United Kingdom **2009**.

[116] Li, Y.-C.; Schulz, J.; Grunlan, J. C., Polyelectrolyte/nanosilicate thin-film assemblies: influence of pH on growth, mechanical behavior, and flammability. *ACS Appl. Mater. Interfaces* **2009**, *1*, 2338.

[117] Li, Y. C.; Mannen, S.; Morgan, A. B.; Chang, S.; Yang, Y. H.; Condon, B.; Grunlan, J. C., Intumescent all-polymer multilayer nanocoating capable of extinguishing flame on fabric. *Adv. Mater.* **2011**, *23*, 3926.

[118] Malucelli, G., Surface-engineered fire protective coatings for fabrics through sol-gel and layer-by-layer methods: An overview. *Coatings* **2016**, *6*, 33.

[119] Carosio, F.; Alongi, J., Ultra-fast layer-by-layer approach for depositing flame retardant coatings on flexible PU foams within seconds. *ACS Appl. Mater. Interfaces* **2016**, *8*, 6315.

[120] Kamal, M.; Jinnah, I.; Utracki, L., Permeability of oxygen and water vapor through polyethylene/polyamide films. *Polym. Eng. Sci.* **1984**, *24*, 1337.

[121] Charton, C.; Schiller, N.; Fahland, M.; Holländer, A.; Wedel, A.; Noller, K., Development of high barrier films on flexible polymer substrates. *Thin Solid Films* **2006**, *502*, 99.

[122] Mattox, D. M., Vacuum evaporation and vacuum deposition. In *Handbook of Physical Vapor Deposition (PVD) Processing;* William Andrew Publishing: Boston, MA **2010**, p 1.

[123] Plichta, A.; Habeck, A.; Knoche, S.; Kruse, A.; Weber, A.; Hildebrand, N., Flexible glass substrates. In *Flexible Flat Panel Displays*; John Wiley & Sons: Weinheim, Germany **2005**, p 35.

[124] Hagen, D. A.; Box, C.; Greenlee, S.; Xiang, F.; Regev, O.; Grunlan, J. C., High gas barrier imparted by similarly charged multilayers in nanobrick wall thin films. *RSC Adv.* **2014**, *4*, 18354.

[125] Holder, K. M.; Priolo, M. A.; Secrist, K. E.; Greenlee, S. M.; Nolte, A. J.; Grunlan, J. C., Humidity-responsive gas barrier of hydrogen-bonded polymer-clay multilayer thin films. *J. Phys. Chem. C* **2012**, *116*, 19851.

[126] Priolo, M. A.; Holder, K. M.; Greenlee, S. M.; Grunlan, J. C., Transparency, gas barrier, and moisture resistance of large-aspect-ratio vermiculite nanobrick wall thin films. *ACS Appl. Mater. Interfaces* **2012**, *4*, 5529.

[127] Tzeng, P.; Maupin, C. R.; Grunlan, J. C., Influence of polymer interdiffusion and clay concentration on gas barrier of polyelectrolyte/clay nanobrick wall quadlayer assemblies. *J. Membr. Sci.* **2014**, *452*, 46.

[128] Nielsen, L. E., Models for the permeability of filled polymer systems. *J. Macromol. Sci. A* **1967**, *1*, 929.

[129] Kim, D.; Tzeng, P.; Barnett, K. J.; Yang, Y. H.; Wilhite, B. A.; Grunlan, J. C., Highly size-selective ionically crosslinked multilayer polymer films for light gas separation. *Adv. Mater.* **2014**, *26*, 746.

[130] Fuoss, R.; Sadek, H., Mutual interaction of polyelectrolytes. *Science* **1949**, *110*, 552.

[131] Thünemann, A. F.; Müller, M.; Dautzenberg, H.; Löwen, J.-f. J., Polyelectrolytes with defined molecular architecture II. *Adv. Polym. Sci.* **2004**, *166*, 113.

[132] Vanerek, A.; van de Ven, T. G. M., Coacervate complex formation between cationic polyacrylamide and anionic sulfonated kraft lignin. *Colloids Surf., A* **2006**, *273*, 55.

[133] Wang, Q.; Schlenoff, J. B., The polyelectrolyte complex/coacervate continuum. *Macromolecules* **2014**, *47*, 3108.

[134] Pogodina, N. V.; Tsvetkov, N. V., Structure and dynamics of the polyelectrolyte complex formation. *Macromolecules* **1997**, *9297*, 4897.

[135] Cini, N.; Tulun, T.; Blanck, C.; Toniazzo, V.; Ruch, D.; Decher, G.; Ball, V., Slow complexation dynamics between linear short polyphosphates and polyallylamines: analogies with "layer-by-layer" deposits. *PCCP* **2012**, *14*, 3048.

[136] Dautzenberg, H., Polyelectrolyte complex formation in highly aggregating systems. 1. effect of salt: Polyelectrolyte complex formation in the presence of NaCl. *Macromolecules* **1997**, *9297*, 7810.

[137] Petzold, G.; Schwarz, S., Polyelectrolyte complexes in flocculation applications. *Adv. Polym. Sci.* **2014**, *256*, 25.

[138] Gärdlund, L.; Wågberg, L.; Gernandt, R., Polyelectrolyte complexes for surface modification of wood fibres: II. Influence of complexes on wet and dry strength of paper. *Colloids Surf., A* **2003**, *218*, 137.

[139] Rojas, O. J.; Neuman, R. D., Adsorption of polysaccharide wet-end additives in papermaking systems. *Colloids Surf., A* **1999**, *155*, 419.

[140] Kim, S.-G.; Ahn, H.-R.; Lee, K.-H., Pervaporation characteristics of polyelectrolyte complex gel membranes based on two anionic polysaccharides having a chelating structure. *Curr. App. Phys.* **2009**, *9*, 42.

[141] Zhao, Q.; An, Q. F.; Ji, Y.; Qian, J.; Gao, C., Polyelectrolyte complex membranes for pervaporation, nanofiltration and fuel cell applications. *J. Membr. Sci.* **2011**, *379*, 19.

[142] Balachandra, A. M.; Dai, J.; Bruening, M. L., Enhancing the anion-transport selectivity of multilayer polyelectrolyte membranes by templating with Cu^{2+}. *Macromolecules* **2002**, *35*, 3171.

[143] Dong, L. C.; Hoffman, A. S., Thermally reversible hydrogels: III. Immobilization of enzymes for feedback reaction control. *J. Control. Rel.* **1986**, *4*, 223.

[144] Hoffman, A. S., Applications of thermally reversible polymers and hydrogels in therapeutics and diagnostics. *J. Control. Release* **1987**, *6*, 297.

[145] Shiroya, T.; Tamura, N.; Yasui, M.; Fujimoto, K.; Kawaguchi, H., Enzyme immobilization on thermosensitive hydrogel microspheres. *Colloids Surf., B* **1995**, *4*, 267.

[146] Bajpai, A. K.; Shukla, S. K.; Bhanu, S.; Kankane, S., Responsive polymers in controlled drug delivery. *Prog. Poly. Sci.* **2008**, *33*, 1088.

[147] Lankalapalli, S.; Kolapalli, V., Polyelectrolyte complexes: A review of their applicability in drug delivery technology. *Indian J. Pharm. Sci.* **2009**, *71*, 481.

[148] Qiu, Y.; Park, K., Environment-sensitive hydrogels for drug delivery. *Adv. Drug Deliv. Rev.* **2001**, *53*, 321.

[149] York, A. W.; Kirkland, S. E.; McCormick, C. L., Advances in the synthesis of amphiphilic block copolymers via RAFT polymerization: Stimuli-responsive drug and gene delivery. *Adv. Drug Deliv. Rev.* **2008**, *60*, 1018.

[150] Sukhishvili, S. A.; Kharlampieva, E.; Izumrudov, V., Where polyelectrolyte multilayers and polyelectrolyte complexes meet. *Macromolecules* **2006**, *39*, 8873.

[151] Cundall, R. B.; Lawton, J. B.; Murray, D., The effect of ph and ionic strength on the stoichiometry of model polycation - polyanion complexes. *Macromol. Chem. and Phys.* **1979**, *2922*, 2913.

[152] Izumrudov, V.; Kharlampieva, E.; Sukhishvili, S. A., Salt-induced multilayer growth: correlation with phase separation in solution. *Macromolecules* **2004**, *37*, 8400.

[153] Izumrudov, V.; Sukhishvili, S. A., Ionization-controlled stability of polyelectrolyte multilayers in salt solutions. *Langmuir* **2003**, *19*, 5188.

[154] Dautzenberg, H.; Jaeger, W., Effect of charge density on the formation and salt stability of polyelectrolyte complexes. *Macromol. Chem. Phys.* **2002**, *203*, 2095.

[155] Birch, N. P.; Schiffman, J. D., Characterization of self-assembled polyelectrolyte complex nanoparticles formed from chitosan and pectin. *Langmuir* **2014**, *30*, 3441.

[156] Li, J.; Huang, P.; Chang, L.; Long, X.; Dong, A.; Liu, J.; Chu, L.; Hu, F.; Liu, J.; Deng, L., Tumor targeting and pH-responsive polyelectrolyte complex nanoparticles based on hyaluronic acid-paclitaxel conjugates and Chitosan for oral delivery of paclitaxel. *Macromol. Res.* **2013**, *21*, 1331.

[157] Lin, W.-C.; Yu, D.-G.; Yang, M.-C., pH-sensitive polyelectrolyte complex gel microspheres composed of chitosan/sodium tripolyphosphate/dextran sulfate: swelling kinetics and drug delivery properties. *Colloids Surf., B* **2005**, *44*, 143.

[158] Hamman, J. H., Chitosan based polyelectrolyte complexes as potential carrier materials in drug delivery systems. *Marine Drugs* **2010**, *8*, 1305.

[159] Chen, J.; Hubbe, M. A.; Heitmann, J. A.; Argyropoulos, D. S.; Rojas, O. J., Dependency of polyelectrolyte complex stoichiometry on the order of addition: 2. Aluminum chloride and poly-vinylsulfate. *Colloids Surf., A* **2004**, *246*, 71.

[160] Ankerfors, C.; Ondaral, S.; Wågberg, L.; Ödberg, L., Using jet mixing to prepare polyelectrolyte complexes: Complex properties and their interaction with silicon oxide surfaces. *J. Coll. Inter. Sci.* **2010**, *351*, 88.

[161] Ghostine, R. A.; Shamoun, R. F.; Schlenoff, J. B., Doping and diffusion in an extruded saloplastic polyelectrolyte complex. *Macromolecules* **2013**, *46*, 4089.

[162] Shamoun, R. F.; Hariri, H. H.; Ghostine, R. A.; Schlenoff, J. B., Thermal transformations in extruded saloplastic polyelectrolyte complexes. *Macromolecules* **2012**, *45*, 9759.

[163] Reisch, A.; Tirado, P.; Roger, E.; Boulmedais, F.; Collin, D.; Voegel, J.-C.; Frisch, B.; Schaaf, P.; Schlenoff, J. B., Compact saloplastic poly(acrylic acid)/poly(allylamine) complexes: Kinetic control over composition, microstructure, and mechanical properties. *Adv. Funct. Mater.* **2013**, *23*, 673.

[164] Fu, J.; Wang, Q.; Schlenoff, J. B., Extruded superparamagnetic saloplastic polyelectrolyte nanocomposites. *ACS Appl. Mater. Interfaces* **2014**, *7*, 895.

[165] Zhao, Q.; An, Q.-F.; Liu, T.; Chen, J.-T.; Chen, F.; Lee, K.-R.; Gao, C.-J., Bio-inspired polyelectrolyte complex/graphene oxide nanocomposite membranes with enhanced tensile strength and ultra-low gas permeability. *Polym. Chem.* **2013**, *4*, 4298.

[166] Ball, V.; Michel, M.; Toniazzo, V.; Ruch, D., The possibility of obtaining films by single sedimentation of polyelectrolyte complexes.n *Ind. Eng. Chem. Res.* **2013**, *52*, 5691.

[167] Cain, A. A.; Murray, S.; Holder, K. M.; Nolen, C. R.; Grunlan, J. C., Intumescent nanocoating extinguishes flame on fabric using aqueous polyelectrolyte complex deposited in single step. *Macromol. Mater. Eng.* **2014**, *299*, 1180.

[168] Kelly, K. D.; Schlenoff, J. B., Spin-coated polyelectrolyte coacervate films. *ACS Appl. Mater. Interfaces* **2015**, *7*, 13980.

[169] Shovsky, A.; Varga, I.; Makuska, R.; Claesson, P. M., Formation and stability of water-soluble, molecular polyelectrolyte complexes: Effects of charge density, mixing ratio, and polyelectrolyte concentration. *Langmuir* **2009**, *25*, 6113.

[170] Acar, N.; Huglin, M. B.; Tulun, T., Complex formation between poly(sodium phosphate) and poly(4-vinylpyridinium chloride) in aqueous solution. *Polymer* **1999**, *40*, 6429.

[171] Cini, N.; Tulun, T.; Blanck, C.; Toniazzo, V.; Ruch, D.; Decher, G.; Ball, V., Slow complexation dynamics between linear short polyphosphates and polyallylamines: analogies with "layer-by-layer" deposits. *PCCP.* **2012**, *14*, 3048.

[172] von Harpe, A.; Petersen, H.; Li, Y. X.; Kissel, T., Characterization of commercially available and synthesized polyethylenimines for gene delivery. *J. Controll. Release* **2000**, *69*, 309.

[173] Dobrynin, A. V.; Rubinstein, M., Theory of polyelectrolytes in solutions and at surfaces. *Prog. Polym. Sci.* **2005**, *30*, 1049.

[174] Choi, J.; Rubner, M. F., Influence of the degree of ionization on weak polyelectrolyte multilayer assembly. *Macromolecules* **2004**, *38*, 116.

[175] Bourbigot, S.; Le Bras, M.; Duquesne, S.; Rochery, M., Recent advances for intumescent polymers. *Macromol. Mater. Eng.* **2004**, *289*, 499.

[176] Horrocks, A. R.; Price, D. *Fire Retardant Materials*; CRC Press: Boca Raton, FL **2001**.

[177] Alongi, J.; Carosio, F.; Malucelli, G., Current emerging techniques to impart flame retardancy to fabrics: An overview. *Polym. Degrad. Stab.* **2014**, *106*, 138.

[178] Carosio, F.; Alongi, J.; Malucelli, G., Layer by layer ammonium polyphosphate-based coatings for flame retardancy of polyester–cotton blends. *Carbohydr. Polym.* **2012**, *88*, 1460.

[179] Zhang, T.; Yan, H.; Wang, L.; Fang, Z., Controlled formation of self-extinguishing intumescent coating on ramie fabric via layer-by-layer assembly. *Ind. Eng. Chem. Res.* **2013**, *52*, 6138.

[180] Li, Y.-C.; Schulz, J.; Mannen, S.; Delhom, C.; Condon, B.; Chang, S.; Zammarano, M.; Grunlan, J. C., Flame retardant behavior of polyelectrolyte-clay thin film assemblies on cotton fabric. *ACS Nano* **2010**, *4*, 3325.

[181] Wang, X.; Romero, M. Q.; Zhang, X.-Q.; Wang, R.; Wang, D.-Y., Intumescent multilayer hybrid coating for flame retardant cotton fabrics based on layer-by-layer assembly and sol-gel process. *RSC Adv.* **2015**, *5*, 10647.

[182] Hammond, P. T., Form and function in multilayer assembly: new applications at the nanoscale. *Adv. Mater.* **2004**, *16*, 1271.

[183] Haile, M.; Fincher, C.; Fomete, S.; Grunlan, J. C., Water-soluble polyelectrolyte complexes that extinguish fire on cotton fabric when deposited as pH-cured nanocoating. *Polym. Degrad. Stab.* **2015**, *114*, 60.

[184] Fang, M.; Kim, C. H.; Saupe, G. B.; Kim, H.-N.; Waraksa, C. C.; Miwa, T.; Fujishima, A.; Mallouk, T. E., Layer-by-layer growth and condensation reactions of niobate and titanoniobate thin films. *Chem. Mater.* **1999**, *11*, 1526.

[185] Kumar, R. S.; Auch, M.; Ou, E.; Ewald, G.; Jin, C. S., Low moisture permeation measurement through polymer substrates for organic light emitting devices. *Thin Solid Films* **2002**, *417*, 120.

[186] Roberts, A. P.; Henry, B. M.; Sutton, A. P.; Grovenor, C. R. M.; Briggs, G. A. D.; Miyamoto, T.; Kano, A.; Tsukahara, Y.; Yanaka, M., Gas permeation in silicon-oxide/polymer (SiOx/PET) barrier films: role of the oxide lattice, nano-defects and macro-defects. *J. Membr. Sci.* **2002**, *208*, 75.

[187] Affinito, J. D.; Gross, M. E.; Coronado, C. A.; Graff, G. L.; Greenwell, E. N.; Martin, P. M., A new method for fabricating transparent barrier layers. *Thin Solid Films* **1996**, *290*, 63.

[188] Xiang, F.; Givens, T. M.; Ward, S. M.; Grunlan, J. C., Elastomeric polymer multilayer thin film with sustainable gas barrier at high strain. *ACS Appl. Mater. Interfaces* **2015**, *7*, 16148.

[189] Ariga, K.; Yamauchi, Y.; Rydzek, G.; Ji, Q.; Yonamine, Y.; Wu, K. C. W.; Hill, J. P., Layer-by-layer nanoarchitectonics: invention, innovation, and evolution. *Chem. Lett.* **2014**, *43*, 36.

[190] Chollakup, R.; Smitthipong, W.; Eisenbach, C. D.; Tirrell, M., Phase behavior and coacervation of aqueous poly(acrylic acid)-poly(allylamine) solutions. *Macromolecules* **2010**, *43*, 2518.

[191] Spruijt, E.; Stuart, M. A. C.; van der Gucht, J., Linear viscoelasticity of polyelectrolyte complex coacervates. *Macromolecules* **2013**, *46*, 1633.

[192] Perry, S. L.; Li, Y.; Priftis, D.; Leon, L.; Tirrell, M., The effect of salt on the complex coacervation of vinyl polyelectrolytes. *Polymers* **2014**, *6*, 1756.

[193] Dan, B.; Irvin, G. C.; Pasquali, M., Continuous and scalable fabrication of transparent conducting carbon nanotube films. *ACS Nano* **2009**, *3*, 835.

[194] Ploehn, H. J.; Liu, C. Y., Quantitative analysis of montmorillonite platelet size by atomic force microscopy. *Ind. Eng. Chem. Res.* **2006**, *45*, 7025.

[195] Ying, Q.; Chu, B., Overlap concentration of macromolecules in solution. *Macromolecules* **1987**, *20*, 362.

[196] Meng, Y.; Xu, X.-B.; Li, H.; Wang, Y.; Ding, E.-X.; Zhang, Z.-C.; Geng, H.-Z., Optimisation of carbon nanotube ink for large-area transparent conducting films fabricated by controllable rod-coating method. *Carbon* **2014**, *70*, 103.

[197] Benedek, I.; Feldstein, M. M. *Technology of Pressure-Sensitive Adhesives and Products*; CRC Press: Boca Raton, FL **2008**.

[198] Lagaron, J. M.; Catala, R.; Gavara, R., Structural characteristics defining high barrier properties in polymeric materials. *Mater. Sci. Technol.* **2004**, *20*, 1.

[199] Lagaron, J. M.; Powell, A. K.; Bonner, G., Permeation of water, methanol, fuel and alcohol-containing fuels in high-barrier ethylene-vinyl alcohol copolymer. *Polym. Test.* **2001**, *20*, 569.

[200] Yang, Y.-H.; Bolling, L.; Haile, M.; Grunlan, J. C., Improving oxygen barrier and reducing moisture sensitivity of weak polyelectrolyte multilayer thin films with crosslinking. *RSC Adv.* **2012**, *2*, 12355.

[201] Möller, M. W.; Kunz, D. A.; Lunkenbein, T.; Sommer, S.; Nennemann, A.; Breu, J., UV-cured, flexible, and transparent nanocomposite coating with remarkable oxygen barrier. *Adv. Mater.* **2012**, *24*, 2142.

[202] Priolo, M. A.; Gamboa, D.; Holder, K. M.; Grunlan, J. C., Super gas barrier of transparent polymer−clay multilayer ultrathin films. *Nano Lett.* **2010**, *10*, 4970.

[203] Holder, K. M.; Spears, B. R.; Huff, M. E.; Priolo, M. A.; Harth, E.; Grunlan, J. C., Stretchable gas barrier achieved with partially hydrogen- bonded multilayer nanocoating. *Macromol. Rapid Commun.* **2014**, *35*, 960.

[204] Xiang, F.; Ward, S. M.; Givens, T. M.; Grunlan, J. C., Super stretchy polymer multilayer thin film with high gas barrier. *ACS Macro Lett.* **2014**, *3*, 1055.

[205] Park, Y. T.; Ham, A. Y.; Grunlan, J. C., Heating and acid doping thin film carbon nanotube assemblies for high transparency and low sheet resistance. *J. Mater. Chem.* **2011**, *21*, 363.

[206] Park, Y. T.; Ham, A. Y.; Yang, Y.-H.; Grunlan, J. C., Fully organic ITO replacement through acid doping of double-walled carbon nanotube thin film assemblies. *RSC Adv.* **2011**, *1*, 662.

[207] Shim, B. S.; Zhu, J.; Jan, E.; Critchley, K.; Kotov, N. A., Transparent conductors from layer-by-layer assembled SWNT films: importance of mechanical properties and a new figure of merit. *ACS Nano* **2010**, *4*, 3725.

[208] Dikin, D. A.; Stankovich, S.; Zimney, E. J.; Piner, R. D.; Dommett, G. H.; Evmenenko, G.; Nguyen, S. T.; Ruoff, R. S., Preparation and characterization of graphene oxide paper. *Nature* **2007**, *448*, 457.

[209] Karter, M. J. *Fire Loss in the United States During 2012*; National Fire Protection Association, **2013**.

[210] Grand, A. F.; Wilkie, C. A. *Fire Retardancy of Polymeric Materials*; CRC Press: Boca Raton, FL **2000**.

[211] Kim, Y. S.; Davis, R., Multi-walled carbon nanotube layer-by-layer coatings with a trilayer structure to reduce foam flammability. *Thin Solid Films* **2014**, *550*, 184.

[212] Patra, D.; Vangal, P.; Cain, A. A.; Cho, C.; Regev, O.; Grunlan, J. C., Inorganic nanoparticle thin film that suppresses flammability of polyurethane with only a single electrostatically-assembled bilayer. *ACS Appl. Mater. Interfaces* **2014**, *6*, 16903.

[213] Thirumal, M.; Khastgir, D.; Nando, G. B.; Naik, Y. P.; Singha, N. K., Halogen-free flame retardant PUF: Effect of melamine compounds on mechanical, thermal and flame retardant properties. *Polym. Degrad. Stab.* **2010**, *95*, 1138.

[214] Huang, G.; Yang, J.; Gao, J.; Wang, X., Thin films of intumescent flame retardant-polyacrylamide and exfoliated graphene oxide fabricated via layer-by-layer assembly for improving flame retardant properties of cotton fabric. *Ind. Eng. Chem. Res.* **2012**, *51*, 12355.

[215] Ai, H.; Gao, J., Size-controlled polyelectrolyte nanocapsules via layer-by-layer self-assembly. *J. Mater. Sci.* **2004**, *39*, 1429.

[216] Aulin, C.; Karabulut, E.; Amy, T.; Wagberg, L.; Lindstrom, T., Transparent nanocellulosic multilayer thin films on polylactic acid with tunable gas barrier properties. *ACS Appl. Mater. Interfaces* **2013**, *5*, 7352.

[217] Zhu, J.; Morgan, A. B.; Lamelas, F. J.; Wilkie, C. A., Fire properties of polystyrene-clay nanocomposites. *Chem. Mater.* **2001**, *13*, 3774.

[218] Laachachi, A.; Ferriol, M.; Cochez, M.; Lopez Cuesta, J. M.; Ruch, D., A comparison of the role of boehmite (AlOOH) and alumina (Al2O3) in the thermal stability and flammability of poly(methyl methacrylate). *Polym. Degrad. Stab.* **2009**, *94*, 1373.

[219] Kogel, J. E. *Industrial Minerals & Rocks: Commodities, Markets, and Uses*; Society for Mining: Littleton, CO **2006**.

[220] Lvov, Y. M.; Pattekari, P.; Zhang, X.; Torchilin, V., Converting poorly soluble materials into stable aqueous nanocolloids. *Langmuir* **2011**, *27*, 1212.

[221] Kim, D.; Tzeng, P.; Barnett, K. J.; Yang, Y.-H.; Wilhite, B. A.; Grunlan, J. C., Highly size-selective ionically crosslinked multilayer polymer films for light gas separation. *Adv. Mater.* **2014**, *26*, 746.

[222] Kashiwagi, T.; Shields, J. R.; Harris, R. H.; Davis, R. D., Flame-retardant mechanism of silica: Effects of resin molecular weight. *J. Appl. Polym. Sci.* **2003**, *87*, 1541.

[223] Laoutid, F.; Bonnaud, L.; Alexandre, M.; Lopez-Cuesta, J. M.; Dubois, P., New prospects in flame retardant polymer materials: From fundamentals to nanocomposites. *Materials Science & Engineering R-Reports* **2009**, *63*, 100.

[224] Jiao, L.; Xiao, H.; Wang, Q.; Sun, J., Thermal degradation characteristics of rigid polyurethane foam and the volatile products analysis with TG-FTIR-MS. *Polym. Degrad. Stab.* **2013**, *98*, 2687.

[225] Morgan, A. B.; Liu, W., Flammability of thermoplastic carbon nanofiber nanocomposites. *Fire Mater.* **2011**, *35*, 43.

[226] Qin, F.; Brosseau, C., A review and analysis of microwave absorption in polymer composites filled with carbonaceous particles. *J. Appl. Phys.* **2012**, *111*, 061301.

[227] Irin, F.; Shrestha, B.; Canas, J. E.; Saed, M. A.; Green, M. J., Detection of carbon nanotubes in biological samples through microwave-induced heating. *Carbon* **2012**, *50*, 4441.

[228] Bourdiol, F.; Dubuc, D.; Grenier, K.; Mouchet, F.; Gauthier, L.; Flahaut, E., Quantitative detection of carbon nanotubes in biological samples by an original method based on microwave permittivity measurements. *Carbon* **2015**, *81*, 535.

[229] Li, S.; Irin, F.; Atore, F. O.; Green, M. J.; Cañas-Carrell, J. E., Determination of multi-walled carbon nanotube bioaccumulation in earthworms measured by a microwave-based detection technique. *Sci. Total Environ.* **2013**, *445*, 9.

[230] Imholt, T. J.; Dyke, C. A.; Hasslacher, B.; Perez, J. M.; Price, D. W.; Roberts, J. A.; Scott, J. B.; Wadhawan, A.; Ye, Z.; Tour, J. M., Nanotubes in microwave fields: Light emission, intense heat, outgassing, and reconstruction. *Chem. Mater.* **2003**, *15*, 3969.

[231] Kuang, T.; Chang, L.; Chen, F.; Sheng, Y.; Fu, D.; Peng, X., Facile preparation of lightweight high-strength biodegradable polymer/multi-walled carbon nanotubes nanocomposite foams for electromagnetic interference shielding. *Carbon* **2016**, *105*, 305.

[232] Risch, S. J., Food packaging history and innovations. *J. Agric. Food Chem.* **2009**, *57*, 8089.

[233] Azoubel, S.; Magdassi, S., Controlling adhesion properties of SWCNT–PET films prepared by wet deposition. *ACS Appl. Mater. Interfaces* **2014**, *6*, 9265.

[234] Saib, A.; Bednarz, L.; Daussin, R.; Bailly, C.; Lou, X.; Thomassin, J.-M.; Pagnoulle, C.; Detrembleur, C.; Jérôme, R.; Huynen, I., Carbon nanotube composites for broadband microwave absorbing materials. *Microwave Theory and Techniques, IEEE Transactions on* **2006**, *54*, 2745.

[235] Zhao, T.; Hou, C.; Zhang, H.; Zhu, R.; She, S.; Wang, J.; Li, T.; Liu, Z.; Wei, B., Electromagnetic wave absorbing properties of amorphous carbon nanotubes. *Scientific Reports* **2014**, *4*, 5619.

[236] Cho, C.; Wallace, K.; Tzeng, P.; Hsu, J.-H.; Yu, C.; Grunlan, J., Outstanding low temperature thermoelectric power factor from completely organic thin films enabled by multidimensional conjugated nanomaterials. *Adv. Energ. Mater.* **2016**, *6*, 1502168.

[237] Wu, F.; Li, J.; Su, Y.; Wang, J.; Yang, W.; Li, N.; Chen, L.; Chen, S.; Chen, R.; Bao, L., Layer-by-layer assembled architecture of polyelectrolyte multilayers and graphene sheets on hollow carbon spheres/sulfur composite for high-performance lithium–sulfur batteries. *Nano Lett.* **2016**.

[238] Rydzek, G.; Ji, Q.; Li, M.; Schaaf, P.; Hill, J. P.; Boulmedais, F.; Ariga, K., Electrochemical nanoarchitectonics and layer-by-layer assembly: From basics to future. *Nano Today* **2015**, *10*, 138.

[239] Lee, S. W.; Yabuuchi, N.; Gallant, B. M.; Chen, S.; Kim, B.-S.; Hammond, P. T.; Shao-Horn, Y., High-power lithium batteries from functionalized carbon-nanotube electrodes. *Nat. Nanotechnol.* **2010**, *5*, 531.

[240] Gentile, P.; Frongia, M. E.; Cardellach, M.; Miller, C. A.; Stafford, G. P.; Leggett, G. J.; Hatton, P. V., Functionalised nanoscale coatings using layer-by-

layer assembly for imparting antibacterial properties to polylactide-co-glycolide surfaces. *Acta Biomater.* **2015**, *21*, 35.

[241] Lee, K.-H.; Hong, J.; Kwak, S. J.; Park, M.; Son, J. G., Spin self-assembly of highly ordered multilayers of graphene-oxide sheets for improving oxygen barrier performance of polyolefin films. *Carbon* **2015**, *83*, 40.

[242] Cao, Q.; Kim, H.-S.; Pimparkar, N.; Kulkarni, J. P.; Wang, C.; Shim, M.; Roy, K.; Alam, M. A.; Rogers, J. A., Medium-scale carbon nanotube thin-film integrated circuits on flexible plastic substrates. *Nature* **2008**, *454*, 495.

[243] Kumar, B.; Park, Y. T.; Castro, M.; Grunlan, J. C.; Feller, J. F., Fine control of carbon nanotubes–polyelectrolyte sensors sensitivity by electrostatic layer by layer assembly (eLbL) for the detection of volatile organic compounds (VOC). *Talanta* **2012**, *88*, 396.

[244] Park, Y.; Ham, A.; Grunlan, J., High electrical conductivity and transparency in deoxycholate-stabilized carbon nanotube thin films. *J. Phys. Chem. C* **2010**, *114*, 6325.

[245] Mamedov, A. A.; Kotov, N. A.; Prato, M.; Guldi, D. M.; Wicksted, J. P.; Hirsch, A., Molecular design of strong single-wall carbon nanotube/polyelectrolyte multilayer composites. *Nat. Mater.* **2002**, *1*, 257.

[246] Kovtyukhova, N. I.; Mallouk, T. E., Ultrathin anisotropic films assembled from individual single-walled carbon nanotubes and amine polymers. *J. Phys. Chem. B* **2005**, *109*, 2540.

[247] Loh, K. J.; Kim, J.; Lynch, J. P.; Shi Kam, N. W.; Kotov, N. A., Multifunctional layer-by-layer carbon nanotube-polyelectrolyte thin films for strain and corrosion sensing. *Smart Mater. Struc.* **2007**, *16*, 429.

[248] Gheith, M. K.; Pappas, T. C.; Liopo, A. V.; Sinani, V. A.; Shim, B. S.; Motamedi, M.; Wicksted, J. R.; Kotov, N. A., Stimulation of neural cells by lateral layer-by-layer films of single-walled currents in conductive carbon nanotubes. *Adv. Mater.* **2006**, *18*, 2975.

[249] Moriarty, G. P.; De, S.; King, P. J.; Khan, U.; Via, M.; King, J. A.; Coleman, J. N.; Grunlan, J. C., Thermoelectric behavior of organic thin film nanocomposites. *J. Polym. Sci., B* **2013**, *51*, 119.

[250] Petrov, V.; Gagulin, V., Microwave absorbing materials. *Inorg. Mater.* **2001**, *37*, 93.

[251] Vazquez, E.; Prato, M., Carbon nanotubes and microwaves: interactions, responses, and applications. *ACS Nano* **2009**, *3*, 3819.

[252] Xiao, L.; Chen, Z.; Feng, C.; Liu, L.; Bai, Z. Q.; Wang, Y.; Qian, L.; Zhang, Y. Y.; Li, Q. Q.; Jiang, K. L.; Fan, S. S., Flexible, stretchable, transparent carbon nanotube thin film loudspeakers. *Nano Lett.* **2008**, *8*, 4539.

[253] Suzuki, K.; Sakakibara, S.; Okada, M.; Neo, Y.; Mimura, H.; Inoue, Y.; Murata, T., Study of carbon-nanotube web thermoacoustic loud speakers. *Jpn. J. Appl. Phys.* **2011**, *50*.

[254] Wei, Y.; Lin, X. Y.; Jiang, K. L.; Liu, P.; Li, Q. Q.; Fan, S. S., Thermoacoustic chips with carbon nanotube thin yarn arrays. *Nano Lett.* **2013**, *13*, 4795.

[255] Buzaglo, M.; Shtein, M.; Kober, S.; Lovrincic, R.; Vilan, A.; Regev, O., Critical parameters in exfoliating graphite into graphene. *PCCP* **2013**, *15*, 4428.

[256] Owens, D. K., The mechanism of corona and ultraviolet light-induced self-adhesion of poly(ethylene terephthalate) film. *J. Appl. Polym. Sci.* **1975**, *19*, 3315.

[257] Vargas, E.; Pantoya, M. L.; Saed, M. A.; Weeks, B. L., Advanced susceptors for microwave heating of energetic materials. *Mater. Des.* **2016**, *90*, 47.

APPENDIX A

ALUMINUM HYDROXIDE MULTILAYER ASSEMBLY CAPABLE OF EXTINGUISHING FLAME ON POLYURETHANE FOAM*

A.1 Introduction

An average of 2500 people died each year in home fires in the United States, from 2008 to 2012, according to the National Fire Protection Association.[113,209] The prevalence of polyurethane (PU) foam (commonly found in furniture, bedding, and packaging) provides fuel for these fires. Due to its chemical structure, high surface area, and high permeability to air, PU foams are highly flammable and often require the use of flame retardant (FR) additives, with organohalogen compounds being the most commonly used.[44,210] Although halogen-containing flame retardants have been effective in reducing fire-related deaths and property damage, concerns over their potential threat to the environment and human health have prompted efforts in finding safer alternatives.[44-48]

Layer-by-layer (LbL) assembly has proven to be an effective method to impart non-halogenated FR coatings on PU foam,[31,49,51,54-56,211-213] as well as other flammable materials such as cotton,[59,62-64,67,214] nylon,[21,70,71] and polyester fabric.[59,72] LbL involves alternate adsorption of positively and negatively-charged polyelectrolytes from aqueous

* Reprinted with permission from "Aluminum hydroxide multilayer assembly capable of extinguishing flame on polyurethane foam" by Haile, et. al, 2016. *Journal of Materials Science,* 51, 375-381, Copyright 2016 by Springer.

solution.[1,182] These assemblies can be built from polymers,[19,24,215,216] nanoparticles.[3-6] or biomolecules[7-10] to deposit thin films without altering the desired properties of the bulk material.[2] Flame retardant (FR) nanocoatings, deposited layer-by-layer, are attractive due to their water-based chemistry and ease of fabrication. A significant drawback of LbL remains the number of bilayers (cationic and anionic layer pairs), necessary to build a film of sufficient thickness to achieve the desired FR behavior, which increases processing time and cost. LbL deposition of polymer-clay thin films on PU foam have shown tremendous success with relatively few layers, and are able to maintain the structure of the foam after burning (in addition to significantly reducing heat release rate).[31,49,54,55,57] Clay is a passive flame retardant, functioning as an inflammable barrier to heat that protects the underlying foam.[217]

Boehmite, an active FR mineral was recently paired with vermiculite clay, using LbL assembly, to effectively suppress flame on PU foam.[212] Boehmite is able to release water when decomposing at high temperature (over 450 ˚C), reducing the heat of its surroundings and releasing an inert gas to dilute the flame. Unfortunately, much of boehmite's beneficial activity occurs at a higher temperature than the decomposition temperature of PU foam (around 250 ˚C), which allows the foam to burn before the critical water release is achieved.[49,218] The present work describes the dispersion and LbL deposition of aluminum hydroxide onto foam, which decomposes at a lower temperature than bohemite, and releases more water per unit mass.[219] Cationic polyethylenimine (PEI) and anionic polyacrylic acid-stabilized aluminum hydroxide (PAA-ATH) were alternately deposited on polyurethane foam. Only six PEI/PAA-ATH bilayers eliminate

melt dripping, extinguish flame, and maintain structural integrity of PU foam upon exposure to direct flame from a butane torch. This nanocoating (~ 1 μm thick) reduces the peak heat release rate (pHRR) of the foam by 64%. This novel FR treatment is deposited under ambient conditions, uses environmentally-benign ingredients, and provides effective fire protection for foam with fewer processing steps.

A.2 Experimental

Cationic branched polyethylenimine (M_w = 25,000 g mol^{-1}), anionic polyacrylic acid solution (M_w = 100,000 g mol^{-1}, 35 wt% in water), sodium hydroxide pellets (anhydrous) (reagent grade, ≥ 98%), and nitric acid (red, fuming, HNO_3 > 90%) were purchased from Sigma–Aldrich (Milwaukee, WI). Aluminum hydroxide (Martinal OL-111 LE) was purchased from Albemarle Corporation (Baton Rouge, LA). P-doped, single side polished (1 0 0) silicon wafers (University Wafer, South Boston, MA), with a thickness of 500 μm, were used as substrates for profilometer thickness measurements. Flexible, open-celled polyether-based 1850 polyurethane foam with a density of 1.75 lbs ft^{-1} was purchased from Future Foam (High Point, NC).

All aqueous solutions were prepared with 18.2 MΩcm deionized water. The pH of 0.2 wt% PEI was adjusted to 10.0 using 1 M hydrochloric acid, and the pH of 0.2 wt% PAA was altered to 4.0 using 1.0 M sodium hydroxide. To prepare solutions of 0.2 wt% PAA with 0.5 wt% ATH, the aluminum hydroxide was added to a solution of PAA and the suspension was ultrasonicated for 30 min. The pH of the suspension was finally adjusted to 4.0 for deposition. Foam was primed for deposition by soaking a 4 x 4 x 1 in. piece in 1 wt% PAA for 30 s. The pH of this solution was adjusted to 2.0 using nitric acid

prior to this deposition step. The nitric acid oxidizes the surface of the foam and polyacrylic acid adsorbs by hydrogen bonding, giving the polyurethane a negative surface charge. The foam was then coated layer-by-layer using alternating dips. Plasma-treated silicon wafers and foam were dipped in the positively charged PEI solution for 5 min, rinsed by a stream of deionized water, and then dried (foam was simply squeezed dry). The procedure was followed by the same dipping, rinsing, and drying cycle in the anionic solution (i.e. PAA with or without ATH). After the deposition of this initial bilayer (BL), the same procedure was followed with 1 min PEI and 1 min PAA dip times for every subsequent deposition until the number of desired layers was reached. Films were placed in an oven for 1 h at 70 ˚C prior to characterization. The LbL procedure is depicted in Fig. 1. Each deposition was followed by dip rinsing in deionized water and wringing out to remove excess polymer. The foam was dried for a minimum of 12 h in 70 ˚C prior to testing.

Film thickness was measured on silicon wafers with a P-6 profilometer (KLA-Tencor, Milpitas, CA). Thermal stability of uncoated and coated PU foam (approximately 20 mg) was evaluated using a Q-50 thermogravimetric analyzer (TA Instruments, New Castle, DE), under a controlled heating ramp of 20 ˚C min^{-1}, from ambient temperature up to 600 ˚C, with a sample purge flow of 60 mL s^{-1} air and a balance purge flow of 40 mL s^{-1} nitrogen. Control and coated foam was exposed to the direct flame of a butane micro hand torch (Model ST2200, Benzomatic, Huntersville, NC) for 10 s to provide a visual demonstration of flame suppression. Cone calorimetry was performed on each foam sample in triplicate at the University of Dayton Research Institute, using a FTT Dual Cone

Calorimeter, with a 35 kW m^{-2} heat flux and an exhaust flow of 24 L s^{-1}, using a standardized procedure (ASTM E-1354-07). Other thermal properties were measured using a Q20 differential scanning calorimeter [DSC] (TA Instruments, New Castle, DE). 5–10 mg of foam was placed in an aluminum pan and scanned from 40 to 500 ˚C at a heating rate of 5 ˚C min^{-1}. Particle size and zeta potential of ATH particles were determined by analysis of 0.1% ATH dispersions using a Brookhaven ZetaPALS instrument (Brookhaven Instruments Corp., Holtsville, NY).

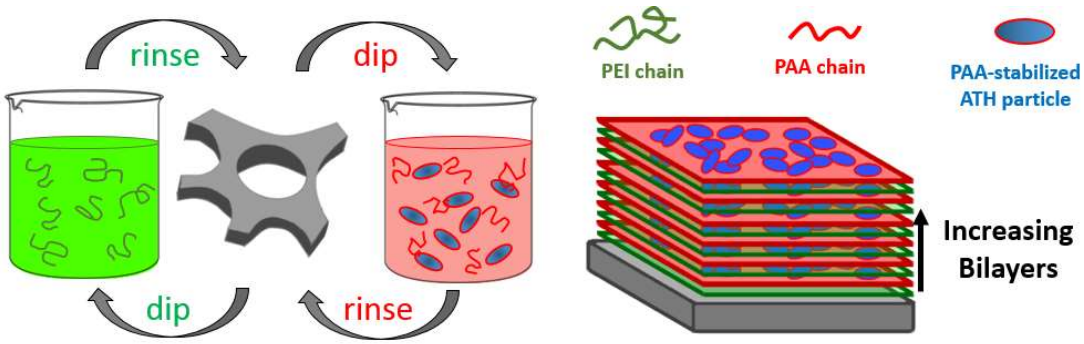

Figure A1. Schematic of layer-by-layer deposition of PEI/PAA-ATH bilayers on a substrate.

A.3 Results and Discussion

Aluminum hydroxide [$Al(OH)_3$] or ATH is known to be an effective flame retardant filler for polymers.[210,219] When exposed to heat in a fire, ATH degrades to aluminum oxide, releasing water as an inert gas to dilute the flame [2 $Al(OH)_3 \rightarrow Al_2O_3$ + 3 H_2O]. This decomposition also acts to cool the system, as the reaction is highly endothermic, absorbing about 280 calories per gram of ATH.[219] With a decomposition

temperature of ~ 200 ˚C, it is an ideal flame retardant as a coating on PU foam, which is a challenging substrate due to its low onset of degradation (≈ 250 ˚C).[210] The key challenge to incorporating ATH into an LbL coating is its low dispersibility in water. Even when ultrasonicated in water, aluminum hydroxide settles out of solution. Zeta potential measurements indicated the particles had an average zeta potential of -41.7 ± 0.8 mV. When ATH was ultrasonicated in the presence of PAA, a stable milky white suspension was formed. ATH remained suspended in the PAA with no appreciable precipitation over 6 h. The negatively-charged poly(acrylic acid) chains likely adsorb to the surface of the ATH particles, allowing the coated particles to disperse by mutual electrostatic repulsion. [220] The zeta potential of the particles in dilute PAA was measured to be -60.9 ± 2.1 mV. The average diameter of the particles was measured to be 708 ± 34 nm, using dynamic light scattering. This somewhat large nanoparticle apparently requires a greater surface charge to remain suspended.

Aluminum hydroxide nanoparticles were deposited onto polyurethane foam using the LbL process, as depicted in Figure 1. The foam was alternately dipped in cationic PEI and anionic PAA-ATH solutions until the desired thickness of the film was achieved.

Thickness of the multilayer assemblies as a function of the number of deposited bilayers was measured with profilometry, as shown in Figure A2. Polyelectrolyte multilayers with ATH (PEM-ATH) grow thicker with each bilayer compared to PEI/PAA multilayer films without ATH (PEM). PEI/PAA is a particularly thick-growing system, achieving greater than one micrometer of thickness with only 6 BL on silicon wafer.[24] PEM-ATH was deposited onto polyurethane in an effort to determine the effect of ATH

particles on its flame retardancy. 6 BL of PEM without ATH was deposited on foam as a control. The weight of coating deposited was determined by weighing before and after coating (reported as the percentage of the original mass in Table A1).

Table A1. Torch test and cone calorimeter results for polyurethane foam with and without nanocoatings.

	Weight gain (%)	ATH in coating (%)[a]	Residue[b] (%)	Peak HRR (kW m^{-2})	Total heat release (MJ m^{-2})	Total smoke release (m^2 m^{-2})	MARHE
Uncoated	-	-	-	877 ± 61	21.3 ± 1.5	159 ± 9	348 ± 23
6 BL PEM	14 ± 2	0	13 ± 7	736 ± 85	23.5 ± 0.3	217 ± 2	361 ± 2
6 BL PEM-ATH	32 ± 3	47	82 ± 1	314 ± 11	21.8 ± 2.2	189 ± 22	195 ± 14

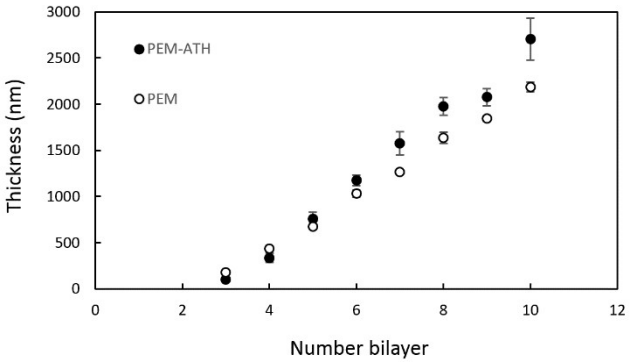

Figure A2. Thickness of LbL assemblies as a function of bilayers deposited.

Figure A3 shows SEM micrographs of uncoated and coated foam. The micrographs of 6 BL PEM-ATH on foam reveals the presence of ATH nanoparticles embedded in a polyelectrolyte matrix (Figure A3c). In comparison, the surface of the 6 BL PEM film deposited without ATH is relatively smooth with the exception of large cracks (Fig. A3b), which are the result of the film being very glassy.[221] The ATH particles

are less than one micrometer in size (Fig. A3d), agreeing with the average particle size measured by DLS. Both coating systems are very conformal, maintaining the open cellular structure of the foam.

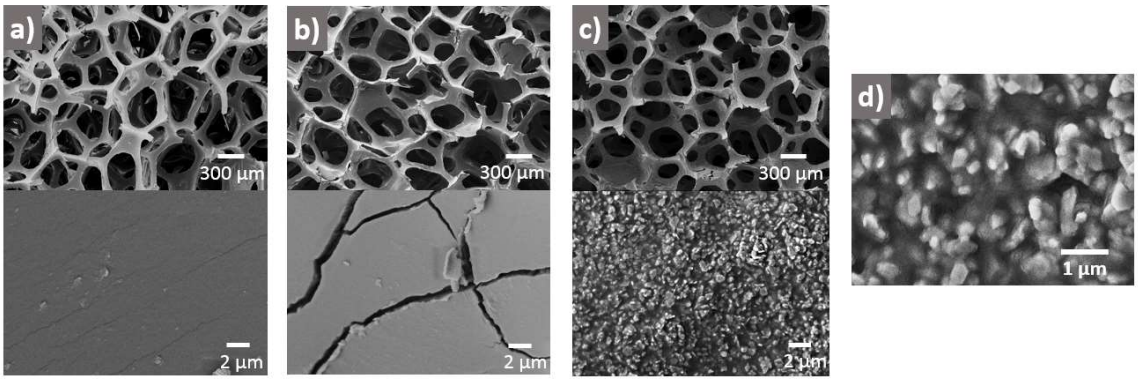

Figure A3. SEM micrographs of PU foam: **a** uncoated foam, **b** 6 BL PEM coated foam, **c-d** 6 BL PEM-ATH coated foam.

Foam flammability was evaluated by exposing samples to the flame from a butane torch for 10 s. Figure A4 shows images of foam 30 s after exposure. Uncoated foam ignites and melt drips upon flame exposure, leaving no residue (Figure A4a). Melt dripping is a major concern due to its ability to spread fire to surrounding furniture, carpeting, and fabric. PEM coating on foam (6 BL of PEI/PAA) completely eliminates melt dripping, but the foam ignites and burns vigorously after flame exposure, leaving only 13 wt% residue (Fig. A4b). The incorporation of ATH in this nanocoating greatly improves flame retardancy, as shown in the torch test results of samples coated with 3 and 6 BL PEM-ATH. 3 BL of PEI/PAA-ATH maintains the shape of the foam during burning, leaving 43 wt% residue (Figure A4c). A thicker 6 BL coating of PEM-ATH affords excellent fire

suppression, extinguishing the flame on the foam's surface to prevent full flashover (Fig. A4d). Figure A4e shows a cross-section of the foam coated with 6 BL PEM-ATH after torch testing. Most of the foam is left completely untouched, leaving 82 wt% residue.

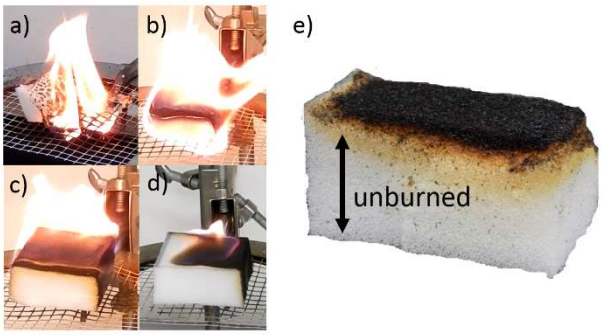

Figure A4. Images of torch testing of PU foam 30 s after removal of external flame: **a** uncoated, **b** 6 BL PEM, **c** 3 BL PEM-ATH, **d** 6 BL PEM-ATH. (**e**) shows a cross-section of foam coated with 6 BL PEM-ATH after torch testing.

The effectiveness of the PEM-ATH coating is partially due to the ability of the ATH particles to release water upon flame exposure, cooling the substrate and diluting combustible gases in the flame. As a decomposition product, alumina also provides protection as an insulating ceramic that protects underlying flammable material from heat, similar to the effect observed in clay-based LbL assemblies.[222,223] Uncoated foam, along with foam coated with PEM and PEM-ATH, was heated from an ambient temperature up to 800˚C in an oxidizing atmosphere, using a thermogravimetric analyzer (TGA), at a heating rate of 10 ˚C min^{-1} (Figure A5). ATH appears to be an appropriate candidate as a flame retardant for PU foam, as its decomposition temperature (measured to be 260 ˚C) coincides with the measured degradation onset of foam (~270 ˚C). This temperature

correspondence allows the ATH to act before the foam starts burning. The degradation onset of the foam is unaffected by the presence of either of the layer-by-layer coating systems, as evidenced by the overlapping derivative curves. Using the mass residue of the foam coated with PEM-ATH, the percentage of ATH in the coating was estimated to be 47 wt%.

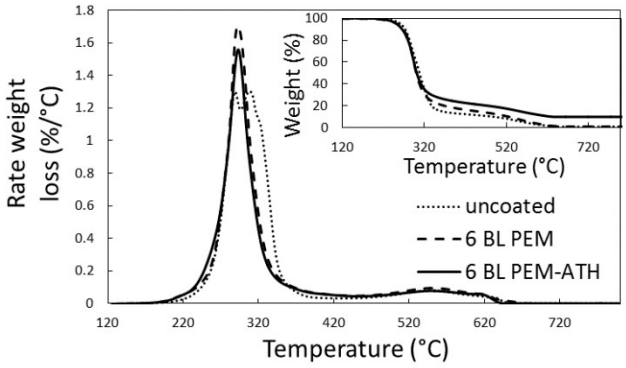

Figure A5. Representative weight loss rate as a function of temperature for uncoated (control) foam and coated foam measured in an oxidizing atmosphere. Weight percent as a function of temperature measured by TGA is shown as inset. Weight loss rate is the derivative of the weight loss curves.

Cone calorimetry was performed to quantitatively assess the FR performance of the PEM-ATH nanocoating on foam. Foam coated with 6 BL PEM and 6 BL of PEM-ATH were evaluated and compared with uncoated foam. Samples were exposed to an external heat flux over time, forcing the material to ignite and undergo combustion. The heat release rate (HRR), an indicator of flammability, was measured as a function of time (Figure A6). Typical combustion behavior was observed for the uncoated polyurethane, releasing a total heat (THR) of 21.3 MJ m^{-2}. Two peaks associated with the combustion of

decomposition products are observed from the HRR curve of uncoated foam, the first being polyisocyanate (261 kW m^{-2}) and then polyether (877 kW m^{-2}).[224] The peak HRR was the polyether peak, occurring after 40 s.

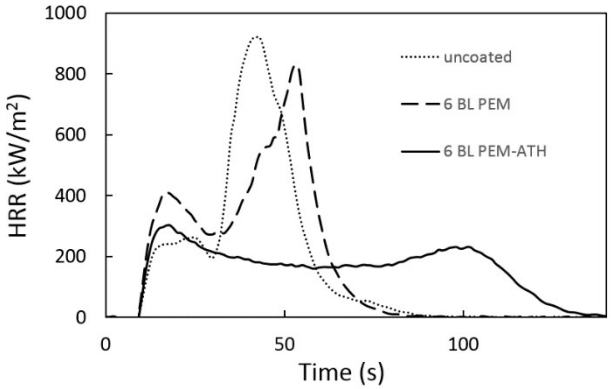

Figure A6. Heat release rate as a function of time for coated and uncoated foam, measured with a cone calorimeter.

6 BL of the PEM did not significantly reduce the flammability of the foam. The peak HRR of 6 BL PEM-coated foam (736 kW m^{-2}) represented a reduction of only 16 %. The total heat release was actually increased to 23.5 MJ m^{-2} due to the coating adding more flammable material to the system. Cone calorimetry of foam coated with 6 BL PEM-ATH, indicates that ATH nanoparticles greatly improve the FR behavior of the foam. This ATH-based coating reduced the peak HRR by 64 %. This effect is similar to that observed with LbL coatings incorporating clay, but the reduction with ATH is more significant. The maximum average rate of heat emission (MARHE) is reduced by 44 % with this PEM-ATH coating (44 %). MARHE ranks materials by their ability to spread flame to other objects,[225] indicating a reduced fire hazard imparted by the PEM-ATH coating.

The total heat release of foam coated with 6 BL PEM-ATH is within error of being the same as the control foam, but lower than the THR of foam coated with 6 BL PEM. This is likely due to the highly endothermic decomposition of the ATH nanoparticles. Differential scanning calorimetry was performed on foam samples to better observe this effect (see Supplementary Material). Polyurethane degraded in two decomposition steps, both endothermic and totaling 435.2 J g^{-1}. When coated with 6 BL PEM-ATH, this energy balance is more endothermic, with a total enthalpy of 633.6 J g^{-1}. It is important to note the exothermic reactions associated with combustion were eliminated in the DSC due to the absence of oxygen. PEI and PAA alone do not impart reduced flammability.

This work demonstrates the use of ATH nanoparticles in a polyelectrolyte multilayer nanocoating and its effectiveness in flame retarding polyurethane foam. This concept could be applied to the incorporation of other water-insoluble particles in FR nanocoatings. The aqueous dispersion of aluminum hydroxide using a fast, environmentally-benign process, as well as its incorporation in an LbL film on PU foam, was successful in suppressing flame without altering the open-celled structure of the foam. Foam coated with only six PEI/PAA-ATH bilayers (~ 1 μm thick) was able to self-extinguish the fire from a butane torch, retaining 82 % of the sample mass. Cone calorimetry revealed the nanocoating reduced the peak heat release rate by 64 % and the MARHE by 44 %. This protective nanocoating provides a low cost, scalable FR treatment for foam that could be a safe alternative to the halogenated systems currently being used. The fact that this is a coating rather than an additive is also noteworthy, allowing foam to be protected without altering its processing and properties.

APPENDIX B

ULTRATHIN CARBON NANOTUBE THIN FILM ASSEMBLIES AS POWERFUL MICROWAVE SUSCEPTORS

B.1 Results and Discussion

One of the lesser known properties of carbon nanotubes (CNTs) is their exceptional ability to absorb microwave radiation.[226] This peculiar phenomenon has been used for CNT detection, electromagnetic shielding and CNT cross-linking.[227-231] Due to their versatility, chemical resistance, and absorption efficiencies, even at low loading levels, CNTs are excellent materials for microwave-absorbing (MWA) applications. There is growing demand for MWA materials in the fields of radar detection, electromagnetic shielding and electronics. Upon exposure to microwave fields, CNTs efficiently attenuate incident propagating waves and evolve tremendous heat. This ability to heat as powerful microwave susceptors could be useful in food packaging, where coatings are used to heat and brown foods during microwave cooking. Conventional MWA materials such as aluminum present some health concerns.[232]

Polymer composites incorporating CNTs offer a wide range of applications and the possibility of tuning desirable properties, including MWA, by varying CNT loading. Although many studies have observed the MWA behavior of CNT bulk nanocomposites, there is little research on how such composites behave when their thickness is on the scale of nanometers.[226,233-235] The present work investigates the microwave absorption of thin films composed of anionically-stabilized carbon nanotubes and a polycation, deposited

layer-by-layer (LbL). LbL assembly involves the "bottom-up" fabrication of thin films by alternately exposing a substrate to positively and negatively charged materials in aqueous suspensions. Film thickness is controlled by the number of deposition cycles, with each positive and negative layer pair referred to as a bilayer (BL).[1,2] This is a powerful coating technique, capable of coating many substrates to impart a variety of properties such as energy generation,[236-239] antimicrobial,[19,240] gas barrier,[27,241] and flame retardancy.[53,65] LbL assembly provides an elegant approach to constructing thin CNT composites on complex substrates with high loading and exceptional electrical conductivity.[84,205,242-249] In the present study, CNT-based films were deposited on polyester (PET) substrates using LbL assembly under ambient conditions and aqueous suspensions. These sub-300 nm thick coatings provide an attractive alternative to common MWA coatings, such as magnetic materials or ceramic ferroelectrics, which require more complex processing and add undesirable mass.[250]

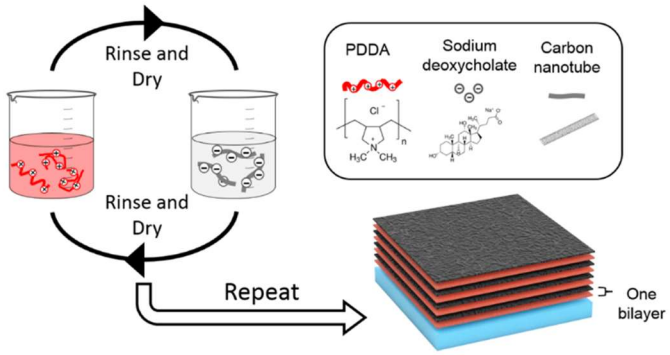

Figure B1. Schematic of the LbL process for fabricating CNT thin films. The substrate is alternately dipped into a cationic PDDA and an anionic DOC-stabilized CNT mixture, with rinsing and drying in between. These steps deposit one bilayer and are repeated to grow a film of desired thickness.

Multilayer thin films composed of either single-walled (SWNT) or multiwall CNTs (MWNT), stabilized by deoxycholate, were paired with poly(diallyldimethylammonium chloride) [PDDA] and deposited according to a previously reported procedure.[244] Substrates were first dipped in the polycationic solution containing PDDA, depositing one positively-charged layer (Figure B1). After rinsing and drying, the substrate was dipped in the anionic suspension containing CNTs and sodium deoxycholate (DOC), depositing one negatively charged layer that was rinsed and dried. This cycle was repeated until the desired number of bilayers was achieved. Both assemblies exhibit linear growth beyond 20 BL, depositing on average 3.1 nm and 2.3 nm per bilayer, respectively. The growth per bilayer is thinner and non-linear at 10 BL, which is typical of multilayer thin films as they are establishing a coherent base layer. These recipes were deposited on PET for the microwave experiments, and on silicon for determining thickness via ellipsometry and profilometry. Each substrate results in a similar thickness value for a given number of bilayers, as reported in earlier studies.[85,205,206,243] The transparency of these films on PET was measured using UV-Vis spectroscopy. Although both coating recipes had comparable thicknesses, PDDA/MWNT films were generally much more opaque than PDDA/SWNT films, with only 53% transmittance at 5 BL and less than 10% transmittance at 20 BL and above. PDDA/SWNT exhibited over 90% visible light transmittance 10 BL and below. Very low transmittances of less than 50% were only achieved at 60 BL and above. Differences in nanotube loading were seen between the two CNT types, when scanning electron microscopy was used to observe the surface morphology of the 40 BL films. The PDDA/MWNT film has a

considerably rougher surface, due to larger nanotube size, and has a considerably higher concentration of CNTs than that of the PDDA/SWNT film. Thermogravimetric analysis (TGA) performed on PDDA/CNT delaminated films indicates that the concentration of MWNT and SWNT are 71.6 and 15.6 wt%, respectively.

In an effort to observe the thermal response of these microwave-absorbing LbL films, coated PET samples were microwaved in a waveguide assembly while temperatures were recorded using a FLIR camera (A655sc). Each sample was irradiated for approximately 30 seconds at 10 W forward power. The heating curves for both SWNT and MWNT films (Figure B2) demonstrate these films' ability to rapidly attenuate microwave energy, converting it to radiant heat. The films rapidly respond to the applied microwave field to reach temperatures over 130° C. This result suggests that the PDDA/CNT films are excellent microwave susceptors, capable of efficiently converting incident microwave power into thermal energy via Joule heating. To better understand the mechanism for this rapid heating response, the microwave absorbing properties of the LbL films on PET were measured using a microwave network analyzer (Agilent E5071C) and a two port coaxial transmission line technique. Round discs of each film thickness were fitted into a coaxial adapter while ensuring that air gaps were eliminated. The network analyzer measures the scattering parameters (S_{11} and S_{21}) by detecting the incident, reflected, and transmitted microwave signals. The ratios of the reflected and transmitted powers to the incident power are equal to $|S_{11}|^2$ and $|S_{21}|^2$, respectively. The power absorbed by the sample and dissipated as heat, normalized to the incident power, is calculated using Equation (B1):

$$\frac{P_{diss}}{P_{inc}} = 1 - |S_{11}|^2 - |S_{21}|^2 \quad \text{(B1)}$$

Higher temperatures are achieved with a higher number of bilayers for both the PDDA/SWNT and PDDA/MWNT assemblies, as predicted by the dissipated power trends observed during coaxial measurements. Notably, the jump in heating rate from 40 to 60 SWNT bilayers is clearly visible in both the relative power measurements (Figure B2c) and the heating curve in Figure B2b. The rate at which the samples cool upon the cessation of microwave heating is also remarkable. Cooling of over 100 °C in less than 30 seconds is observed for some samples, indicating that the high temperature is localized in the nanocoating and is quickly transferred to the still-cool substrate and air.

In Figure B2d, the maximum temperature as a function of film thickness at 30 seconds of heating is shown for both PDDA/SWNT and PDDA/MWNT films. Both nanotube films display a similarly increasing maximum temperature as film thickness is increased by adding more bilayers. This positive correlation between film thickness and heating response appears logical, however, this trend is not typical for MWA thin film susceptors. The thermal response of sputtered aluminum films on PET was plotted for comparison (Figure 2d). For the aluminum films, a decreasing maximum temperature is observed as film thickness is increased from 7 nm to 100 nm. This inverse relationship of thickness to heat evolved clearly indicates that the aluminum films are highly reflective to incident microwaves, which means thicknesses below 20 nm are useful as microwave susceptors. In contrast, the PDDA/CNT assemblies have a wide range of thicknesses

displaying different heating profiles, providing greater flexibility for tuning their heating response.

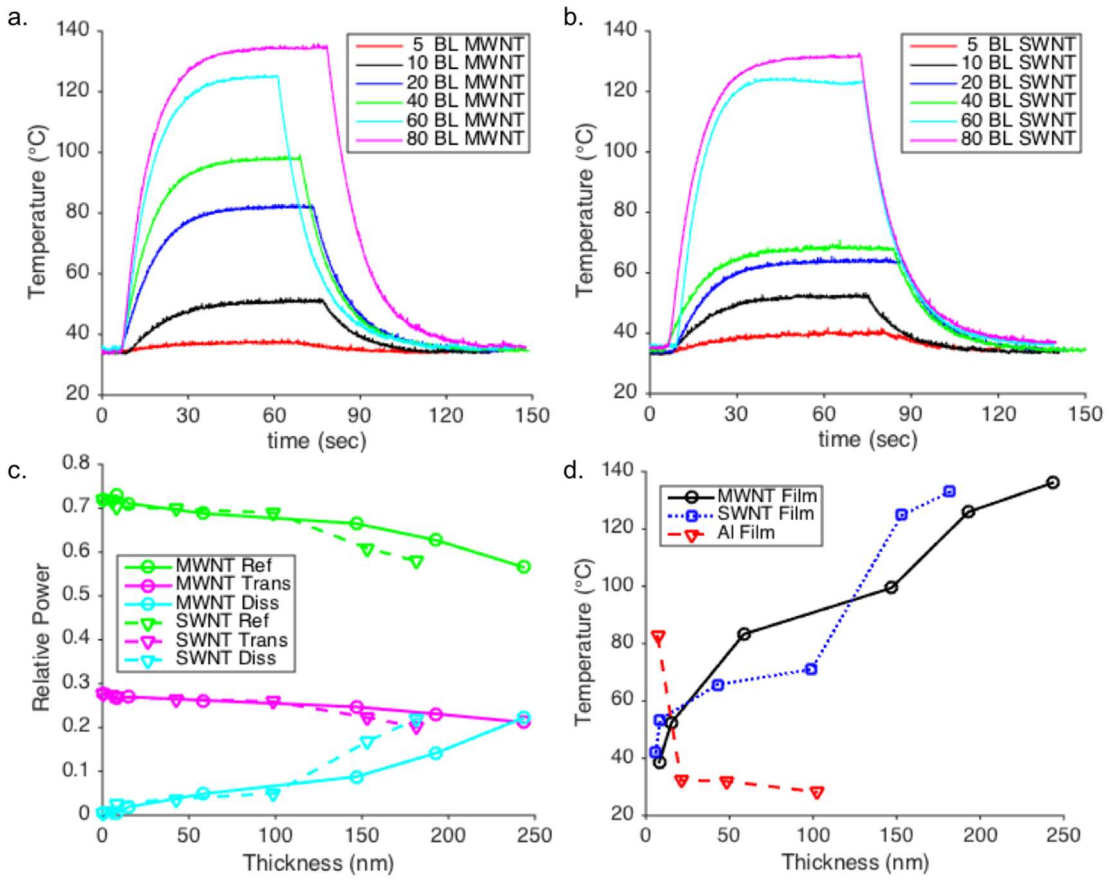

Figure B2. FLIR temporal plots of the maximum temperature recorded of the (a) PDDA/MWNT and (b) PDDA/SWNT films during microwave heating at 10 W. (c) Relative power curves: reflected, transmitted, and dissipated (absorbed) of the LbL films measured with a two-port coaxial method. (d) Maximum temperature versus film thickness for MWNT, SWNT, and Al films.

The spatial heating profiles of the nanotube films were recorded for each sample, as shown in Figure B3. The electric field and thus deposited power in the waveguide are maximized at the center. No difference in the spatial heating profile is observed for the

MWNT or SWNT-based films, which suggests the same thermal heating mechanism is responsible in each case. The exact nature of the heating response of CNTs and their composites to microwave irradiation is still not well understood. It is generally accepted that incident microwave radiation interacts with CNTs through electric field coupling, causing the excitation of electrons and electric currents in the film that leads to Joule heating concentrated at resistive lattice defect sites and nanotube-nanotube junctions.[251] It is believed that the observed rapid heating and cooling rates stem from CNT-related heating phenomena reported in prior studies. For instance, it is well known that CNT films can rapidly heat (and cool) from a stimulated direct current (DC) biased audio signal to produce a thermoacoustic effect.[252-254] The CNT film loudspeakers are able to drive audio signals up to many hundreds of kilohertz due to their low heat capacity and thermal cycling efficiency. Further studies involving wide-band terahertz spectroscopy of CNT films in response to stimulated electric currents, ranging from DC to the gigahertz region, may be helpful in elucidating the exact mechanisms responsible for the rapid heating observed. Regardless of the exact heating mechanism, this work demonstrates the efficient frequency up-conversion from S-band (2-4 GHz) microwave energy to long wave infrared (LWIR) (20-40 THz) radiant thermal energy in these carbon nanotube-based thin film assemblies.

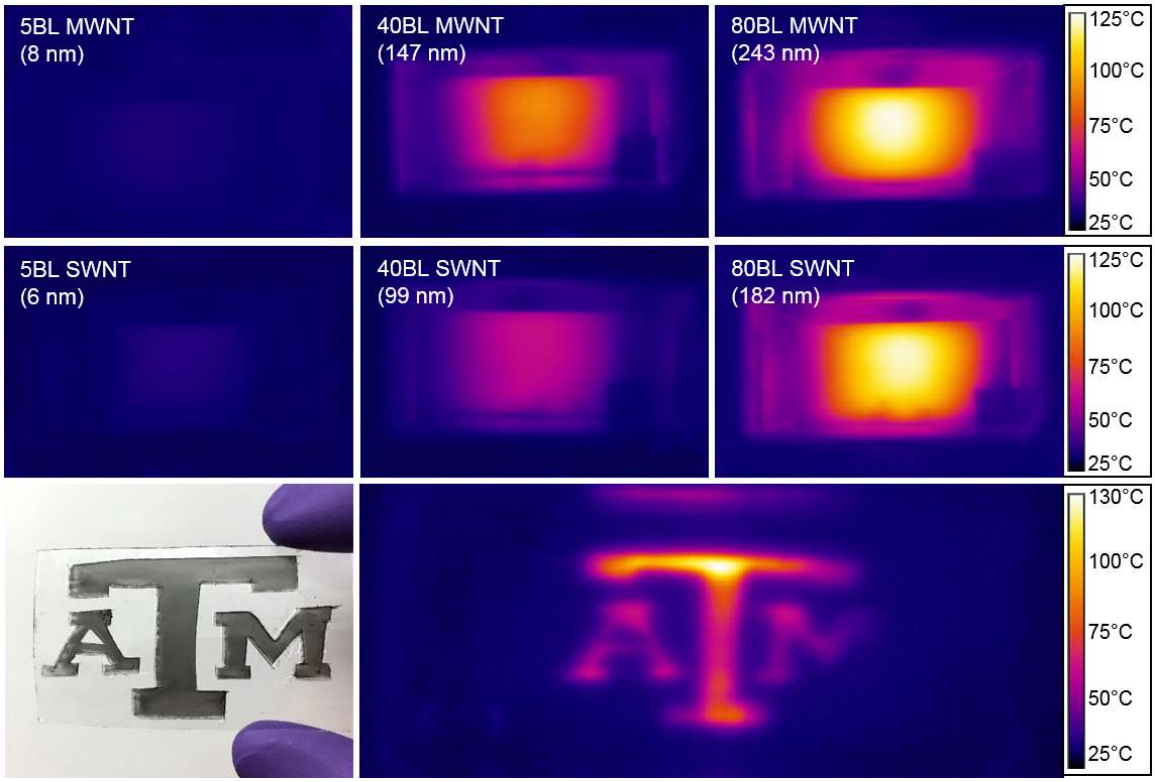

Figure B3. FLIR images of the MWNT (top) and SWNT-based (middle) LbL films of increasing thickness in the microwave waveguide at 10W after 30 seconds of heating. A patterned logo (bottom) made with the carbon nanotube LbL process demonstrates the ability to remotely heat discrete areas of interest.

In this report, both SWNT and MWNT-based layer-by-layer films of varying thicknesses were prepared and exposed each to microwave energy. The microwave response of these thin CNT films (< 300 nm) was outstanding, evolving significant heat in low-power fields. High localized temperatures at the coated surfaces were achieved without appreciably heating the bulk PET substrate. The ease of deposition and process scalability, bolstered by the useful range of film thicknesses that respond to incident microwaves, confirm the utility and advantage these films have over current susceptors materials. By selectively depositing carbon nanotube susceptor films, precise control of

material interface temperatures may be realized by an applied external electric field. This spatial temperature control could be used for material bonding, curing, and thermally-driven microstructure evolution. Beyond susceptors, these multilayer films could be used as radar absorbing materials for stealth vehicles and aircraft, EMI shielding films, as well as antennas for radio frequency identification (RFID) tags.

B.2 Experimental Section

B.2.1 Materials

MWNTs (20-30 nm outer diameter and 10-30 μm length, C ≥ 95 wt %) were provided by Cheap Tubes Inc. (Cambridgeport, VT). SWNTs (0.7-1.3 nm diameter, (7,6) chirality, C ≥ 70 wt %) were purchased from SouthWest NanoTechnologies (Norman, OK). PDDA (Mw ~ 200,000 g mol^{-1}), and DOC were purchased from Sigma-Aldrich (St. Louis, MO). Sulfuric acid (H_2SO_4, 98%), hydrogen peroxide (H_2O_2, 30%), and methanol (99.8%) were also purchased from Sigma-Aldrich and used as received. P-doped, single side polished (1 0 0) silicon wafers (University Wafer, South Boston, MA), with a thickness of 500 μm, were used as substrates for elipsometer and profilometer thickness measurements. Films for microwave testing were deposited on 179 μm-thick poly(ethylene terephthalate) (PET) film (ST505, Dupont-Teijin) purchased from Tekra (New Berlin, WI).

B.2.2 Layer-by-Layer Assembly

All solutions were prepared using 18.2 MΩ cm deionized water. A cationic 0.25 wt % PDDA aqueous solution was prepared by diluting a 20 wt% PDDA solution with deionized water. The anionic solution was prepared by dissolving 0.05 wt % CNTs in deionized water containing 2 wt% DOC, followed by a three step ultrasonication process to remove large nanotube bundles: 30 min of bath sonication, then 20 min using a tip sonicator, and a final 30 min of additional bath sonication.[255] Single-side polished (1 0 0) silicon wafers (University Wafer, South Boston, MA) were cleaned by immersion into a piranha solution (4:1 mixture of H_2SO_4 and H_2O_2; caution: dangerous oxidizing agent) and sonicating for 30 min, followed by thoroughly rinsing with deionized water and drying with filtered air. 175 μm thick PET (trade name ST505 by DuPont Teijin, Tekra Corp., New Berlin, WI) film was cut to size, followed by rinsing with methanol and water. The cleaned PET substrates were then corona treated with a BD-20C Corona Treater (Electro-Technic Products Inc., Chicago, IL). Corona treatment oxidizes the surface of PET, increasing the surface energy and allowing for positively-charged polymers to better adhere.[256] PDDA/ CNT assemblies were deposited on a given substrate according to the procedure shown in Figure 1, using automated rinsing, dipping, and drying. Substrates were immersed into the cationic PDDA solution for 5 min, then rinsed with deionized water and dried using filtered air. Immersion into the DOC-stabilized CNT suspension for 5 min came next, followed by rinsing and drying. These four steps comprised one cycle, yielding one BL. Dipping times were 1 min for every subsequent cycle until the desired

number of bilayers was deposited. All samples were stored in a drybox for a minimum of 12 h prior to testing.

Film thickness was measured on silicon wafers with a P-6 profilometer (KLA-Tencor, Milpitas, CA) and alpha-SE Ellipsometer (J.A. Woollam Co., Inc., Lincoln, NE). Coated PET samples were mounted on aluminum stubs in preparation for surface images that were acquired with a field-emission scanning electron microscope (SEM) (Model JSM-7500F, JEOL; Tokyo, Japan).

B.2.3 Electrical Characterization

DC electrical conductivity of the prepared PDDA/CNT films was measured with a four-point-probe (Signatone HR4-620850FN). Samples approximately 3 x 5 cm were centered on a four-point-probe stand (Lucas Labs) and measured using a differential voltage system (two Keithley 6514 electrometers, Keithley 2000 digital multimeter) with current sourced by a Keithley 6221. Starting at the lowest possible current for each sample, voltage drops were measured at three increasing decades to ensure the linear Ohmic behavior of the samples. Volume resistivity (inverse conductivity) was calculated according to the following formula:

$$\rho = \frac{\pi}{\ln 2} \cdot \frac{V}{I} \cdot t \cdot k \qquad \text{(B2)}$$

where ρ is the resistivity in Ohm-m, V is the voltage drop in Volts, I is the current in Amps, t is the thickness in meters, and k is a correction factor for geometry based on the probe

spacing to sample diameter. For the sample geometry tested, k is taken to be 0.983 (short sample dimension [3 cm] divided by probe spacing 0.15875 cm and correction applied from lookup table).

Microwave dielectric properties of the films were measured using a coaxial technique using a microwave network analyzer (Agilent E5071C) that measures the scattering (S) parameters of two-port networks. The measurement technique uses a disk shaped sample sandwiched between two transmission lines. The parts of the dielectric disk that are outside the coaxial lines are completely enclosed with a conductor. For convenience, two 7 mm Amphenol Precision Connectors (APC-7) were used as the sample holder. The films to be measured were prepared by laminating both faces with clear packing tape to insulate and protect the surfaces from the coaxial sample holder. A disc punch was used to punch out samples 14.8 mm in diameter, ensuring the films would fit precisely in the sample holder with minimal air gaps at the edges. All power measurements were carried out at approximately 2.45 GHz to match the frequency used for the waveguide heating experiments.

B.2.4 Microwave Heating

PDDA/CNT films were heated in a rectangular waveguide (AMCSS-284-F/F-12-B, AMC LLC.) powered by a solid state microwave source (GMP 150, Opthos Instruments Inc.) operated at 2.45 GHz at various power levels. Spatial temperature measurements were carried out using an infrared camera system (A655sc, FLIR Systems Inc.) calibrated to measure temperatures of a sample located behind a brass mesh covering the open end of the waveguide.[257] The samples were inserted into the waveguide at the location of a

maximum of the electric field standing wave, approximately 57.9 mm from the brass mesh. This ensures the samples were exposed to the strongest and most uniform electric field in the waveguide. Various power levels were used to heat the samples and their temperature response was recorded using the FLIR supplied software (ReseachIR MAX). Aluminum-coated films were deposited onto PET using a PVD 75 Metal Sputter (Lesker Company, Jefferson Hills, PA). Thickness of aluminum films was determined by profilometry of coated silicon concurrently sputtered alongside PET samples.